# Anatomy of *Haplomastodon chimborazi* (Mammalia, Proboscidea) from the late Pleistocene of Ecuador and its bearing on the phylogeny and systematics of South American gomphotheres

Author(s): Marco P. Ferretti
Source: Geodiversitas, 32(4):663-721. 2010.
Published By: Muséum national d'Histoire naturelle, Paris
DOI: http://dx.doi.org/10.5252/g2010n4a3
URL: http://www.bioone.org/doi/full/10.5252/g2010n4a3

# Anatomy of *Haplomastodon chimborazi* (Mammalia, Proboscidea) from the late Pleistocene of Ecuador and its bearing on the phylogeny and systematics of South American gomphotheres

**Marco P. FERRETTI**
Università di Firenze, Dipartimento di Scienze della Terra,
via G. La Pira 4, I-50121 Firenze (Italy)
mferretti@unifi.it

Ferretti M. P. 2010. — Anatomy of *Haplomastodon chimborazi* (Mammalia, Proboscidea) from the late Pleistocene of Ecuador and its bearing on the phylogeny and systematics of South American gomphotheres. *Geodiversitas* 32 (4): 663-721.

**ABSTRACT**
I present here a revision of the late Pleistocene *Haplomastodon chimborazi* (Proaño, 1922) material from Bolivar, Ecuador and a comparison with other New World trilophodont gomphotheres, and provide new morphological data in order to develop a novel phylogenetic hypothesis of South American (SA) proboscideans. *Haplomastodon* Hoffstetter, 1950 includes a single SA species whose valid name is *H. chimborazi*. *Haplomastodon waringi* (Holland, 1920) is considered to be an invalid taxon as it is based on undiagnosed material. Phylogenetic analysis supports the monophyly of SA gomphotheres (Cuvieroniinae) *H. chimborazi*, *Cuvieronius hyodon* (Fischer de Waldheim, 1814), and "*Stegomastodon*" *platensis* (Ameghino, 1888), based on five unambiguous characters. Conflicting evidence regarding the interrelationships of SA gomphotheres leads to three possible alternative hypotheses: two paired associations ((*H. chimborazi*,"*S.*" *platensis*) *C. hyodon*) and ((*C. hyodon*,"*S.*" *platensis*) *H. chimborazi*), and a trichotomy. These imply that the ancestral separation of the three SA taxa might be either the result of two successive dichotomous branchings or of a single trichotomous branching event. The latter hypothesis would be consistent with the disjunct fossil distribution of the three SA gomphothere species. "*Stegomastodon*" *platensis* is shown to be not closely related to North American (NA) *Stegomastodon* Pohlig, 1912, supporting its removal from the latter genus. The NA species *Rhynchotherium* cf. *falconeri* Osborn, 1923 is placed as the sister taxon of SA gomphotheres, on the basis of four unequivocal characters. NA *Stegomastodon* and the Asian *Sinomastodon* Tobien, Chen & Li, 1986 form successive outgroups to the previous clade together with whom they form a monophyletic group which includes all the brevirostrine species considered, along with the "depressed-beaked" gomphothere *Rhynchotherium* Falconer, 1868. The results of the present phylogenetic analysis indicate a rather high level of homoplasy in the evolution of New World gomphotheres.

**KEY WORDS**
Mammalia,
Proboscidea,
Gomphotheriidae,
*Haplomastodon*,
*Stegomastodon*,
South America,
Ecuador,
Pleistocene,
osteology,
phylogeny.

**RÉSUMÉ**
*Anatomie de* Haplomastodon chimborazi *(Mammalia, Proboscidea) du Pléistocène supérieur de l'Équateur et ses implications sur la phylogénie et sur la systématique des gomphothères de l'Amérique du Sud.*
La révision du matériel du Pléistocène tardif de Bolivar, Équateur, associé à *Haplomastodon chimborazi* (Proaño, 1922), et sa comparaison avec les autres gomphothères trilophodontes du Nouveau Monde, fournissent des données morphologiques inédites permettant de développer une nouvelle hypothèse phylogénétique pour les proboscidiens d'Amérique du Sud (SA). *Haplomastodon* Hoffstetter, 1950 comprend une seule espèce SA dont le nom valide est *H. chimborazi*. Le taxon *H. waringi* (Holland, 1920), fondé sur l'étude d'un matériel non diagnostique, est considéré invalide. L'analyse cladistique soutient la monophylie des gomphothères SA (Cuvieroniinae) *H. chimborazi*, *Cuvieronius hyodon* (Fischer de Waldheim, 1814), et "*Stegomastodon*" *platensis* (Ameghino, 1888), définis par cinq caractères non ambigus. Des résultats contradictoires quant aux relations internes des gomphothères SA conduisent à trois hypothèses alternatives : deux paires exclusives ((*H. chimborazi*,"*S.*" *platensis*) *C. hyodon*) et ((*C. hyodon*,"*S.*" *platensis*) *H. chimborazi*)), ou une trifurcation. Elles impliquent que la séparation ancestrale des trois taxons SA serait le résultat, soit de deux branchements dichotomiques successifs, soit d'un unique évènement de trifurcation. La dernière hypothèse serait cohérente avec la distribution fossile séparée des trois espèces de gomphothères SA. "*Stegomastodon*" *platensis* n'apparait pas directement lié aux *Stegomastodon* Pohlig, 1912 nord-américains (NA), ce qui soutient son exclusion de ce genre. L'espèce NA *Rhynchotherium* cf. *falconeri* Osborn, 1923 se place en groupe frère des gomphothères SA, sur la base de quatre caractères non équivoques. Les *Stegomastodon* NA et *Sinomastodon* Tobien, Chen & Yuqing, 1986 asiatiques forment les groupes externes successifs du clade précédent avec lequel ils forment un groupe monophylétique qui inclut toutes les espèces brévirostres considérées, associées au gomphothère à symphyse mandibulaire inclinées vers le bas *Rhynchotherium* Falconer, 1868. Les résultats de l'analyse phylogénétique présente indiquent un niveau relativement élevé d'homoplasie au sein de l'évolution des gomphothères du Nouveau Monde.

**MOTS CLÉS**
Mammalia,
Proboscidea,
Gomphotheriidae,
*Haplomastodon*,
*Stegomastodon*,
Amérique du Sud,
Équateur,
Pléistocène,
ostéologie,
phylogénie.

## INTRODUCTION

South American (SA) gomphotheres have received extensive attention from vertebrate paleontologists for over 200 years, thanks in particular to the very rich fossil record from Ecuador, Bolivia, Chile, Brazil, and Argentina (see Hoffstetter 1952; Prado *et al.* 2005; and Ferretti 2008a for an overview). Despite this, many problems associated with the phylogeny, classification, and paleobiogeographic patterns of this proboscidean group still exist. Within SA gomphothere systematics, the taxonomic status of *Haplomastodon chimborazi* (Proaño, 1922) is a particularly contentious issue (Hoffstetter 1955; Simpson & Paula Couto 1957; Ficcarelli *et al.* 1995; Prado *et al.* 2005; Shoshani & Tassy 2005; Lucas 2008, 2009). In fact, both the validity of the species *H. chimborazi*, considered by some authors as a junior synonym of "*Mastodon*" *waringi* Holland, 1920 and that of the genus *Haplomastodon* Hoffstetter, 1950 as a distinct taxon from *Stegomastodon* Pohlig, 1912 have been questioned. The relationships between *H. chimborazi* and the other Pleistocene SA gomphotheres, *Cuvieronius hyodon* (Fischer de Waldheim, 1814) and "*S.*" *platensis* (Ameghino, 1888),

are still not completely resolved, though there is a general consensus in considering the three taxa as forming a monophyletic group (Hoffstetter 1952; Tobien 1973; Tassy 1985; Webb 1992; Shoshani 1996; Lambert & Shoshani 1998; Ferretti 2008a; Prado & Alberdi 2008). The phylogenetic relationships of SA gomphotheres with other gomphothere taxa (both from North America and Eurasia) is also problematic. In fact, it is questionable as to whether "*S*". *platensis* should be included in *Stegomastodon* which is otherwise an exclusively North American taxon (Madden 1984; Webb 1992).

The species name "*Masthodon*" *chimborazi* was based on a complete skeleton from the Late Pleistocene of Quebrada Chalán, near Punin, Chimborazo Province, Ecuador (Proaño 1922; Spillmann 1928) and was later selected by Hoffstetter (1950) as the type species of the new genus *Haplomastodon*. A second skeleton was discovered in 1928 at Quebrada Callihuaico, near Alangasi, Quito Province (Spillmann 1928; 1931). These two remarkable specimens were almost completely lost in a fire that destroyed part of the fossil collections of the University of Quito in 1929. Subsequently, *Haplomastodon* remains have been found from various other Ecuadorian sites, including both high plains and coastal localities (Hoffstetter 1952).

The principal works on the dental, cranial and postcranial anatomy of Ecuadorian *Haplomastodon* are those of Spillmann's (1928, 1931) and Hoffstetter's (1950, 1952). Little attempt was made by these authors at detailed comparison of skeletal features (especially cranial) with other gomphotheres, so that the phylogenetic information of the skeletal anatomy of *Haplomastodon* has remained largely unexplored. In 1991, fieldwork in Northern Ecuador by the Dipartimento di Scienze della Terra and Museo di Storia Naturale, Sezione di Geologia e Paleontologia of the University of Firenze, in collaboration with the Museo Ecuatoriano de Ciencias Naturales of Quito, and the Escuela Politecnica National of Quito, resulted in the discovery of new fossil vertebrate localities near Bolivar, Carchi province (Fig. 1; Ficcarelli *et al.* 1992, 1993). Two collecting sites in the Bolivar area (known as Quebrada Pistud and Q. Cuesaca, respectively) provided abundant material, mostly representing mylodonts and gomphotheres. In particular, an almost complete skeleton of *H. chimborazi* was retrieved from the Cangahua Formation at the Q. Pistud site.


FIG. 1. — Map of Ecuador, showing the location of the Bolivar area and of other Ecuadorian sites with *Haplomastodon chimborazi* (Proaño, 1922).

The Bolivar sample represents the most complete material of this species and is also, at present, the only sample suitable for a comprehensive diagnosis of this taxon which includes cranial, dental and postcranial elements, complemented by precise stratigraphic information. Ficcarelli *et al.* (1993, 1995) provided a general description of the skull, mandible, and atlas of the Bolivar skeleton.

The aim of this paper is to review the taxonomy of *Haplomastodon* and to provide a new comprehensive and detailed description of the dental and skeletal anatomy of *Haplomastodon chimborazi*. A comparative analysis of dental and osteological characters of American trilophodont gomphotheres is presented in order to develop a new phylogenetic hypothesis of New World gomphotheres, focusing on the South American taxa. The classification and taxonomy of South American proboscideans are thus discussed based on the results of the cladistic analysis.

## MATERIAL AND METHODS

The present description and revision of *Haplomastodon chimborazi* are based on the Bolivar sample (material kept at MECN). Observations made from other Ecuadorian *H. chimborazi* specimens, including the S. Elena sample (material kept at EPN) described by Hoffstetter (1952), were also integrated in the description, as they have details not preserved in the Bolivar material. Comparisons with the two specimens from Punin (holotype of *H. chimborazi*) and Alangasi, were based on the published descriptions and figures made by Proaño (1922), Spillmann (1928, 1931), and Osborn (1936). The individual from Punin had the M3 in use. The specimen from Alangasi was a young adult with both M1 and M2 in use and the M3 completely formed but yet unerupted. In the comparative analysis, dental and skeletal material of the following elephantoid taxa were studied (repository of directly studied material and published sources are indicated within brackets): *Mammut americanum* (Kerr, 1792) from North America (Late Pleistocene; AMNH, NHM); *Gomphotherium sylvaticum* Tassy, 1985 from Artenay, France (Early Miocene; MNHN; Tassy 1977); *Gomphotherium angustidens* (Cuvier, 1817) from Sansan, France (Middle Miocene; MNHN; Tassy 1985) and the Dinotheriensande, Germany (Middle Miocene; SMNS); *Gomphotherium productum* (Cope, 1875) from Clarendon, Texas (Late Miocene; AMNH; Osborn 1936); *Eubelodon morilli* Barbour, 1914 from Brown County, Nebraska (Late Miocene; AMNH; Osborn 1936); *Rhynchotherium edensis* Frick, 1921 from Mt Eden, California (Early Pliocene; AMNH; Osborn 1936); *Rhynchotherium* cf. *falconeri* Osborn, 1923 from Arizona (Late Pliocene; LVMNH; Miller 1990; Ferretti 2008a); *Cuvieronius hyodon* from Tarija, Bolivia (Late Pleistocene; MLP, MACN, MNHN, NMR; Boule & Thevenin 1920); "*Stegomastodon*" *platensis* from various localities of the Provinces of Buenos Aires and Entre Rios, Argentina (Late Pleistocene; MLP, MACN, NHM; Cabrera 1929); *Stegomastodon texanus* Osborn, 1924 (= *S. mirificus* Leidy, 1858, according to Savage 1955) from Llano Estacado, Texas (Late Pliocene; AMNH; Osborn 1936); *Anancus perimensis* (Falconer & Cautley, 1847) from Perim Island, India (Late Miocene; NHM); *Anancus arvernensis* (Croizet & Jobert, 1828) from Asti, Italy (Early Pliocene; MGT, MGB), and Valdarno Inferiore, Italy (Middle Pliocene; IGF); *Elephas maximus* Linnaeus, 1758 (Recent; ACM, MCZR, MNHN, MSNFZ, NHM); *Loxodonta africana* (Blumenbach, 1792) from various African localities (Recent; MNHN, MSNFZ, NHM). Data on the dental and skeletal anatomy of *Megabelodon lulli* Barbour, 1914, *Gnathabelodon thorpei* Barbour & Sternberg, 1935, *Sinomastodon intermedius* (Teilhard de Chardin & Trassaert, 1935), and *Sinomastodon hanjiangensis* Tang & Zong, 1987, were obtained from the following publications: Barbour (1914), Barbour & Sternberg (1935), Osborn (1936), Tobien (1973), Tobien *et al*. (1986) and Zong *et al*. (1989).

The Peruvian gomphothere *Amahuacatherium peruvium* Romero-Pittman, 1996 was not included in the analysis as the interpretation of its anatomy and age is still highly controversial (Campbell *et al*. 2000; Alberdi *et al*. 2004; Shoshani & Tassy 2005; Ferretti 2008a; Campbell *et al*. 2009).

The nomenclature of dental characters follows Tassy (1985, 1996a).

To test hypotheses about the phylogenetic relationships of New World gomphotheres, a parsimony analysis was performed based on the matrix shown in Appendix 7. The matrix consists 11 taxa and 24 characters (Appendix 6).

The 11 taxa analyzed in the cladistic analysis include representatives of all the trilophodont non-amebelodontine gomphothere genera recognized in North America by Lambert & Shoshani (1998) and the three South American taxa recognized by Prado *et al.* (2005) and Ferretti (2008a). The Old World brevirostrine gomphothere *Sinomastodon* Tobien, Chen & Li, 1986 was also included in the analysis as several authors consider this genus closely related to South American proboscideans (Tobien *et al*. 1986; Tassy 1990; Shoshani 1996; Prado & Alberdi 2008). Fifteen characters are taken or modified from previous studies (Tassy 1990; Shoshani 1996). Eleven are new characters. Polarity was defined by outgroup comparison using *G. angustidens* as outgroup. The analysis was performed using PAUP 4.0b10 (Swofford 2003). All 24 characters were weighted equally and treated as ordered (except for the multistate

character number 9). A set of exhaustive searches was conducted, implementing both the ACCTRAN (accelerated transfomation) and DELTRAN (delayed transformation) optimization criteria.

ABBREVIATIONS

*Institutions*

| | |
|---|---|
| ACM | Museo di Anatomia Comparata, Bologna; |
| AMNH | American Museum of Natural History, New York; |
| EPN | Escuela Politecnica Nacional, Quito; |
| IGF | Museo di Storia Naturale – Sezione di Geologia e Paleontologia, Firenze; |
| MCZR | Museo Civico di Zoologia, Roma; |
| MECN | Museo Ecuatoriano de Ciencias Naturales, Quito; |
| MGB | Museo di Paleontologia "G. Capellini", Bologna; |
| MGT | Museo di Geologia, Torino; |
| MICN | Museo de Historia Natural del Instituto de Ciencias Naturales, Universidad Central, Quito; |
| MLP | Museo de La Plata, La Plata; |
| MNHN | Muséum national d'Histoire naturelle, Paris; |
| MSNFZ | Muso di Storia Naturale (sezione di Zoologia), Firenze; |
| MUT | Museo Nacional Paleontologico-Arquelogico, Tarija; |
| NHM | Natural History Museum, London; |
| NMR | Swedish Museum of Natural History, Stockholm; |
| SMNS | Staatlichen Museum Naturkunde, Stuttgart; |
| UCE | Universidad Central de Ecuador, Quito; |
| UCMP | University of California, Museum of Paleontology, Berkeley. |

*Anatomy*

| | |
|---|---|
| C | cervical vertebra; |
| DP | upper deciduous premolar; |
| dp | lower deciduous premolar; |
| I | upper incisor (tusk); |
| L | lumbar vertebra; |
| M | upper molar; |
| m | lower molar; |
| Mc | metacarpal; |
| Mt | metatarsal; |
| T | thoracic vertebra. |

## GEOLOGY AND TAPHONOMY OF THE BOLIVAR GOMPHOTHERE SITE

The Cangahua Formation is a Late Pleistocene loess-like pyroclastic unit, deposited under periglacial conditions, present in the interandean depression of northern Ecuador (Sauer 1965; Ficcarelli *et al.* 1992; Coltorti *et al*. 1998). It yielded abundant vertebrate remains, including articulated skeletons of large mammals (Hoffstetter 1952). At Quebrada Pistud (Bolivar), two main vertebrate-rich levels and other minor ones were recognized in the Cangahua sequence. The lower and upper main fossiliferous levels, consisting of torrential stream sediments, were dated to 18 720±90 and 12 350±70 y respectively, on the base of radiometric analysis of bone carbonate (Coltorti *et al.* 1998). Both ages are consistent with the biochronological interpretation of the fauna from this site, which indicates a Lujanian age (Ficcarelli *et al.* 1992; 1993; 1997).

The *H. chimborazi* skeleton was recovered from the lowermost main fossiliferous bed, in an area of about 5 m$^2$. It consists of the cranium, mandible and 68 postcranial elements (Table 1).

Different catalogue numbers were given to the various skeletal elements of this individual as they were collected during successive excavations. Nevertheless, in the following description the skeleton will be referred to as individual "MECN 82".

Some of the bones of MECN 82 were in anatomical connection (e.g., right humerus and ulna), position of other parts, when not in anatomical connection, was however anatomically coherent. The skull was lying on its dorsal part on the first cervical vertebrae, the mandible was in front of the skull. Bone disposition indicates that the animal was decomposed *in situ* and that the skeleton was only slightly displaced by a current responsible of the skull upturning and mandible disarticulation. Bones do not show any sign of butchering nor carnivore tooth marks.

The exploited area at Q. Pistud, some tens of square meters, allowed recovery of 160 proboscidean elements, representing at least seven individuals, including the MECN 82 skeleton. Vertebrae and ribs are the most abundant elements. Smaller elements (sesamoids, phalanges) are somewhat underrepresented, indicating a certain size bias. On the other hand, large but fragile parts, as skulls, scapulae and pelvis are extremely rare. Finally, elements of the anterior limbs are slightly more abundant than that of the posterior ones.

## TAXONOMY OF ECUADORIAN GOMPHOTHERES

The complex taxonomy of Ecuadorian gomphotheres has been revised by Hoffstetter (1950, 1952, 1955), Simpson & Paula Couto (1957) and Ficcarelli *et al.* (1993, 1995; see Ferretti 2008a and Lucas 2008 for an overview). In this section, we shall discuss the taxonomy and nomenclature of those specimens from Ecuador allocated by Hoffstetter (1952) to *Haplomastodon*.

### *Haplomastodon chimborazi*

In 1894, J. F. Proaño reported the discovery of a partial proboscidean skeleton at Quebrada de Chalán, a small gorge near Punin (Chimborazo Province, Central Ecuador), providing a summary description and pictures of the skull and mandible (Arauz 1950; Costales 1950; Hoffstetter 1952). The author referred to the specimen as "Mastodonte del Chimborazo", considering it a new, exclusively South American taxon. Proaño (1894) mentioned as distinctive characters of the Punin gomphothere, distinguishing it from the other species known from the Andean highplains, i.e. *Mastodon andium* Cuvier, 1824 (= *Cuvieronius hyodon* Fischer de Waldheim, 1814), the higher cranium and the more massive upper tusks with converging tips and no enamel band.

Elements of the Punin skeleton, namely the skull, the atlas, a humerus and other postcranials, were then figured in an anonymous paper published in the French magazine *Cosmos* in 1903 (Hoffstetter 1952).

The species name "*Masthodon*" *chimborazi* was first published by Proaño in 1922.

The fact that the name appeared in the caption of a picture of the Punin skull in an unpaged leaflet inserted in a religious tract (see Arauz 1950 and Hoffstetter 1952), has led some authors to question the adequacy of Proano's publication to the purpose of zoological nomenclature. However, the work by Proaño meets all the criteria set by the ICZN code (ICZN 1999) to be regarded as published and therefore the species name "*M.*" *chimborazi* should be considered as valid, within the meaning of the *Code*.

Spillmann (1931), in his review of the Pleistocene mammals from Ecuador, provided a new description of the Punin skull, based on data and photographs taken before the specimen was destroyed in 1929. He referred this specimen to *Bunolophodon ayora* Spillmann, 1928, a specific name he had previously created for the Punin skeleton (Spillmann, 1928), completely disregarding Proaño's species. In the same paper, Spillmann named a nearly complete skeleton from Q. Callihuaico near Alangasi (Quito Province) as *B. postremus* Spillmann, 1931. Hoffstetter (1950, 1952, 1955) revised all the gomphothere material from Ecuador then known. The author concluded that the Punin and Alangasi gomphotheres were conspecific and that the specific name "*M.*" *chimborazi* had priority over Spillmann's *B. ayora* and *B. postremus*. Hoffstetter (1950) created the new name *Haplomastodon* as a subgenus of *Stegomastodon* to accommodate "*M.*" *chimborazi* (Hoffstetter 1950). Later, based on the presence/absence of transverse foramina on the atlas and axis, Hoffstetter (1952) established a full generic separation of *Haplomastodon* (atlas without foramina) from *Stegomastodon* (atlas and axis with foramina) and based the separation of the former into the two subgenera *Haplomastodon* (axis lacks the foramina) and *Aleamastodon* Hoffstetter, 1952 (axis with foramina). The latter subgenus was established on material from the S. Elena peninsula, on the southern coast of Ecuador, and attributed to the new species *H.* (*Aleamastodon*) *guayasensis* Hoffstetter, 1952. Simpson & Paula Couto (1957), based on a larger *Haplomastodon* sample from Aguas do Araxà (Brazil) demonstrated that the absence/presence of transversal foramina in the first and second cranial vertebrae is a variable character in this genus. They considered therefore *H. guayasensis* as a junior synonym of *Haplomastodon chimborazi*. On the other hand, Simpson & Paula Couto (1957), following Hoffstetter's (1950) original diagnosis, accepted *Haplomastodon* as a valid genus distinct from *Stegomastodon*. Based on the comparison of the Ecuadorian and Brazilian material referred to *Haplomastodon*, Simpson & Paula Couto (1957) concluded that this represents one and the same species and that the nominal taxon "*Mastodon*" *waringi* Holland, 1920, a species based on a Brazilian type

TABLE 1. — *Haplomastodon chimborazi* (Proaño, 1922) from Bolivar, Ecuador. List of skeletal elements of individual MECN 82.

| Element | Catalogue number | Element | Catalogue number |
|---|---|---|---|
| skull | MECN 82 | right humerus | MECN 95 |
| mandible | MECN 133 | left humerus | MECN 100 |
| atlas | MECN 83 | right ulna | MECN 134 |
| axix | MECN 84 | left ulna | MECN 418 |
| C3 | MECN 85 | right radius | MECN 210 |
| C5 | MECN 102 | left radius | MECN 421 |
| C6 | MECN 94 | right unciform | MECN 216 |
| C7 | MECN 403 | right magnum | MECN 217 |
| T2 | MECN 404 | right pyramidal | MECN 219 |
| T3 or T4 | MECN 405 | left scaphoid | MECN 428 |
| T4 or T5 | MECN 406 | left trapezoid | MECN 429 |
| T6 or T7 | MECN 407 | left lunar | MECN 427 |
| T7 or T8 | MECN 408 | left pisiform | MECN 426 |
| T9 or T10 | MECN 135a | right Mc3 | MECN 218 |
| T11 or T12 | MECN 135b | right Mc4 | MECN 220 |
| T12 or T13 | MECN 135c | right Mc5 | MECN 221 |
| T13 or T14 | MECN 214 | pelvis | MECN 415 |
| T16-lastT | MECN 177 | right femur | MECN 420 |
| T16-lastT | MECN 211 | left femur | MECN 98 |
| L1 | MECN 101 | right patella | MECN 90 |
| L3 | MECN 113 | right tibia | MECN 99 |
| L4 | MECN 106 | left tibia | MECN 424 |
| sacrum | MECN 107 | right fibula | MECN 423 |
| caudal | MECN 436 | left fibula | MECN 422 |
| caudal | MECN 435 | right astragalus | MECN 425 |
| caudal | MECN 87 | right Mt1 | MECN 434 |
| 1st left rib | MECN 409 | right Mt4 | MECN 430 |
| 1st right rib | MECN 410 | left Mt3 | MECN 432 |
| 9 ribs | MECN 91, 92, 93, 207, 208, 411, 412, 457, 470 | left Mt4 | MECN 431 |
| right scapula | MECN 82 | phalanx | MECN 89 |
| left scapula | MECN 82 | left phalanx | MECN 433 |

specimen (see below), has priority over "*Masthodon*" *chimborazi* Proaño, 1922. Simpson & Paula Couto (1957) treated then *Haplomastodon waringi* (Holland, 1920) as the type species *Haplomastodon*, contrary to the rule of the *Code* (Lucas 2008, 2009). Hoffstetter (1955, 1986), however, strongly questioned the validity of Holland's species, considering it as a *nomen dubium*. Ficcarelli *et al.* (1993), based on new material from Bolivar, demonstrated that Ecuadorian *Haplomastodon* display a variability in the presence/absence of transverse foramina similar to that known in the Aguas do Araxà population. Following Hoffstetter (1955), they accepted the validity of the species name *H. chimborazi* over "*M.*" *waringi*. However, considering that the type material, in particular the skull, of the former species was lost, Ficcarelli *et al.* (1995) proposed as neotype of *H. chimborazi* the complete skeleton from Q. Pistud, Bolivar. More recently, Lucas (2009) presented a case to the International Commission on Zoological Nomenclature to conserve the usage of the name *Mastodon waringi* by designating as neotype the Bolivar specimen. As noted by Lucas (2009), *H. chimborazi* would still retain its status as the type species of *Haplomastodon* under the rules of the *Code*. The usage of the name *H. waringi* is indeed far more widespread in the literature, after the systematic revison of Simpson & Paula Couto (1957). To note, however, is that, contrary to common opinion, the type skeleton of *H. chimborazi* was not completely lost in the 1929 fire of the Quito University. Hoffstetter (1952: 195) mentioned in fact an atlas and two humeri (left and right), then housed in the collection of the UCE, as probably

representing what was left of the type specimen of *H. chimborazi* described by Proaño (1922). The left and right humeri are currently kept at the MICN (catalog numbers MICN-UCE 1982 and 1981, respectively), along with other post-cranial material from Punin (T. Gordón pers. comm.). The atlas, however, is not among the MICN gomphothere material. Though this specimen might probably be in other collections of the UCE, it has not yet been located by the author.

The two humeri housed at the MICN still bear an old label reporting the site of provenance (Chalán, Punin). Indeed, a comparison with the published figures of the Punin skeleton leaves no doubt that the two humeri pertain to the type specimen of *H. chimborazi*. For these reasons, the proposal of Ficcarelli's *et al.* (1995) and Lucas (2009) to designate the Bolivar skeleton as the neotype of the species is not valid according to the *Code* (Ferretti 2009).

Alberdi & Prado (1995), accepted the synonymies and species-level nomenclature proposed by Simpson & Paula Couto (1957), but included *waringi* within *Stegomastodon*, considering *Haplomastodon* a junior synonym of the former.

Based on new character information and on the results of the cladistic analysis presented here, *Haplomastodon* is conservatively considered a valid genus, characterized by two autapomorphic features, with respect to both "*Stegomastodon*" *platensis* and the North American (NA) representatives of the genus.

### Status of "*Mastodon*" *waringi*

The type series of the species is from Pedra Vermelha, Bahia (Brazil). Holland (1920) did not figure the material, providing only a general description of the remains that does not distinguish "*M.*" *waringi* from other similar taxa. The surviving material consists of the tip of a tusk, a tusk dentine fragment, three molar fragments, and the distal end of a tibia, representing at least two individuals (Simpson & Paula Couto 1957; Ficcarelli *et al.* 1995; Ficcarelli pers. comm.; Lucas 2008, 2009). The remains are too poorly preserved to provide any useful systematic information. Thus, "*M.*" *waringi* should be effectively considered as a *nomen dubium*.

### Nomenclature

The taxonomic evidence outlined above leads to the following conclusions concerning the nomenclature of Ecuadorian gomphotheres:

– the species "*M.*" *chimborazi* is valid, as the original description and available published figures of the type skeleton from Punin, clearly distinguish it from other similar brevirostrine gomphotheres. The left and right humeri, and possibly the atlas (not found yet among the UCE collections) represent what is left of the type skeleton described by Proaño (1922);

– *Haplomastodon chimborazi* is characterized by a set of autapomorphic characters that distinguish it from both SA and NA *Stegomastodon* species (see below). It is thus proposed that the generic name *Haplomastodon* is retained, with *Haplomastodon chimborazi* as the only species;

– *Bunolophodon ayora* (sometimes spelled *ayorae* in later papers) is a junior objective synonym of *H. chimborazi*;

– *Bunolophodon postremus* and *H. guayasensis* are junior subjective synonyms of *H. chimborazi*;

– "*Mastodon*" *waringi* is a *nomen dubium* because it is based on undiagnostic material.

It should be kept in mind, however, that such a treatment has no formal standing until ratified by the ICZN.

## SYSTEMATICS

Order PROBOSCIDEA Illiger, 1811
Superfamily Elephantoidea Gray, 1821
Family Gomphotheriidae Hay, 1922

Genus *Haplomastodon* Hoffstetter, 1950

Type species. — *Masthodon chimborazi* Proaño, 1922 by monotypy.

Diagnosis. — As for the only species *H. chimborazi*, see Revised diagnosis below.

### ***Haplomastodon chimborazi*** (Proaño, 1922)

Mastodonte del Chimborazo Proaño, 1894: unnumbered page.

*Mastodon waringi* Holland, 1920: 229, *nomen dubium.*

*Masthodon chimborazi* Proaño, 1922: unnumbered page.

*Tetrabelodon ayora* Spillmann, 1928: unnumbered page preceding p. 70.

*Bunolophodon ayorae* (Spillmann, 1931): 67.

*Bunolophodon postremus* Spillmann, 1931: 73.

*Cuvieronius ayora* – Osborn 1936: 567.

*Cuvieronius postremus* – Osborn 1936: 595.

*Haplomastodon* (*Haplomastodon*) *chimborazi* – Hoffstetter 1952: 192.

*Haplomastodon* (*Aleamastodon*) *guayasensis* Hoffstetter, 1952: 208.

*Haplomastodon waringi* – Simpson & Paula Couto 1957: 171.

*Haplomastodon waringi* – Ficcarelli *et al.* 1993: 233. — Casamiguela *et al.* 1996: 316.

*Stegomastodon waringi* – Alberdi & Prado 1995: 283. — Alberdi *et al.* 2004: 433. — Prado & Alberdi 2005: 4. — Prado & Alberdi 2008: 905.

HOLOTYPE. — A nearly complete adult skeleton of which only the right (MICN-UCE 1981) and left (MICN-UCE 1982) humeri are now preserved.

OTHER MATERIAL EXAMINED. — See Tables 1-19.

ORIGINAL DIAGNOSIS. — Gomphothere with high-domed cranium; upper tusks massive, with converging tips, lacking an enamel band (Proaño 1922). Hoffstetter (1952) listed the following diagnostic characters of *Haplomastodon chimborazi*: 1) cranium high, elephant-like; 2) mandible with short symphysis (brevirostrine); 3) atlas and axis lack transverse foramina; 4) lower tusks absent; 5) upper tusks are relatively short, upturned with no torsion; 6) enamel band present in some juvenile tusks, never at adult age; 7) molars show slight tendency to anancoidy (displacement of buccal and lingual half-lophs); 8) posttrite central conules absent to poorly developed; 9) third molar tetra- to pentalophodont.
Characters 1, 2, 4, and 7 are shared with "*Stegomastodon*" *platensis*, whilst characters 3, 8 and 9 have a wider distribution within SA gomphotheres, with character 3 showing intraspecific variability. Characters 5 and 6 are derived relative to the condition in *Cuvieronius hyodon*. The phylogenetic significance of these two latter characters, in particular concerning the relationships between *Haplomastodon* and SA "*Stegomastodon*" will be discussed below.

REVISED DIAGNOSIS. — Medium to large brevirostrine gomphotheriid of trilophodont grade that differs from other South American gomphotheres by the presence of relatively short, massive and upwardly curved upper tusk, which always lacks an enamel band in the adult growth stage, and in possessing only slightly divergent tusk alveoli in the premaxillaries. In addition, *H. chimborazi* has a unique combination of the following characters: 1) high, elephantine skull; 2) inflated frontals and parietals forming sagittaly a wide fronto-parietal plane; 3) anterior border of bony orbit laying forward of the mesialmost cheek tooth in use; 4) nasal aperture wide and shallow, separated by a thin bony lamina from a deep subnasal fossa; 5) supraorbital foramen of maxillary absent; 6) alveolar portion of premaxillaries relatively long and robust; 7) presence of a shallow fossa for muscular insertion (lateral coronoid fossa) at the base of the ascending ramus of the mandible; 8) position of the mandibular foramen on the medial side of the ascending ramus markedly higher than the occlusal plane; 9) transversal foramina of the first and second cervical vertebrae with tendency to obliterate; 10) dorsal arch of atlas very thick, with strong dorsal concavity; 11) large and robust ventral tubercle of transverse process of atlas; 12) lower tusks absent; 13) DP3/dp3 trilophodont; 14) P3-P4/p3-p4 absent; 15) M3 with fully developed tretraloph; m3 with 4 to 5 lophids; 16) posttrite central conules (forming secondary trefoils under wear) absent to weakly developed.

Character 1, is shared with "*S.*" *platensis*. Characters 2-10 and 12-15 are shared with both "*S.*" *platensis* and *C. hyodon*, whilst character states 11 and 16 are as in *C. hyodon*.

TYPE LOCALITY. — Quebrada de Chalán near Punin, Chimborazo province, Central Ecuador (Proaño 1922; Hoffstetter 1952).

TYPE HORIZON. — No stratigraphic data were provided by Proaño (1894, 1922). Recent geological investigations in the Punin area, however, indicate that the sedimentary sequence cropping out at Quebrada Chalán is part of the Late Pleistocene Cangahua Formation and contains a typical Lujanian fauna (Ficcarelli *et al.* 1997; Coltorti *et al.* 1998). A radiometric dating of bone carbonate from mammalian fossil remains newly collected from Q. Chalán gave an age of 20 980±530 years BP (Coltorti *et al.* 1998).

OCCURRENCE. — Late Pleistocene to earliest Holocene (Ficcarelli *et al.* 2003; Coltorti *et al.* 1998). Ecuador: it is distributed both in the Andean provinces (Carchi, Pichincha, Chimborazo) and on the coast (Santa Elena Peninsula, Guayas province). Remains referable to this species have been collected from many other sites in South America, including Brazil (Simpson & Paula Couto 1957), Colombia, Venezuela (Hoffstetter 1986), and Peru (Alberdi *et al.* 2004).

TABLE 2. — *Haplomastodon chimborazi* (Proaño, 1922) from Bolivar, Ecuador. Measurements (in mm) of the skull (see Appendix 1).

| Measures | Specimen MECN 82 |
|---|---|
| 1. Total length: akrokranion-prosthion | 930 |
| 2. Akrokranion-rhinion (base of nasal aperture) | 270 |
| 3. Tusk alveolus length | 590 |
| 4. Length of zygomatic arch | 450 |
| 5. Greatest breadth of neurocranium | *c.* 780 |
| 6. Diameter between most lateral points of orbital processes of frontals | *c.* 550 |
| 7. Breadth of tusk alveoli between infraorbital foramina | 422 |
| 8. Greatest breadth of tusk alveoli | 515 |
| 9. Maximum dorso-ventral diameter of tusk alveoli | 213 |
| 10. Greatest length of occipital condyle | 110 |
| 11. Transversal diameter of occipital condyle | 75 |

## ANATOMICAL DESCRIPTION AND COMPARISONS

### *Cranium (Figs 2-5; Table 2)*

The description of the cranium of *H. chimborazi* is mainly based on the study of the Bolivar specimen (MECN 82). Additional data were obtained from Spillmann's (1928, 1931) description and figures of the Punin (Fig. 2) and Alangasi skulls. Though these three specimens are at slightly different ontogenetic stage (see the Material and methods section), they represent adult individuals as in all of them the M3 is completely formed. The skull of the Bolivar skeleton suffered a dorso-ventral crushing of the neurocranium and a distortion that altered in part the orientation of the distal end of the premaxillaries, that of the right tusk, and of the molars along the tooth row (see below). The Punin and Alangasi skulls were, on the other hand, in good state of preservation. Unfortunately, some aspects of these skulls were not figured before they were lost, so we have a partial knowledge of their morphology. Of the Punin skull only the left lateral aspect was figured by both Proaño (1894, 1922) and Spillmann (1928, 1931). Of the Alangasi skull the anterior, antero-lateral and ventral aspects were figured by Spillmann (1931).

**Antero-dorsal view (Figs 3A, B; 4A).** The parietal bones are transversally expanded and dorsally form two small bulges separated by a sagittal depression. The forehead (fronto-parietal plane) is wide, sagittally convex, and transversely flat. The temporal lines are very faint and smooth postero-ventrally. The postorbital process of the frontal bone is relatively small. The nasals are bounded posteriorly by a sulcus for the attachment of the *m. maxillo labialis* (levator of the trunk), marking the limit between the nasals and the frontals. The sulcus is shallow medially and deeper laterally. It continues laterally into the nasal process of the premaxillary bone, along the limit between the premaxillary and frontal. Rostrally, the nasals constitute the dorsal limit of the external nasal aperture. The nasal processes are very small. The external nasal aperture is wide and low (Fig. 4A). The dorsal margin, formed by the nasals and the nasal processes of the premaxillaries, is thick, forming a step-like border. Laterally, the nasal aperture is delimited by the nasal processes of the premaxillaries. The thickness of the lateral border of the nasal aperture rapidly decreases ventrally. The ventral border, made up by the body of the premaxillary, is not very distinct. The lateral and dorsal inner walls of the nasal aperture do not show any opening communicating with the paranasal sinuses, or with the lacrimal conduct. Medially, just below the ventral margin of the nasal aperture is a fossa that deepens into the body of the premaxillary (Fig. 4A). This structure, here called the *sub-nasal fossa*, is contiguous anteriorly with the incisive fossa, from which it is clearly distinct. The alveolar processes of the premaxillaries, bearing the alveoli for the tusks, are long and very robust. In particular, the distal anterior margin is very thick. Seen in anterior view, the tusk alveoli only slightly diverge distally. The maximum distal width of the premaxillaries do not exceed the diameter between the orbital processes of the frontals. The *incisura dentalis* only slightly separates distally the two premaxillaries.

**Lateral view (Figs 2; 5A, B).** In lateral view, the outline of the cranial vault is regularly convex (Punin skull; Fig. 2). The skull vertex is on the perpendicular passing just behind the tuber maxilla. The orbits are large, with their anterior margin laying at the front of the mesial-most molar. The proximo-distal axis of the tusk alveoli is parallel to the plane of the forehead, and forms a wide open angle with the occlusal plane. The dorsal side of the alveolar processes of the premaxillaries is longitudinally concave.

The maxillary bones have a single large orbital perforation, ventral to the orbit, corresponding to the infraorbital foramen. The foramen is oval-shaped and relatively large, with a maximum diameter comparable to that of extant *Loxodonta africana*. The infraorbital process of the maxillaries, forming the lateral wall of the infraorbital foramen, is thick and antero-posteriorly expanded. The zygomatic arch is deep and robust. The anterior half of the zygomatic is deep, with a straight dorsal margin. On the ventral margin, is a slightly concave surface, possibly representing the origin of the *m. masseter*. A marked step separates dorsally the anterior half of the zygomatic from the shallower posterior portion (*pars temporalis*), whose dorsal side is occupied by the elongated articular surface for the zygomatic process of the temporal. The zygomatic ends posteriorly in a small tuberosity.

**Posterior view (Fig. 3C).** The dorso-ventral crushing of the MECN 82 cranium caused the posterior tilting of the occipital squama. Dorsally and laterally, the occipital squama is bounded by the nuchal crest. The latter is a thick and markedly wrinkled crest, evidence of a powerful dorsal nuchal musculature (*m. splenius capits* and *m. semispinalis capitis*). Viewed from behind and slightly from above, the cranium shows two lateral swellings separated by a median depressed area at the bottom of which is the nuchal fossa.

**Ventral view (Fig. 3D).** Because of the post-mortem crushing, the occipital and basicranial regions of the Bolivar cranium are quite damaged preventing a detailed anatomical description. Anterior to the condyles is the stoutly built basilar process (basiocipital). Along its lateral margins are two contiguous depressed areas, likely representing the area for insertion of the *m. rectus capitis ventralis* and *m. longus capitis*. The auditory bullae are not preserved, except for the anterior portion of the right one, represented by a thin bony lamina (muscular process). Anterior and lateral to the muscular process is an aperture here interpreted as the *foramen lacerum orale* (= *foramen lacerum medium* + *foramen ovale*; Eales 1928). Anterior and lateral to the basioccipital are, on both sides, the pterygoid processes of the sphenoids, extending to the palatine region.

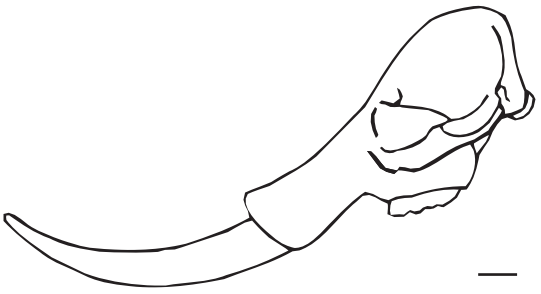

FIG. 2. — Diagrammatic representation of the skull of *Haplomastodon chimborazi* (Proaño, 1922) from Q. Chalán, Punin, Ecuador (holotype, now destroyed), left lateral view (based on Spillmann 1931). Scale bar: 10 cm.

The angle between the plane of the basicranium and the occlusal plane in *H. chimborazi* is greater than in *G. angustidens* and *G. productum*, approaching the condition in *L. africana*. The articular-mastoid region is characterized by the stout zygomatic process of the temporal and by its auricular part. The area posterior to the articular fossa is not preserved in the Bolivar skull, so it is not possible to control the occurrence of a retroarticular fossa (present in elephants and stegodonts, and absent in primitive gomphotheres and in mammutids; Tassy 1985).

The palate is relatively long and narrow. Sagittally there is a prominent *crista palatina*. Lateral to the palatine crista, on both sides, are two sulci deepening posteriorly. No palatine foramina are discernable in both the MECN 82 and Alangasi skull. Both the palatine crista and the palatine sulci gradually weaken and eventually disappear anteriorly. The palatines reach posteriorly and laterally the pterygoid processes at the contact with the sphenoids, where they


FIG. 3. — *Haplomastodon chimborazi* (Proaño, 1922) from Q. Pistud, Bolivar, Ecuador, skull (MECN 82): **A**, cranium, anterior view; **B**, cranium (cast), antero-dorsal view (tusks have been removed); **C**, cranium and mandible, posterior view; **D**, cranium (cast), ventral view. Abbreviations used in Figures 3-5: **eam**, external acustic meatus; **ena**, external nasal aperture; **FR**, frontal; **id**, incisura dentalis; **if**, infraorbital foramen; **inf**, incisive fossa; **ipm**, infraorbital process of maxillary; **MX**, maxillary; **M2**, second upper molar; **M3** third upper molar; **mf**, mandibular fossa; **NA**, nasal; **nc**, nuchal crest; **nf**, nuchal fossa; **npp**, nasal process of premaxillary; **o**,opening on the internal lateral face of the nasal aperture, leading to perinasal fossae; **OC**, occipital; **occ**, occipital condyle; **PA**, parietal; **PM**, premaxillary; **ppf**, post-orbital process of frontal; **snf**, subnasal fossa; **TE**, temporal; **zpm**, zygomatic process of maxillary; **zpt**, zygomatic process of temporal. Scale bar: 10 cm.

form a stout protuberance. The posterior border of the palatines lays well behind the distal end of the posteriormost molar (MECN 82, Alangasi skull). In MECN 82, the left and right dental rows diverge at the level of the distal-most and yet non completely erupted molar (M3) to became parallel to each other

at the level of the molars in use (M2). Medial to the mesial-most molar (M2) originates, on both side, the interalveolar crest. The two interalveolar crests diverge anteriorly so that their anterior ends are well separated from one another.

**Discussion.** Compared to *Gomphotherium angustidens* and *G. productum*, *H. chimborazi* is more derived in possessing larger and more robust premaxillaries, whose dorsal face is slightly upwardly concave, a wider and more rounded forehead, and a more pronounced pneumatization of the bones forming the dorsal, lateral, and posterior walls of the braincase, which produces a moderate lateral swelling of the parieto-occipital bulges. These characters are also present in *Rhynchotherium* cf. *falconeri* (LVNHM 871; Ferretti 2008: fig. 3), as well as in the other American brevirostrine gomphotheres considered (i.e. *Stegomastodon texanus*, *C. hyodon*, and "*S.*" *platensis*). *Sinomastodon hanjiangensis*, the only species of this Old World brevirostrine gomphothere genus whose cranial morphology is sufficiently well-known (Zong *et al*. 1989), possesses a similar derived morphology of the neurocranium, while retaining a primitive premaxillary morphology. *Haplomastodon chimborazi* and the other brevirostrine gomphotheres considered are derived with respect to *G. angustidens* and *G. productum* in having the anterior margin of the orbit laying just at the front of the mesial end of the tooth row. The more forward position of the orbit in the brevirostrine forms with respect to the condition in *G. angustidens* and other longirostrine gomphotheres (e.g., *Eubelodon morilli*, *R.* cf. *falconeri*), is correlated to a modification of the skull toward a more "elephant-like" morphology, characterized by a relatively higher, vertically tilted, and more for-aft compressed cranium than that of primitive gomphotheres. Such derived skull shape is likely linked to the development of a large proboscis, and evolved in parallel in other elephantoid lineages, such as Elephantidae Gray, 1821 and Stegodontidae Hopwood, 1935. Another derived character of the skull of *H. chimborazi* with respect to primitive gomphotheriids, is the absence of a supraorbital foramen. This last character is shared, among American gomphotheres, with *R.* cf. *falconeri*, *C. hyodon* (Tarija sample), and "*S.*" *platensis* (MLP 8-1, MLP

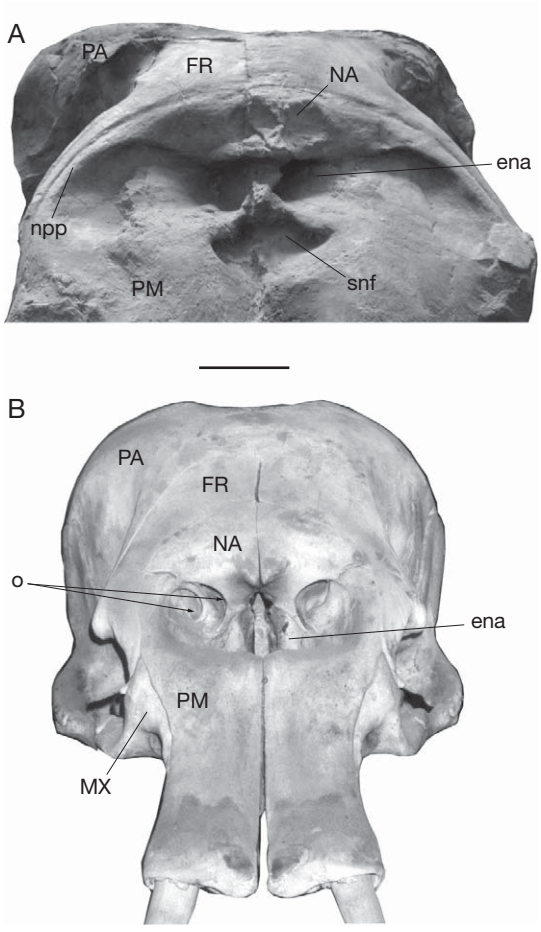


Fig. 4. — Anterior view of skull, showing anatomical details of the anterior nasal aperture: **A**, *Haplomastodon chimborazi* (Proaño, 1922) from Q. Pistud, Bolivar, Ecuador (MECN 82); **B**, *Elephas maximus* Linnaeus, 1758 (Recent; MCZR). Abbreviations: see Figure 3. Scale bar: 10 cm.

8-3). It is noteworthy that *Stegomastodon texanus* (AMNH 10622) retains a well-defined supraorbital foramen (Osborn 1936). On the basis of the figures provided by Zong *et al.* (1989), *Sinomastodon hanjiangensis* seems also to possess a supraorbital foramen. *Haplomastodon chimborazi* shares with "*S.*" *platensis* similarly large and robust premaxillaries, but in the latter (skulls MLP 8-1 and NHM M-19951) these are relatively shorter and distally wider than in *Haplomastodon*. In these characters, "*S.*" *platensis* appears morphologically intermediate between *C. hyodon*, that possesses extremely flaring

TABLE 3. — *Haplomastodon chimborazi* (Proaño, 1922) from Bolivar, Ecuador. Measurements (in mm) of the mandible (see Appendix 1).

| | Specimen/site | | |
|---|---|---|---|
| **Measures** | MECN 82 Q. Pistud | MECN 437 Q. Pistud | MECN 147 Q. Quesaca |
| 1. Length: most aboral margin of condyle-infradentale | 765 | – | – |
| 2. Length: gonion caudale-infradentale | *c.* 740 | – | – |
| 3. Length: infradentale-most oral point of the anterior margin of the ascending ramus | 523 | – | – |
| 4. Length: infradentale-anterior origin of ascending ramus | 450 | – | – |
| 5. Length: infradentale-oral border of m2 | 210 | 175 | – |
| 6. Length: gonion caudale-oral border of m2 | 590 | – | – |
| 7. Length: oral border of m2-anterior origin of ascending ramus | 270 | 270 | – |
| 8. Length: gonion caudale-most oral point of the anterior margin of the ascending ramus | 239 | – | – |
| 9. Horizontal antero-posterior diameter of symphysis projection in sagittal plane | 169 | – | – |
| 10. Oral height of ascending ramus: gonion ventrale-corion | *c.* 316 | – | – |
| 11. Aboral height of ascending ramus: gonion ventrale -heighest point of condyle | 473 | – | – |
| 12. Height of the mandible body at midpoint of the cheektooth row | 154 | 155 | 135 |
| 13. Greatest thickness of the mandible body at midpoint of cheektooth row | 110 | 125 | 139 |
| 14. Maximum breadth between interalveolar crests | 105 | – | – |
| 15. Breadth between the most lingual points of the trigoni retro-molari | 235 | – | – |
| 16. Breadth between anterior margin of ascending rami | 430 | – | – |
| 17. Breadth between most lateral points of the condyles | 570 | – | – |
| 18. Mandibular breadth: gonion laterale-gonion laterale | 478 | – | – |
| 19. Transverse diameter of condyle | 141 | – | – |
| 20. Antero-posterior diameter of condyle | 54 | – | – |

premaxillaries, distally divided by a deep and wide incisura, and *H. chimborazi*. The configuration of the external nasal aperture of *H. chimborazi*, with the occurrence of a deep sub-nasal fossa, differs from the condition seen in *Mammut americanum*, *G. angustidens*, *G. productum*, *Anancus* Aymard, 1855 and elephantines, whereas it is shared by *R.* cf. *falconeri*, *C. hyodon*, and "*S.*" *platensis* (MLP 8-1, MLP 8-3, NHM M-19951). The wide external nasal aperture, the evidence for a strong trunk musculature, and the large infraorbital foramen indicate that *H. chimborazi* possessed a well-developed, elephant-like proboscis.

*Mandible (Figs 3C; 5A; 6; Table 3)*

The mandibular corpus is relatively long and its labial side is moderately inflated. The corpus becomes deeper anteriorly at the level of the posterior mental foramen. The symphyseal portion is short ("brevirostrine"), massive, with no tusk or vestigial tusk alveoli (Fig. 6A-C). In MECN 82, on the labial side, there are three mental foramina: the most posterior one is the largest and is positioned at the level of mesial root of the m2 (Fig. 6D). The ascending ramus is slightly posteriorly inclined. Its anterior and posterior borders are parallel to one another. The posterior margin of the ramus is straight. It continues dorsally into the condylar process. This is dorso-caudally directed and bears a large and transversely elongated condyle. In anterior view, the condyle is very slightly medially inclined (Fig. 6B). The coronoid process is significantly lower than the condyle. On the lateral side of the ramus, there is a deep masseteric fossa, dorsally positioned, just below the sigmoid incisure (Fig. 6D). The posteroventral margin of the


FIG. 5. — *Haplomastodon chimborazi* (Proaño, 1922) from Q. Pistud, Bolivar, Ecuador, skull (MECN 82); **A**, cranium and mandible in right lateral view; **B**, cranium in left lateral view; **C**-**E**, right molar in medial, lateral, and anterior views. Abbreviations: see Figure 3. Scale bars: 10 cm.

fossa makes a marked step with the lateral surface of the ascending ramus. Anteriorly, the fossa becomes gradually shallower and the anterior margin is poorly defined.

At the very base of the anterior margin of the ramus, posterior to the linea obliqua, is a small and not well-delimited depressed surface (Fig. 6D). This structure is here named the *lateral coronoid fossa* (LCF). The LCF could represent the ventral-most point of insertion of the *m. temporalis* on the lateral side of the coronoid process (see Laub 1996).

The mandibular foramen is small and dorsally positioned on the medial side of the ramus, about 5 cm from the posterior border of the ramus. The ventral border of the foramen is V-shaped (Fig. 6E). The anterior border bears a small tuberosity, here interpreted as homologous to the lingula (linguoid process) described in elephants (Beden 1979) and mammutids (Laub 1996). Behind the mandibular foramen, at the posterior margin of the ascending ramus, below the condyle, there is a small depression probably for the *m. pterygoideus externus*. Still, on the medial side of both rami, near to the *trigonus retromolares*, is a well-developed coronoid foramen (Fig. 6E).

**Discussion.** The mandible of *H. chimborazi* closely resembles those of *C. hyodon* and "*S.*" *platensis*. Among the *C. hyodon* sample examined there are specimens (e.g., MUT J1, MUT J2) with relatively long and downward deflected symphyses. This primitive morphotype is unknown in *H. chimborazi* and "*S.*" *platensis*. Several juvenile mandibles of *C. hyodon* from Tarija, Bolivia (MUT) present small alveoli for the deciduous lower tusks (Hoffstetter 1952; Ferretti 2008b). In one specimen (MUT-J69), a left deciduous tusk was indeed found *in situ* (Ferretti pers. obs). Both the tusk and the alveolus have an oval cross-section. No traces of lower incisors were found in the mandibles of any of the other brevirostrine gomphotheres considered. *Stegomastodon texanus* (AMNH 10622) differs from the SA gomphotheres here examined in possessing a lower and more backwardly oriented ascending ramus and the posterior opening of the mandibular canal (mandibular foramen) placed more ventrally on the medial side of the ascending ramus. Absence of a lateral coronoid fossa as described in *H. chimborazi*, in *M. americanum*, *G. angustidens*, *G. productum*, *R.* cf. *falconeri*, *S. texanus*, *Anancus arvernensis*, and elephants and its presence in "*S.*" *platensis* and *C. hyodon* suggests this is a derived feature of SA gomphotheres. The mandibles of *Sinomastodon intermedius* and *S. hanjiangensis* are morphologically very similar to those of South American gomphotheres, but apparently lack a coronoid fossa (Teilhard de Chardin & Trassaert 1937; Tobien *et al.* 1986; Zong *et al.* 1989).

*Dentition*

**Upper incisor (tusk; Figs 3A; 5A, B).** Adults of *H. chimborazi* posses massive and relatively short upper tusks, oval in cross-section. The longitudinal axis of the tusk is distinctly upwardly curved and with no trace of torsion. The curvature becomes more evident as the tusk increases its length during growth, so that adult or, more in general, larger tusks are more curved than smaller juvenile tusks. In MECN 82, the left tusk has a maximum diameter of 115 mm and the length of the extralveolar part on the outer side is of 880 mm.

All known adult tusks of *H. chimborazi* lack enamel. Contrary to what was reported by Ficcarelli *et al.* (1995), the juvenile tusk MECN 258 from Bolivar also has no trace of enamel. However, a juvenile fragmentary skull with the DP4 in use from the Late Pleistocene of Quebrada Los Milagros near Llano Chico (EPN V-1980; Hoffstetter 1952), bears a tusk with a distinct lateral enamel band. The enamel band is very thin and straight. The tusk is rectilinear, with a flattened sub-circular cross section and no torsion, that would exclude it from *C. hyodon*.

**Cheek teeth (Figs 7; 8; Table 4).** Cheek tooth categories represented at the Bolivar sites are DP4-M3 and m1-m3. No permanent premolars (P3-P4-p3-p4) are present in the Bolivar sample nor among the La Carolina and Punin samples studied by Hoffstetter (1952). All intermediate cheek teeth (DP4-M2 and m1-m2) are trilophodont. M3s posses four lophs and a small distal talon (Fig. 7C, D, I, J). The fourth loph is sensibly narrower and with a more simple structure than the preceding ones. The lower m3s have four to five lophids and a distal talonid. They possess well-developed pretrite central conules. The emerging wear figure is a typical trefoil pattern. In all molar categories, posttrite central conules could be either absent (morphotype a) or moderately developed (morphotype b). In the latter morphotype a poorly defined secondary trefoil pattern emerges in advanced stages of wear. Cement is absent or filling the very base of the interloph(id)s. Enamel is even and never wrinkled as in "*S.*" *platensis*. Two complete m3s from Bolivar (MECN 133, MECN 438;

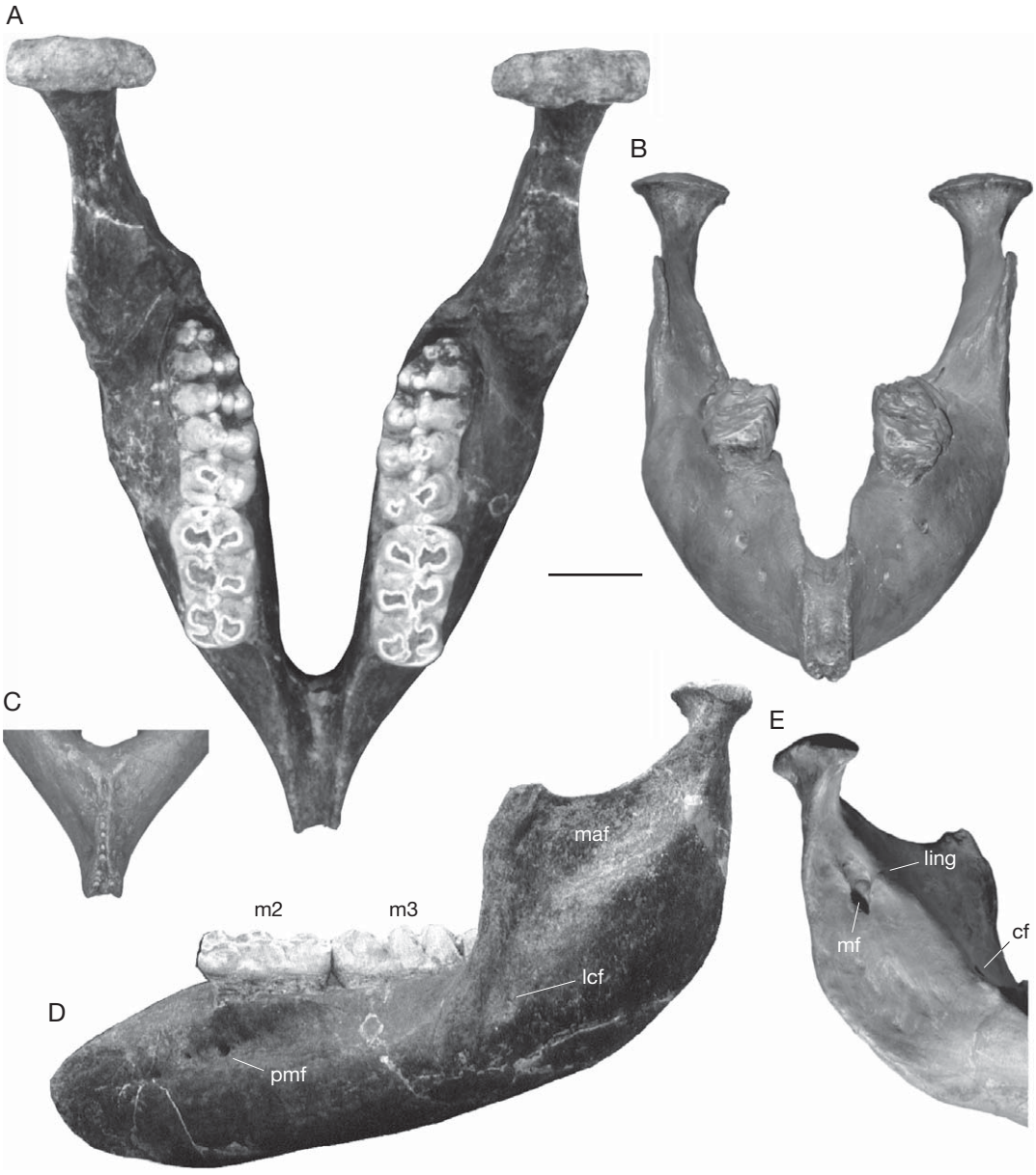


FIG. 6. — *Haplomastodon chimborazi* (Proaño, 1922) from Q. Pistud, Bolivar, Ecuador, mandible (MECN 82): **A**, **B**, **D**, mandible in occlusal, anterior (cast), and left lateral view; **C**, detail of the ventral aspect of the symphysis (anterior to the bottom); **E**, medial view of the left ascending ramus. Abbreviations: **cf**, coronoid foramen; **lcf**, lateral coronoid fossa; **ling**, linguoid process; **m2**, second lower molar; **m3**, third lower molar; **maf**, masseteric fossa; **mf**, mandibular foramen; **pmf**, posterior mental foramen. Scale bar: 10 cm.

Fig. 8F, H) preserve their roots. The root of the second lophid is divided into two branches, with the mesial one joining the main anterior root and the posterior one coalescing with the posterior root system, formed by the fusion of the roots of the third to fifth lophids.

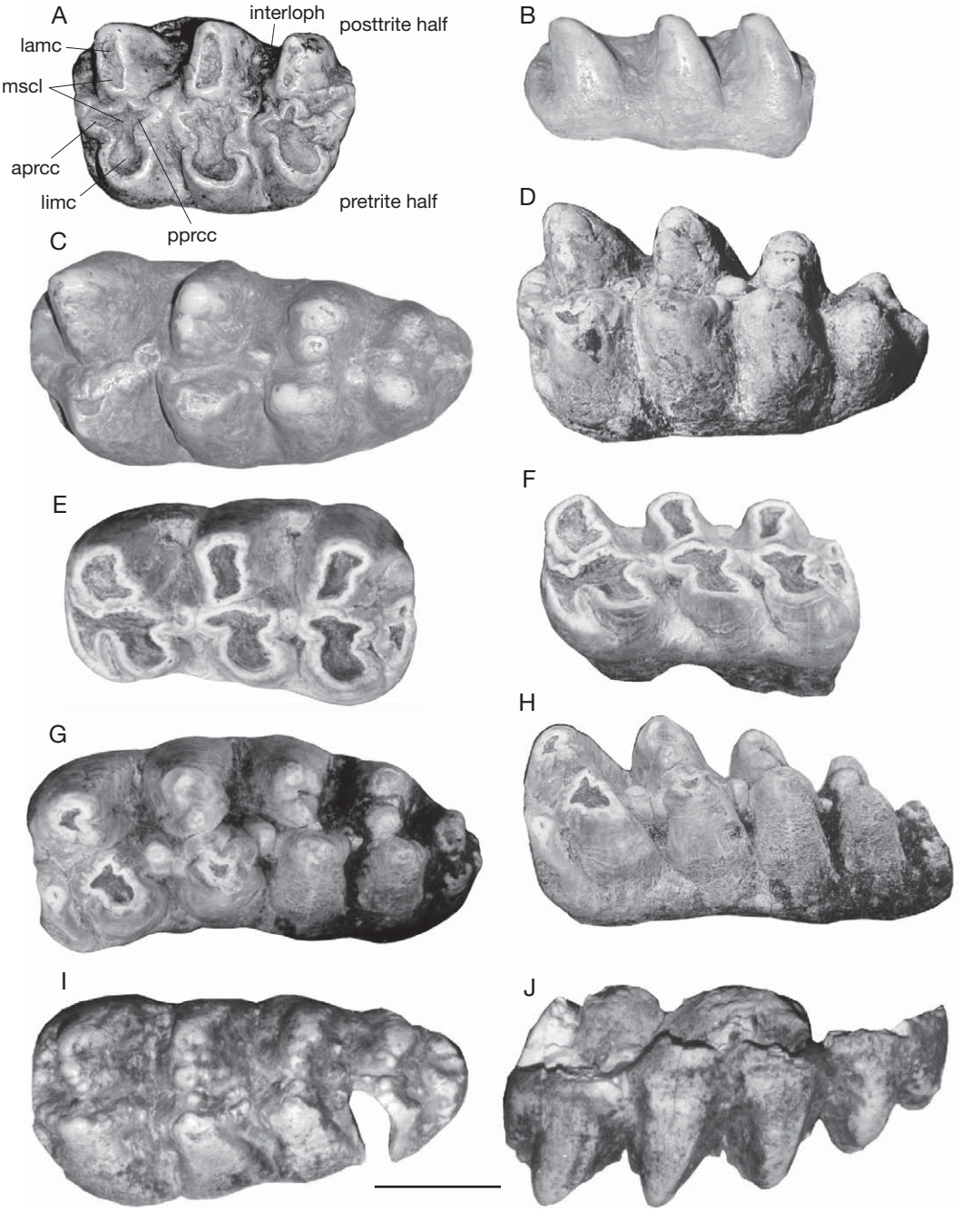


FIG. 7. — *Haplomastodon chimborazi* (Proaño, 1922) from Bolivar, Ecuador, upper and lower second and third molars (M2/m2 and M3/m3): **A**, **B**, left M2 (MECN 82) in occlusal and lingual views; **C**, **D**, left M3 (MECN 82) in occlusal and oblique lingual views; **E**, **F**, left m2 (MECN 82) in occlusal and oblique labial views; **G**, **H**, left m3 (MECN 82) in occlusal and oblique labial view; **I**, **J**, left M3 (MECN 4) from Q. Cuesaca, in occlusal and labial (reversed) views. Abbreviations: **aprcc**, anterior pretrite central conule; **lamc**, labial main cone; **limc**, lingual main cone; **mscl**, mesoconelets; **pprcc**, posterior pretrite central conule. In all figures, mesial is to the left. Scale bar: 5 cm.

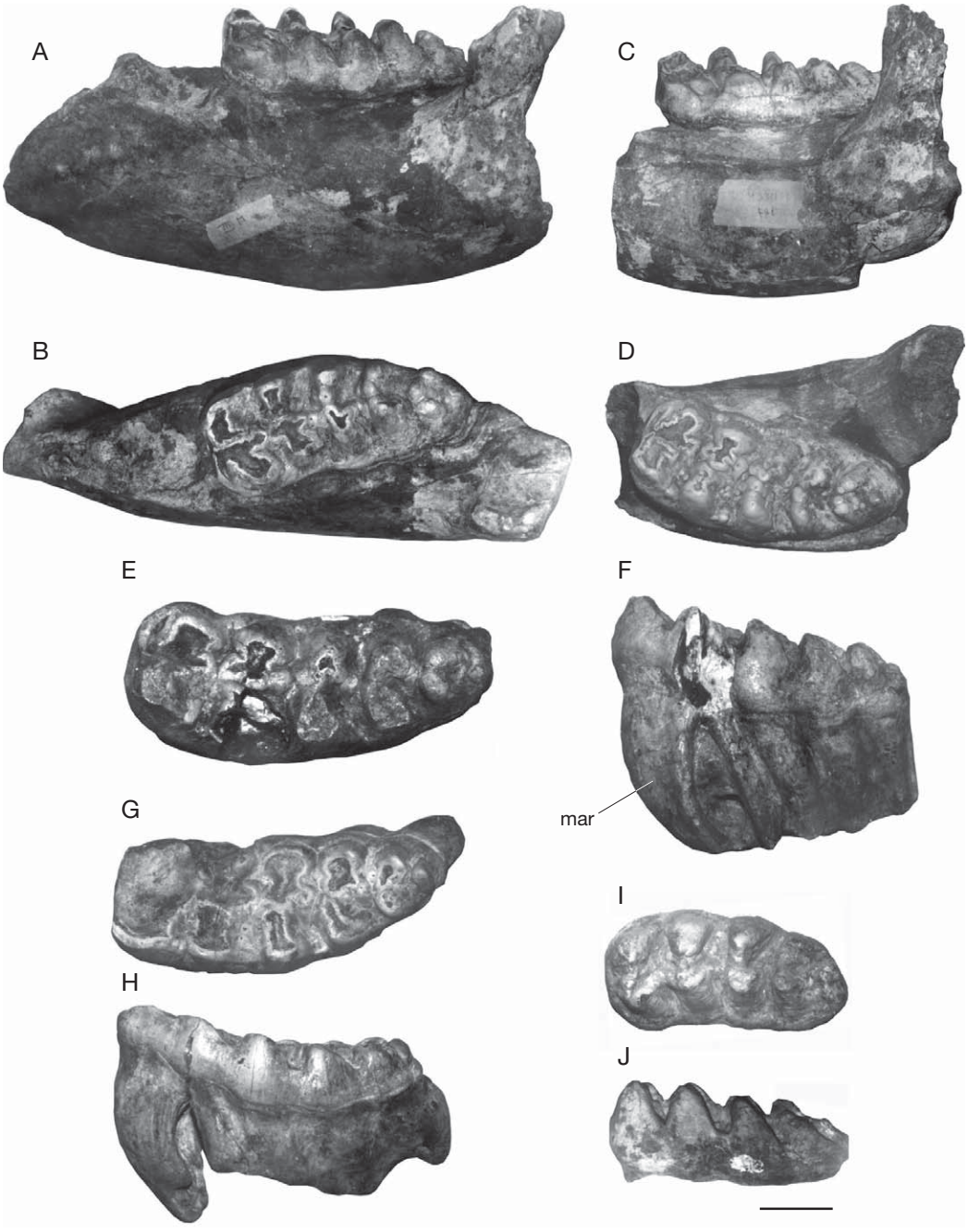


FIG. 8. — *Haplomastodon chimborazi* (Proaño, 1922) from Bolivar, Ecuador, mandibles and lower molars: **A**, **B**, left mandibular body with m3 (MECN 437; Q. Pistud) in lateral and occlusal views; **C**, **D**, incomplete right half mandible with m3 (MECN 147; Q. Cuesaca), in lateral (reversed) and occlusal view; **E**, **F**, right m3 (MECN 189; Q. Pistud), in occlusal and lingual views; **G**, **H**, right m3 (MECN 438; Q. Pistud), in occlusal and lingual views; **I**, **J**, left m3 (MECN 272; Q. Cuesaca), in occlusal and lingual (reversed) views. Abbreviation: **mar**, main anterior root. In all figures, mesial is to the left. Scale bar: 5 cm.

Though no DP3s are present in the Bolivar dental sample, information on the anatomy of this tooth is given by Hoffstetter (1952) who describes, without figuring them, two isolated *H. chimborazi* DP3s from the Late Pleistocene of Alangasi and Calderon, in the surrounding of Quito. The specimen from Alangasi (EPN V1244) is formed by three lophs and a small distal talon. Its size (length 56 mm; width 43 mm) is comparable to that the DP3 of *C. hyodon* from Tarija, where complete upper molar series are known (Boule & Thevenin 1920). Specimen EPN V1244 is, on the other hand, significantly smaller than the DP4s of *C. hyodon* and also than that from Q. Pistud, described above. In EPN V1244 only pretrite trefoils are present. Between the first and second lophs, at the labial end of the interlpohid, is a small cone ("bouton"). The enamel sectioned on the occlusal surface is rather wrinkled.

The second DP3 from Calderon (EPN V1231) is very similar to that from Alangasi both in size (57.3 mm in length; 47.5 mm in width) and morphology.

**Discussion.** The tusks of *H. chimborazi* differ from those of primitive gomphotheres (e.g., *G. angustidens*) in being more robust, not downwardly curved and with no enamel band in adults. With respect to "*S.*" *platensis* and *C. hyodon*, the tusks of *H. chimborazi* are relatively shorter. The type specimen of "*S.*" *platensis* (MLP-8-1) possesses long and nearly straight tusks, a morphotype absent in Ecuadorian *H. chimborazi*. No adult tusks from Ecuador show traces of an enamel cover. Also, in the Aguas do Araxá sample described by Simpson & Paula Couto (1957), all tusks are without enamel. On the other hand, this occurs in some "*S.*" *platensis* isolated tusks from Argentina (MLP; material previously referred to a distinct taxon, *Notiomastodon ornatus* Cabrera, 1929) belonging to both juvenile and adult individuals (Ferretti pers. obs.). Therefore, even though the occurrence of an enamel band is a variable character in both *H. chimborazi* and "*S.*" *platensis*, the latter has a tendency to retain an enamel band in later stages of growth.

The morphology of *H. chimborazi* molars is generally conservative (as far as South American gomphotheres is concerned), very similar to the condition in *C. hyodon*, but with morphotypes that approach the more derived complex structure of "*S.*" *platensis*. *Haplomastodon chimborazi* is more progressive than species of *Gomphotherium* Burmeister, 1837 and *Rhynchotherium* Falconer, 1868 in the greater development of the accessory conules and in possessing well-developed tetraloph and pentalophid on M3 and m3 respectively. The most primitive NA bona-fide species of *Stegomastodon*, *S. primitivus* Osborn, 1936 from the Late Hemphillian to Early Blancan (Latest Miocene-Early Pliocene) of North America, is already more derived than *H. chimborazi* in possessing a more developed pentaloph on the M3 (Osborn 1936). Ecuadorian *H. chimborazi* possesses DP3 with three lophs and a distal talon. This character is also present in *C. hyodon* and "*S.*" *platensis*. As evidenced by Tassy (1990) and Shoshani (1996), the full development of a third loph in the DP3/dp3 could represent a distinct feature of SA gomphotheres, and a convergence with tetralophodont gomphotheres (*Tetralophodon* Falconer, 1857, *Anancus*, *Paratetralophodon* Tassy, 1983; Tassy 1985, 1990). Primitive trilophodon gomphotheres, like *G. angustidens* and *G. productum*, posses DP3/dp3s formed by two loph(id)s and a distal talon. Savage (1955) described a dp3 (UCMP 44749) of *Stegomastodon mirificus* from Cita Canyon, Texas, as consisting of three lophids, though the third one is much lower and structurally less complex than the anterior ones. A similar incipient development of the third loph(id) of the third deciduous premolars is observed in the juvenile material of *Rhynchotherium edensis* from Mt Eden, California, described by Frick (1926) and Osborn (1936).

Available evidence from Ecuador and Brazil (Simpson & Paula Couto 1957) indicates that in *Haplomastodon* deciduous premolars are not replaced by permanent premolars. This derived feature is also known in *C. hyodon* (Boule & Thevenin 1920), in "*S.*" *platensis* (Cabrera 1929; Ferretti pers. obs.) and in NA *Stegomastodon* (Shoshani 1996). In contrast, P3-P4 are present in more primitive gomphotheriids from NA and Europe, like *G. productum* and *G. angustidens* (Frick 1926; Tassy 1985, 1990). Evidence from a juvenile skull and mandible (AMNH 18218, 18216a, 18216b) of *Rhynchotherium edensis*

TABLE 4. — *Haplomastodon chimborazi* (Proaño, 1922) from Bolivar and Quebrada Colorada (Punin), Ecuador. Molar measurements (in mm ) and complexity. Abbreviations: **a**, absent; **p**, present; **Q.P**: Q. Pistud; **Q.C**: Q. Cuesaca; **Q.Co**: Q. Colorada; **l(id)**: loph(id); **L**, length; **W**: width.

| | | | | Measures | | | | | | | | | | |
|---|---|---|---|---|---|---|---|---|---|---|---|---|---|---|
| **Tooth** | **Specimen** | **Site** | **Wear stage** | Greatest L | W at 1st l(id) | W at 2nd l(id) | W at 3rd l(id) | W at 4th l(id) | W at 5th l(id) | Greatest height | Enamel thickness | Number of l(id)s | **Secondary trefoil** | **Cement** |
| dP4 | MECN 442 | Q.P | 3 | – | 43 | 47 | – | – | – | – | – | – | – | a |
| M2 | MECN 82 | Q.P | 4 | 130 | 82 | 84 | 79 | – | – | 48 | – | 3 | p | a |
| M3 | MECN 82 | Q.P | 2 | 167 | 85 | 83 | 72 | 53 | – | *c.* 65 | – | 3+ | p | scarce |
| m1 | MECN 441 | Q.P | 4 | 104 | 55 | 59 | 65 | – | – | – | 3.5 | 3 | | a |
| m2 | MECN "82" | Q.P | 4 | 136 | 73 | 77 | 79 | – | – | 44 | 4.0 | 3 | a | a |
| m3 | MECN "82" | Q.P | 2 | *c.* 193 | 78 | 83 | 80 | 66 | 41 | 77 | – | 4+ | a | scarce |
| m3 | MECN 187 | Q.P | 1 | – | 86 | 87 | – | – | – | 76 | – | 4+ | a | scarce |
| m3 | MECN 189 | Q.P | 2\3 | 216 | 83 | – | 88 | 78 | 60 | 68 | 4.5 | 4+ | a | scarce |
| m3 | MECN 438 | Q.P | 3\4 | 216 | *c.* 89 | *c.* 90 | 86 | 74 | 51 | – | – | 4\5 | a | a |
| m3 | MECN 437 | Q.P | 2 | 203 | 84 | 87 | 90 | 76 | 54 | 65 | – | 4+ | a | scarce |
| M1 | MECN 145 | Q.C | 4 | 86 | 58 | 55 | 48 | – | – | – | – | 3 | – | a |
| M3 | MECN 4 | Q.C | 1 | 178 | 84 | 85 | 75 | 64 | – | 72 | – | 4+ | p | a |
| m3 | MECN 272 | Q.C | 1 | 190 | 91 | 90 | 91 | 78 | – | 76 | – | 4+ | a | a |
| m3 | MECN 267 | Q.C | 1 | 189 | 92 | 90 | 86 | 71 | – | 73 | – | 4+ | a | a |
| m3 | MECN 147 | Q.C | 2 | 210 | 84 | 90 | 87 | 78 | – | 66 | – | 4\5 | p | a |
| m3 | EPQ-V1254 | Q.Co | 3 | *c.* 250 | 90 | 100 | 98 | 94 | 66 | *c.* 77 | *c.* 5 | 5+ | s | scarce |

TABLE 5. — *Haplomastodon chimborazi* (Proaño, 1922) from Bolivar and Tumbaco, Ecuador. Measurements (in mm) of the atlas (see Appendix 2).

| | Specimen (site) | | |
|---|---|---|---|
| **Measures** | MECN 82 (Q. Pistud) | MECN 271 (Q. Cuesaca) | MECN 232 (Tumbaco) |
| 1. Breadth of cranial articular surface | 217 | 191 | 187 |
| 2. Breadth of caudal articular surface | 203 | 160 | 103 |
| 3. Greatest breadth | 392 | 280 | – |
| 4. Height | 225 | 203 | 228 |

from Mt. Eden, with the DP2-DP3/dp2-dp3 in use and the M1/m1 already formed, indicates that this taxon also lacks permanent premolars (Frick 1926; Osborn 1936). Loss of permanent premolars and the acquisition of a "horizontal tooth succession" is a derived trait among proboscideans, that evolved independently in several elephantoid lineages (e.g., mammutids, *Anancus*, and elephants; Tassy 1990). Shoshani (1996) regarded this trait as a possible synapomorphy of SA gomphotheres and NA *Stegomastodon*.

*Axial skeleton*

**Atlas (Fig. 9A-G; Table 5).** The dorsal arch is very stout, dorsally convex, with a strong dorsal tuberosity. The foramen for the passage of the vertebral artery (lateral vertebral foramen), is large, oval in shape, and located near the cranial margin of the dorsal arch. Lateral and slightly ventral to the outer opening of the lateral vertebral foramen, a shallow groove extends to the cranial opening of the transverse foramen. The articular facets for the occipital condyles are deep and concave. The articular facets for the axis are almost circular in shape, low, and slightly concave dorso-ventrally. The transverse processes are large and well extended dorso-ventrally. The dorsal tubercle of both processes is strongly developed, and projects lateralward and dorsalward (Fig. 9F). The ventral tubercle is well developed though smaller than the dorsal one. The dorsal and ventral tubercles are separated by a notch. The transversal foramina are in most specimens unequally developed, with

TABLE 6. — *Haplomastodon chimborazi* (Proaño, 1922) from Bolivar, Ecuador. Measurements (in mm) of the axis (see Appendix 2).

| Measures | Specimen MECN 82 |
|---|---|
| 1. Greatest breadth | 251 |
| 2. Breadth of cranial articular surface | 208 |
| 3. Breadth across the postzygapophyses | 154 |
| 4. Breadth of caudal articular surface | 154 |
| 5. Height of caudal articular surface | 134 |
| 6. Greatest height | 296 |
| 7. Height of the dorsal process | 106 |
| 8. Greatest length | 125 |

one foramen markedly larger than the opposite one (e.g., MECN 82; Fig. 9F). Noticeably, in some specimens, as first noted by Hoffstetter (1952), one or both foramina are completely obliterated (e.g., EPN V2010; Fig. 9C, D). A similar variability in size and presence/absence of transverse foramina of the atlas has been observed in the *C. hyodon* and "*S.*" *platensis* samples analyzed for this study. On the other hand, none of the other proboscideans examined show this feature.

**Cervical vertebrae 2 to 7 (Figs 9H-K; 10A-H; Tables 6; 7).** Five other cervical vertebrae of the Bolivar skeleton are preserved, identified as C2, C3, C5, C6, and C7 respectively. The axis possesses a very high dorsal arch (Fig. 9H) The spinous process is transversally enlarged and terminates with two dorsal tuberosities, separated by a central depression. On the caudal aspect of the process runs a narrow crest, and, lateral to this, on both sides, two intensely wrinkled grooves are present. The pedicles are long and robust. The vertebral body has a ventral crest that terminates caudally in a small tuberosity. Lateral to this crest, the ventral face of the body is cranio-caudally concave and transversally convex. Cranially, the two wide articular surfaces for the atlas are situated lateral to the stout odontoid process. The transverse processes are short and weak and are pierced by an oval-shaped transverse foramen. The process ends laterally with a tuberosity. Medial and ventral to the transverse process there is a small bony spine. A second, nearly complete axis from Punin (EPN V 3744) shows no traces of transverse foramina. On the other hand, two axes from La Carolina (EPN 1265, EPN 1287) described by Hoffstetter (1952) possess well-developed transverse foramina.

The body of C3 has a sub-circular shape in cranial view (Fig. 10A, B). On the ventral side runs a thin median crest. The laminae are thick. The spinous process is broken just above its base. It seems, however, to have been slender and not caudally bent. The vertebral foramen is triangular-shaped with a rounded vertex. The caudal vertebral incision consists, on both sides, in a groove running from the vertebral foramen to the transverse foramen. The transverse process is slender, and its dorsal root is ventrally sloping. The dorsal tubercle of the transverse process is caudally directed. The ventral tubercle forms a thin process, cranially directed.

The morphology of C5 is very similar to that of C3 (Fig. 10C, D). The transversal foramina are however larger than those of C3, while the ventral tubercle of the transverse process is smaller.

The body of C6 of MECN 82 is crushed dorsally (Fig. 10E, F). The vertebral foramen is wide. The spinous process is slender. The transverse processes are more robust relative to those of the previous vertebrae. Ventrally and caudally there is a robust process whose extremity forms a large tubercle (*tuberculum caroticus*) cranially directed.

In C7 the spinous process is incomplete; however, it was evidently larger than in the previous cervical vertebrae. The ventral portion of the body and the transverse processes are crushed and partly broken off. The facet for the articulation with the first left rib is partly preserved on the caudal face of the body. The transverse processes are dorso-ventrally expanded, laterally flattened and without transversal foramina.

**Thoracic vertebrae (Fig. 10I-T; Table 7).** Eleven vertebrae of the thoracic segment of the backbone of MECN 82 are preserved. The approximate position of each vertebra along the vertebral column was assessed by comparison with associated vertebrae of *E. maximus* and *C. hyodon* from Tarija. The cranial-most preserved thoracic vertebra is identified as a T2 or T3 (thereafter T2/T3) based on the size of the spinous process and the fact that it seems not to articulate with C7. The body is heart-shaped and

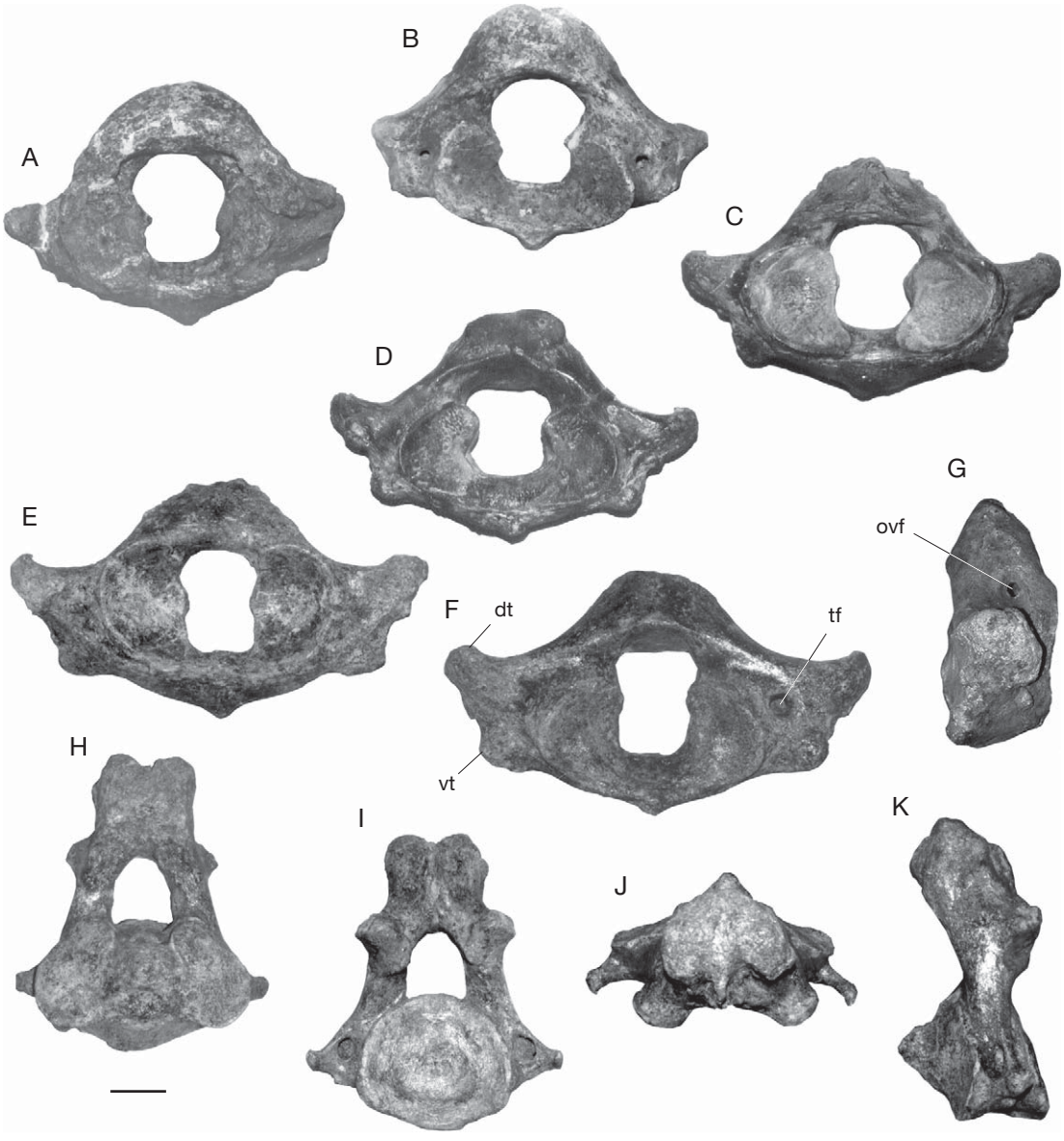


FIG. 9. — *Haplomastodon chimborazi* (Proaño, 1922), from Ecuador (various localities), first (atlas) and second (axis) cervical vertebrae: **A**, **B**, atlas (MECN 271; Q.Cuesaca, Bolivar) in cranial and caudal views; **C**, **D**, atlas (EPN V2010; La Carolina, S. Elena Peninsula), in cranial and caudal views; **E**-**G**, atlas (MECN 82; Q. Pistud, Bolivar), in cranial, caudal, and left lateral views; **H**-**K**, axis (MECN 82), in cranial, caudal, ventral and left lateral views. Abbreviations: **dt**, dorsal tubercle of transverse process; **ovf**, outer opening of lateral vertebral foramen; **tf**, transversal foramen; **vt**, ventral tubercle of transverse process. Scale bar: 5 cm.

its lateral sides are concave (Fig. 10I, J). On both sides, ventral to the base of the transverse process, there are two demi-facets, which articulate, with the heads of the second and third ribs. The incomplete spinous process is large, caudally bent, and originally terminated into an apical tubercle. The cranial margin of the spinous process is sharp. The caudal one, on the contrary, is characterized by a

TABLE 7. — *Haplomastodon chimborazi* (Proaño, 1922) from Bolivar, Ecuador. Measurements (in mm) of cervical (C3-C7), thoracic, and lumbar vertebrae (see Appendix 2).

| | Measures | | | | | |
|---|---|---|---|---|---|---|
| **Specimen MECN 82** | 1. Greatest breadth | 2. Breadth of cranial articular surface | 3. Breadth of caudal articular surface | 4. Greatest height | 5. Height of neural spine | 6. Greatest length of corpus |
| C3 | 250 | 140 | 149 | – | – | 61 |
| C5 | 256 | 150 | 150 | – | – | – |
| C6 | *c.* 275 | 133 | 156 | > 304 | > 76 | *c.* 42 |
| C7 | 117 | 165 | *c.* 179 | > 100 | – | *c.* 62 |
| T2 | 380 | 149 | *c.* 186 | > 450 | > 270 | *c.* 63 |
| T3 or T4 | 339 | 161 | 209 | > 455 | 330 | *c.* 70 |
| T4 or T5 | – | 147 | 205 | > 270 | > 200 | 68 |
| T6 or T7 | 306 | 136 | 208 | – | – | *c.* 61 |
| T7 or T8 | – | 136 | 195 | – | – | *c.* 68 |
| T9 or T10 | – | 125 | *c.* 176 | > 260 | > 207 | *c.* 75 |
| T11 or T12 | – | 128 | 186 | > 290 | > 280 | 70 |
| T12 or T13 | 290 | 126 | – | > 270 | > 280 | 66 |
| T13 or T14 | 292 | 117 | 160 | 310 | 207 | 73 |
| T16–lastT | – | 119 | *c.* 143 | – | – | 77 |
| T16–lastT | – | 132 | *c.* 135 | 265 | 172 | 71 |
| L1 | – | 137 | 132 | – | – | 72 |
| L3 | – | 139 | 155 | – | – | 82 |
| L4 | 310 | 162 | 155 | – | > 109 | 89 |

feeble median groove. The vertebral foramen is triangle-shaped. The very thick transverse processes end in a robust lateral tubercle, on the cranial side of which is present a small, dorsally oriented spine. The cranial articular processes (prezygapophyses) are well separated from each other.

In T3/T4 the body is longer than that of the preceding vertebra (Fig. 10K, L). The vertebral foramen is narrow, due to the position of the cranial articular processes. The spinous process is similar to that of T2/T3. The transverse processes are stout and laterally directed. The articular facet for the tubercle of the fourth rib is not evident. Also the cranial articular facet for the head of the rib is not well defined; it seems however to be positioned on the cranio-ventral margin of the transverse process. The caudal one is positioned laterally with respect to the body, near the dorsal margin.

The corpus of T4/T5 is heart-shaped (Fig. 10M, N). The spinous process is strongly deflected caudally, probably as a consequence of taphonomic distortion. The cranial margin of the process is flattened, while on the caudal one runs a very deep groove. The transverse processes are more slender and the lateral tubercle is less pronounced with respect to the preceding vertebrae. The cranial articular facet for the head of the fourth/fifth rib is concave and dorso-ventrally elongated. The caudal one is wide, concave, semicircular-shaped and positioned lateral to the corpus.

T6/T7 has the same general characteristics as T4/T5. It is missing its spinous process (Fig. 10O, P). The transverse processes are more dorsally positioned than in the preceding vertebrae. The caudal facet for the sixth/seventh rib is smaller than that of T4/T5.

Also in T7/T8 the spinous process is broken (Fig. 10Q, R). This vertebra is very similar in shape to the previous one. The transverse processes are incomplete, laterally and slightly cranially directed.

The shape of T9/T10 is similar to that of the preceding one (Fig. 10S, T). Only the proximal half of the spinous process is preserved. The groove occurring on the caudal side of the process is very deep, and the spine has a V-shaped cross section. The lateral processes are broken.

T11/T12 has a heart-shaped, and dorso-ventrally elongated body. The costal facets are close to each other and positioned dorsally on the body. Their dorsal margin is situated at about half of the ver-

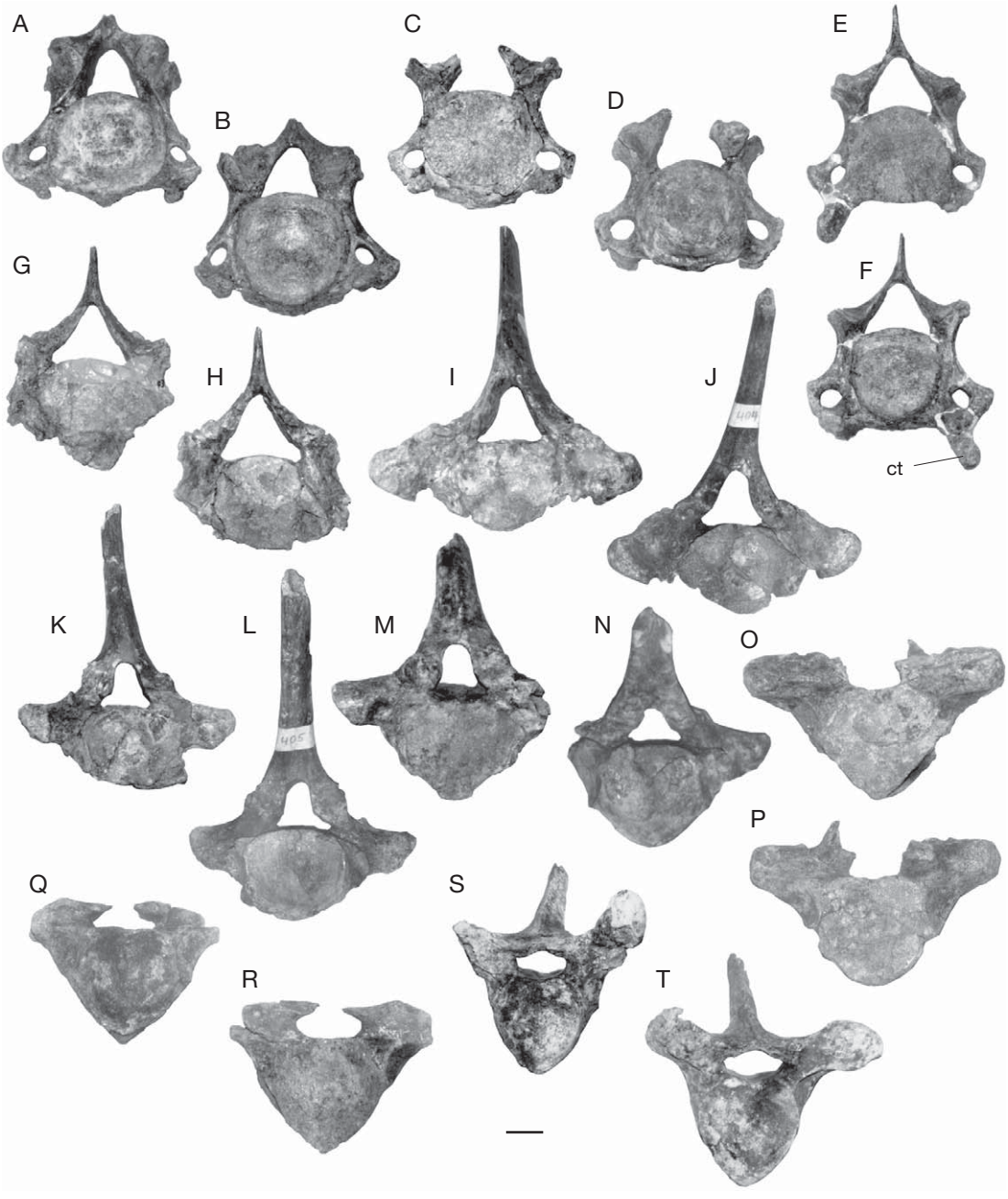


FIG. 10. — *Haplomastodon chimborazi* (Proaño, 1922) from Q. Pistud, Bolivar, Ecuador, posterior (C3-C7) cervical and anterior dorsal (T2-T9) vertebrae (MECN 82): **A**, **B**, C3, in cranial and caudal views; **C**, **D**, C5, in cranial and caudal views; **E**, **F**, C6, in cranial and caudal views; **G**, **H**, C7, in cranial and caudal views; **I**, **J**, T2, in cranial and caudal views; **K**, **L**, T3 or T4, in cranial and caudal views; **M**, **N**, T4 or T5, in cranial and caudal views; **O**, **P**, T6 or T7, in cranial and caudal views; **Q**, **R**, T7 or T8, in cranial and caudal views; **S**, **T**, T9 or T10, in cranial and caudal views. Abbreviation: **ct**, carotic tubercle. Scale bar: 5 cm.

tebral foramen. The vertebral foramen has an oval outline. The spinous process is rather long and possesses a very sharp cranial margin. The lateral processes are broken.

T12/T13 is very similar in shape to the preceding vertebra. The spinous process is slender, long, and caudally inclined. A narrow notch with a rounded floor is found in a median position on the cranial margin of the dorsal arch. The transverse processes are laterally and dorsally directed. The costal articular facets are close to one another. The cranial facet is particularly deep and concave.

In T14/T15, the cranial and caudal costal articular facets are small, and well separated from one another. The spinous process is short and not so much inclined caudally. The cranial notch on the dorsal arch is deep. The transverse processes are dorso-laterally directed. They have a dorso-ventrally flattened base and each ends in a clubbed extremity. A stout crest, possibly homologous to the accessory tubercle of the lumbar vertebrae, is present on caudal margin of the transverse processes.

Two more posterior thoracic vertebrae are present, whose position is between T15 and the last thoracic vertebra. The corpus of the more anterior one is rather long. The spinous process is broken at its very base. A deep cranial groove runs on the dorsal arch. The right transverse process is broken, whilst the left one is only slightly damaged on its ventral side. The left process is short, dorso-ventrally flattened and horizontal in direction. Dorso-cranially there is an elongated tubercle, which is homologous to the mammillary process of the lumbar vertebrae.

The second posterior thoracic is morphologically similar to the preceding one. It is damaged on the right side. It has, on both sides, only one cranial facet for the head of a rib. It bears a short spinous process, caudally inclined. The mammillary processes are large and positioned laterally to the cranial articular processes. The right transverse process is short, flattened and dorsalward and lateralward directed. It articulates with a rudimentary rib. Between the latter and the ventral side of the transverse process persists a small fissure. The caudal articular facet for the rib is absent.

**Lumbar vertebrae** (**Fig. 11A-C, F; Table 7**). Three lumbar vertebrae are preserved in MECN 82. The body of L1 is wide and thick (Fig. 11A). The pedicles diverge. The spinous process is broken. The cranial articular processes are very close to one another, and are separated only by a narrow fissure. The left transverse process is not preserved. The right one is short, thick and latero-caudally directed. The mammillary processes end in two small tubercles. Lateral to each mammillary process arises a bony lamina that reaches the cranio-dorsal margin of transverse processes, bounding a small foramen dorsally.

The body of L3 is subcylindrical in shape and dorso-ventrally flattened (Fig. 11B). The dorsal arch is thin. The distal part of spinous process is not preserved. It has a wide base. The vertebral foramen is wide. The transverse processes are broken at their bases. The mammillary processes end into two small tubercles cranially directed.

L4 has a markedly dorso-ventrally flattened body (Fig. 11C). The spinous process has a wide base. It is laterally flattened, short and caudally inclined. The cranial articular processes and the mammillary processes, on both sides, are fused together into a unique strong process, cranio-dorsally oriented. The transverse processes (costal processes) are thick and are laterally expanded, making up, caudally, a wide articular surface for the ileum (Fig. 11F).

**Sacrum** (**Fig. 11D-F; Table 8**). The sacrum of MECN 82 consists of the first, second and third sacral vertebra (in adult elephants the sacrum is formed usually by five sacral vertebrae that are fused at different times during the individual life history). The width of the vertebrae diminishes in a caudal direction. The ventral face of each vertebra is concave (Fig. 11E). The neural arch is low. All three vertebrae bear a spinous process strongly inclined caudally (in the third one it is broken) and two cranial articular processes, dorso-cranially directed (Fig. 11F). The vertebral canal is flattened and it narrows caudally. The first sacral vertebra has, lateral to the articular facets, a large mammillary process. The transverse processes are wide and flattened, ventrally directed and blended together to form the wrinkled lateral crest. The sacral wing is poorly developed. Laterally, the vertebrae are

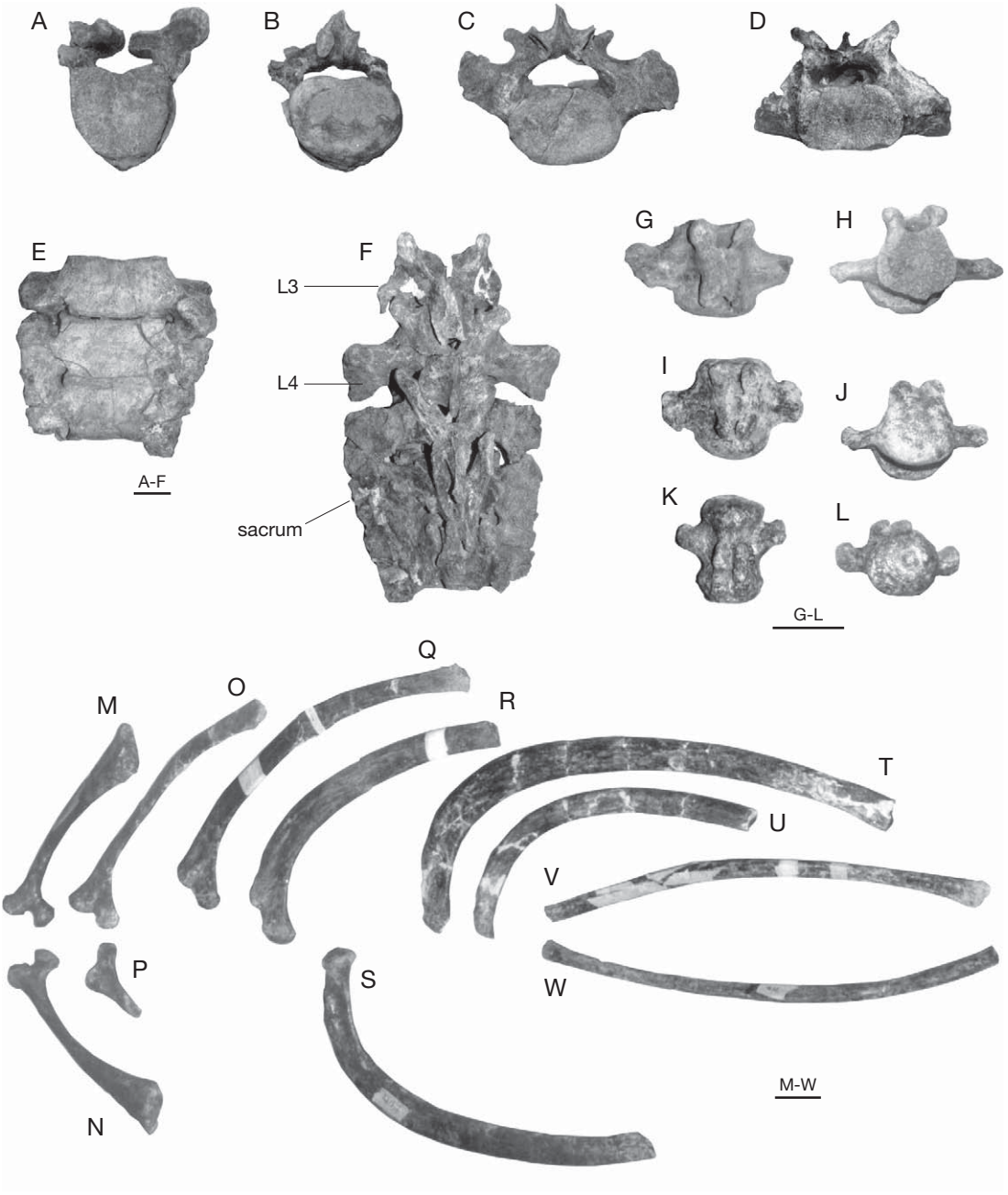


FIG. 11. — *Haplomastodon chimborazi* (Proaño, 1922) from Q. Pistud, Bolivar, Ecuador, lumbar vertebrae, sacrum and caudal vertebrae (MECN 82): **A**, L1, cranial view; **B**, L3, cranial view; **C**, L4, cranial view; **D**, **E**, sacrum, in cranial and ventral view; **F**, L3-L4 and sacrum in anatomical connection, dorsal view; **G**-**L**, caudal vertebrae in dorsal and cranial views; **M**, **N**, first left and right costae; **O**-**R**, anterior costae; **S**-**U**, intermediate costae; **V**, **W**, posterior costae. Scale bars: A-L, 5 cm; M-W, 10 cm.

TABLE 8. — *Haplomastodon chimborazi* (Proaño, 1922) from Bolivar, Ecuador. Measurements (in mm) of the sacrum (see Appendix 2).

| Measures | Specimen MECN 82 |
|---|---|
| 1. Greatest length | *c*. 280 |
| 2. Greatest breadth | 290 |
| 3. Breadth of second sacral vertebra | 280 |
| 4. Breadth of thirdh sacral vertebra | 253 |
| 5. Breadth of cranial articular surface | 150 |
| 6. Height of cranial articular surface | 92 |

separated from each other by a wide intervertebral space, where the supra- and sub-sacral foramina, respectively, are visible.

**Caudal vertebrae (Fig. 11G-L).** Three caudal vertebrae are attributable to individual MECN 82. All three vertebrae have an elongated body. The two most anterior caudals have cranial and caudal convex articular surfaces. Transverse processes are flattened, horizontal, and their length diminishes from the anterior-most to the posterior-most one. The dorsal arches have a base cranio-distally expanded. Cranial and caudal articular processes are button-like. The spinous process is extremely reduced and caudally oriented.

**Ribs (Fig. 11M-W).** Among the collected material, four ribs surely pertain to individual MECN 82. Most probably also specimens MECN 112, MECN 207, MECN 208, MECN 409, MECN 410, MECN 411, MECN 412, MECN 457 and MECN 470 belong to the same individual. The first rib is complete. It is short and slightly curved (Fig. 11M, N). The tuberculum is large and separated by a notch from the head. The latter has two facets, respectively for the seventh cervical and the first thoracic vertebrae. The tubercula of the consecutive ribs become gradually smaller and eventually disappear, while the bodies become longer and more curved.

**Discussion.** The observed asymmetry and variability in the degree of closure of the transverse foramina on the atlas and axis of *H. chimborazi*, *C. hyodon* and "*S.*" *platensis* could be consistent with a regressive process affecting skeletal structures no longer functional. A similar pattern can be observed in C7 of most mammals. In humans, for instance, the transverse foramina of the seventh cervical vertebra rarely give passage to the vertebral artery and vein, and they are generally smaller on one side or even absent (Bell *et al.* 1950). The vertebral artery in humans usually passes in front of the transverse process of C7. A similar condition for the atlas and axis of *H. chimborazi* (and the other SA gomphotheres) is suggested here. According to this hypothesis, in *H. chimborazi* the vertebral artery ran cranially through the transverse foramina of C6-C3 and then just below the transverse processes of the axis and the atlas (Fig. 9). Then it turned upward passing laterally to the articular surface for the occipital condyle and entered the vertebral foramen passing through the lateral vertebral foramen. The latter is present in all the atlases of *H. chimborazi* examined, even in those with completely closed transversal foramina. It is difficult to assign any adaptive significance to the lack of transverse foramina on the first cervicals. Rather, it might represent an anatomic variation, quite frequent among SA gomphotheres, while extremely rare (if present at all) in other proboscideans (actually no other case has been described so far). In this case, it could represent the results of the so-called founder effect, supporting the hypothesis that all South American taxa derived from a single dispersal event.

The preserved vertebrae of MECN 82 indicate that the trunk region of *H. chimborazi* contained a minimum of 16-17 vertebrae (extant elephants typically possess from 19 to 21 thoracic vertebrae). All thoracic vertebrae of *H. chimborazi* possess backwardly bent spinous processes. The inclination increases in the anterior thoracics (T2 to T5), remains nearly constant from T5 to about T12 and then decreases in the remaining posterior vertebrae. Compared to *G. sylvaticum* and *G. productum*, the spinous processes of the anterior thoracics of *H. chimborazi* are more backwardly bent, suggesting the head was kept in a more elevated posture in the latter taxon. In *H. chimborazi*, the length of the spinous processes increases from (T1) T2 to T5 and rapidly decreases passing from the fifth thoracic to consecutive vertebrae.

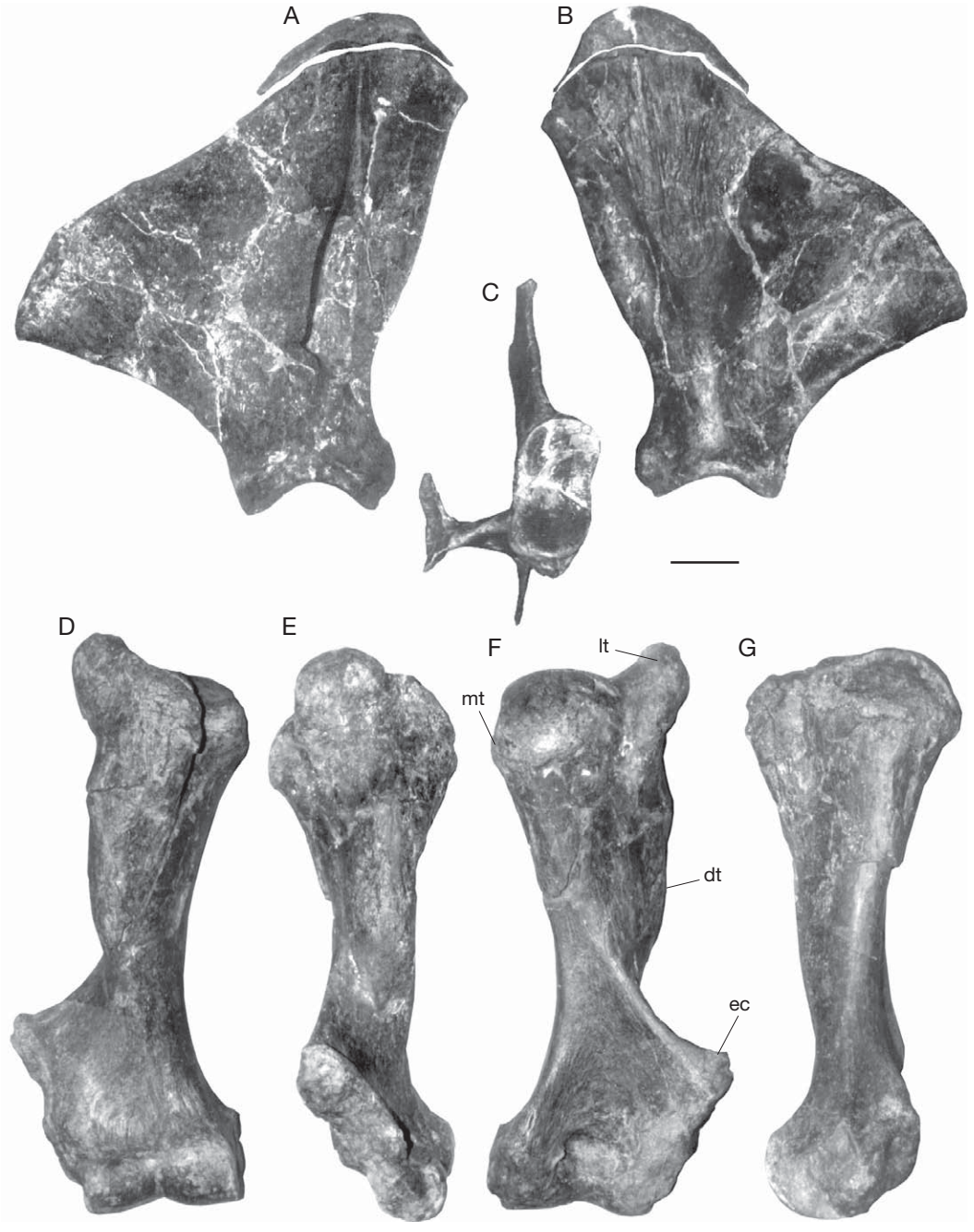


FIG. 12. — *Haplomastodon chimborazi* (Proaño, 1922) from Q. Pistud, Bolivar, Ecuador, anterior limb bones (MECN 82): **A**-**C**, right scapula, in lateral, medial, and articular views; **D**-**G**, right humerus, in anterior, lateral, posterior, and medial views. Abbreviations: **dt**, deltoid tuberosity; **ec**, epicondilar crest; **lt**, lateral tuberosity; **mt**, medial tuberosity. Scale bar: 10 cm.

TABLE 9. — *Haplomastodon chimborazi* (Proaño, 1922) from Bolivar and La Carolina, Ecuador. Measurements (in mm) of the scapula (see Appendix 3).

| | Specimen/site | | |
|---|---|---|---|
| | Q. Pistud | | La Carolina |
| **Measures** | MECN 82, r | MECN 82, l | EPN V-2010 |
| 1. Height | 785 | – | – |
| 2. Length of dorso-posterior margin | 700 | 696 | – |
| 3. Length of the spine (to the tip of the acromion) | – | 530 | – |
| 4. Smallest length of collum scapulae | 233 | 228 | – |
| 5. Greatest length of the glenoid process | 245 | 250 | – |
| 6. Length of glenoid cavity | 193 | 191 | 185 |
| 7. Breatdth of glenoid cavity | 107 | 110 | 120 |

TABLE 10. — *Haplomastodon chimborazi* (Proaño, 1922) from Bolivar and La Carolina, Ecuador. Measurements (in mm) of the humerus.

| | Specimen/site | | | |
|---|---|---|---|---|
| | Q. Pistud | | La Carolina | |
| **Measures** | MECN 95 | MECN 100 | EPN V-165 | EPN V-166 |
| 1. Greatest length from caput | 791 | 790 | 741 | 810 |
| 2. Greates length of lateral part | 866 | 870 | 778 | 846 |
| 3. Greatest breadth of caput | 218 | 206 | – | – |
| 4. Smallest breadth of diaphysis | 125 | 120 | – | – |
| 5. Smallest depth of diaphysis | 138 | 142 | – | – |
| 6. Length of epitroclear crest | 330 | 325 | – | – |
| 7. Breadth of distal articular surface | 230 | 226 | *c.* 214 | *c.* 214 |

On the basis of the preserved thoracic vertebrae of MECN 82, it can therefore be deduced that the dorsal outline originally produced by their spinous processes (Fig. 20) should have been similar to that observed in complete specimens of *M. americanum* (see Olsen 1979) and in "*S.*" *platensis* (Ferretti 2008a).

*Appendicular skeleton*

**Scapula (Fig. 12A-C; Table 9)**. In both scapulae of the Bolivar skeleton, the ossified dorsal cartilage is not fused, and only that of the right scapula was retrieved (Fig. 12A). The supraspinous fossa is sub-rectangular and fairly concave. The infraspinous fossa, more extended caudally than the former, is sub-triangular. Its cranial portion is concave and the caudal portion is convex. The scapular spine is prominent and terminates ventrally into an anterior acromian process (processus hamatus) and a posterior metacromian process (processus suprahamatus), separated by a shallow triangular surface. The acromian process is more developed than the metacromian one. The medial (costal) face cranially displays a shallow subscapular fossa and is rather convex in the central portion (Fig. 12B). In the dorsal half of the costal surface there is a wide, extremely rough triangular area for the origin the *m. serratus ventralis*. Caudally, the surface is flat and is delimited by the caudal angle of the scapula. The glenoid cavity is sub-rectangular, with the main axis directed cranio-caudally. The cavity is markedly concave cranio-caudally, and is less concave transversally. The supraglenoid tubercle is situated cranially to the glenoid cavity. The coracoid process is poorly developed and forms a short crest along the medial aspect of the glenoid cavity. The supraglenoid tubercle is not ventrally bent to a great extent (Fig. 12A).

**Humerus (Fig. 12D-G; Table 10)**. In the MECN 82 skeleton the left humerus is fractured at the epicondylar crest, while the right one is complete and undeformed. The epiphyses are fused to the shaft. The bone appears rather massive. The epicondylar crest, for the extensor of the forearm, is well developed. The deltoid tuberosity is moderately developed.

The tuberosity for *m. teres major* and *m. latissimus dorsi* is weakly pronounced and proximally positioned. The proximal epiphysis is massive and


FIG. 13. — *Haplomastodon chimborazi* (Proaño, 1922) from Q. Pistud, Bolivar, Ecuador, anterior limb bones: **A**-**D**, right ulna (MECN 82), in anterior, proximal, lateral and medial views; **E**-**G**, right radius (MECN 82), in lateral, anterior and medial views; **H**, **I**, incomplete right ulna of a newborn calf (MECN 458), in proximal and anterior views. Scale bars: A-G, 10 cm; H, I, 5 cm.

TABLE 11. — *Haplomastodon chimborazi* (Proaño, 1922) from Bolivar and La Carolina, Ecuador. Measurements (in mm) of the ulna (see Appendix 3).

| | Specimen/site | | | |
|---|---|---|---|---|
| | Q. Pistud | | | La Carolina |
| **Measures** | MECN 134 | MECN 418 | MECN 458 | EPN V-172 |
| 1. Greatest length | 765 | 750 | – | *c*. 800 |
| 2. Physiological length | 585 | 570 | – | 635 |
| 3. Length of olecranon | 230 | 230 | – | – |
| 4. Depth across processus aconaeus | 224 | 222 | – | – |
| 5. Breadth of proximal end | 220 | 224 | 80 | 240 |
| 6. Smallest breadth of diaphysis | 100 | 101 | 30 | – |
| 7. Smallest depth of diaphysis | 114 | 120 | 34 | – |
| 8. Breadth of distal end | 184 | 173 | – | – |
| 9. Depth of distal end | 174 | 190 | – | *c*. 250 |

TABLE 12. — *Haplomastodon chimborazi* (Proaño, 1922) from Bolivar, Ecuador. Measurements (in mm) of the radius (see Appendix 3).

| | Measures | | | |
|---|---|---|---|---|
| **Specimen (Site)** | 1. Length | 2. Breadth of proximal end | 3. Depth of proximal end | 4. Depth of distal end |
| MECN 82 (Q. Pistud) | 605 | 108 | 64 | 150 |

dominated by the articular head. This is very convex both dorso-caudally and latero-medially. The articular surface is wide at the center, tapers cranially and caudally. Medially and posteriorly, it is limited by a sulcus. This is distinct on the medial side, separating the articular surface from the medial tuberosity (trochine). The articular head is separated from the bicipital groove by the lateral tuberosity, which projects above the head. The distal articular surface is strongly convex antero-posteriorly. The trochlea is well developed, with a deep median depression, while the lateral border is weak and practically integrated with the condyle. The articular surface is delimited antero-proximally by a large coronoid fossa confluent to the radial fossa. Posteriorly, there is a deep olecranon fossa, bordered by the epicondyle and epitrochlea. Relative to the humerus long axis, the distal articular surface is latero-distally sloping. The humerus to ulna physiological length ratio in MECN 82 is 1.4.

**Ulna (Fig. 13A-D, H, I; Table 11)**. The ulna is relatively slender. The medial margin is flat and displays marks for the interosseous tendon. The epiphyses are completely fused with the shaft. The olecranon is massive and medially bent. The top of the olecranon is enlarged and rough with two tuberosites, one proximal, the latter medial. The semilunar notch is deeply concave vertically, convex transversally. The medial articular surface for the trochlea of the humerus is more developed than the lateral one, for the condyle, and dorsally-medially has a small articular area for the radius. The distal extremity of the ulna is slightly bent laterally. A strong styloid process occurs laterally. On the medial side, there is a wide diarthrodial surface for the radius. A subtriangular surface occurs distally for the pyramidal, formed by a palmo-lateral condyle, and is concave dorsally. Dorso-medially there is a small articular facet for the lunar. The articular surface for the pyramidal continues palmarly in a proximal direction and fuses with the facet for the pisiform.

Among the *H. chimborazi* remains from the Q. Cuesaca site there is a juvenile right ulna (MECN 458; Fig. 13H, I) belonging to a calf. The olecranic epiphysis is not fused to the shaft and was not retrieved. Distally the shaft is fractured at is palmar side, while dorsally it reaches to the diarthroidal surface for the distal epiphysis. A likely juvenile character is the slenderness of the shaft.

**Radius (Fig. 13E-G; Table 12)**. In MECN 82, the radii do not have completely fused distal ends. The shaft is narrow and flat is its proximal part, and thickens distally, assuming a triangular cross section. The bone axis in concave palmarly and has a lateral bending in its upper part. The proximal end, bearing the surface for the humerus and the ulna is laterally expanded. The surface for the humerus

is trapezoidal and concave antero-posterirorly. It is divided in three parts: the lateral-most part contributes with the ulna to the articulation with the condyle of the humerus. The middle part is convex and forms the coronoid process. The medial-most part is part of the articulation for the humeral trochlea. Palmarly and distally is the articular facet for the ulna and distally to it, an extremely rough triangular area for the insertion of tendons. The distal end, more voluminous than the proximal one, displays a triangular cross section. The articular facets for the lunar and the scaphoid are found on distal face of the radius. Both facets continue for a short distance on the palmar side. The articular facet for the lunar is laterally positioned and has a saddle form: palmarly convex and dorsally concave. The surface for the scaphoid is medial to the convex portion of the articulation for the lunar, and is also concave. In dorsal view the two surfaces form an angle of about 160°.

**Carpus (Figs 14; 15; Table 13).** Only three carpals from the right side and four from the left side of the Bolivar skeleton are preserved. Articular surfaces of each element of the carpus are schematically depicted in Figure 14.

In lateral view the scaphoid (radial carpal bone; Figs 14B, C; 15A-C) is triangular. The medial aspect is concave and rough. A large tuberosity, that projects above the proximal margin, is found on the dorsal margin of the scaphoid. A groove occurs distal to this tuberosity, and reaches to the distal margin of the bone. With its upper extremity it articulates with the radius (proximally) and with the lunar (medially). The lower extremity presents the facets for the lunar (dorsally), the magnum (palmarly), the trapezoid, and the trapezium (distally and palmarly).

The lunar (intermedium carpal bone; Figs 14D-F; 15D-H) is proximo-distally flattened, and subtriangular in proximal view. The proximal face bears the articulation for the radius and the ulna. The former is saddle-like. A strong margin divides, laterally, the surface for the radius from that for the ulna. The latter is very small, laterally facing, palmo-dorsally concave and convex proximo-distally. The dorsal aspect of the bone is sub-rectangular and very rough. The palmar angle is formed by a voluminous square tuberosity. The lateral and medial faces are irregular and dorso-palmarly elongated. Both bear on the proximal and distal margins the articular surfaces for the neighbouring carpals.

The lateral process of the pyramidal (ulnar carpal bone; Figs 14G; 15I-K) is not palmarly curved as in elephants. The pisiform (accessory carpal bone; Fig. 14H) is massive, with the distal tubercle slightly bent medially. It possesses two articular surfaces: proximally is a smaller one for the tibia and below, on the anterior face, a larger one for the pyramidal. The trapezoid (second carpal bone; Figs 14I-L; 15L-O) has a triangle-like shape in proximal view. The proximal face is occupied by the articulation for the scaphoid. This is wide dorsally and narrow palmarly. The medial margin is straight, while the lateral one forms a saddle-like articulation for the magnum. In specimen MECN 82 the sinuosity of the lateral margin of the trapezoid is indeed not particularly pronounced. There is no evidence of a distinct facet for the lunar on the proximal face of the trapezoid,

TABLE 13. — *Haplomastodon chimborazi* (Proaño, 1922) from Bolivar, Ecuador. Measurements (in mm) of carpal bones (see Appendix 3).

| | Measures | | |
|---|---|---|---|
| **Specimen/site** | 1. Breadth | 2. Depth | 3. Height |
| left lunar, MECN 45 (Q. Cuesaca) | 144 | 137 | 78 |
| left magnum, MECN 23 (Q. Cuesaca) | 79 | 104 | 82 |
| left unciform, MECN 46 (Q. Cuesaca) | 88 | 102 | 78 |
| right scaphoid, MECN 82 (Q. Pistud) | 67 | 130 | 109 |
| right lunar, MECN 82 (Q. Pistud) | 133 | 136 | 79 |
| right pyramidal, MECN 82 (Q. Pistud) | 157 | 124 | 55 |
| right trapezoid, MECN 82 (Q. Pistud) | 60 | 114 | 58 |
| right trapezoid, MECN 184 (Q. Pistud) | 70 | 114 | 67 |
| right magnum, MECN 82 (Q. Pistud) | 88 | 127 | 87 |
| right unciform, MECN 82 (Q. Pistud) | 132 | 130 | 92 |
| left unciform, MECN 183 (Q. Pistud) | 107 | 132 | 90 |

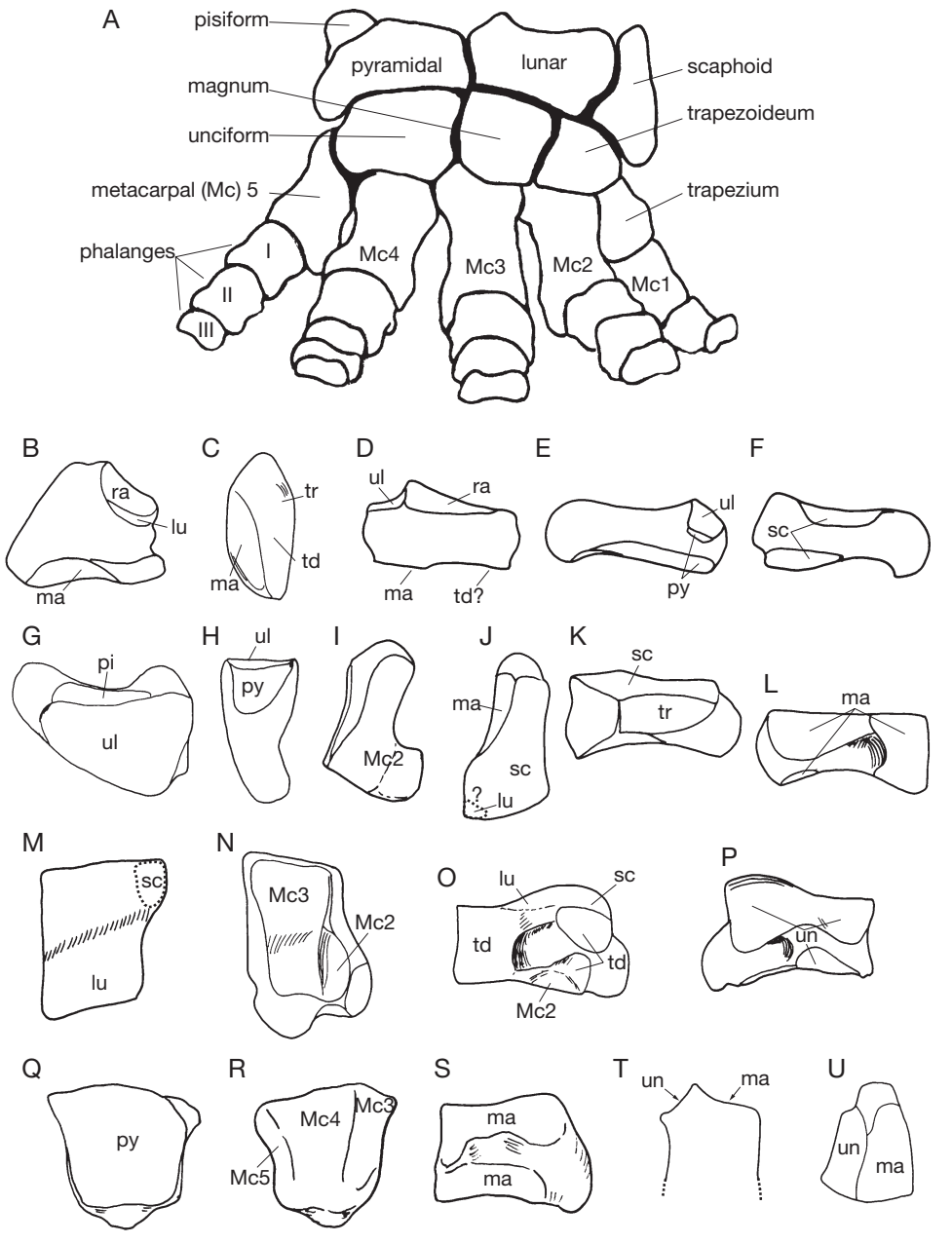


FIG. 14. — Schematic representation of *Haplomastodon chimborazi* (Proaño, 1922) carpals and third metapodial, showing extention of articular surfaces for contiguous bones (based on the Bolivar sample). All bones are from the right manus. **A**, reconstruction of the right manus, dorsal aspect (based on "*S.*" *platensis*, MNHN-PAM191) showing the position of various autopodial bones; **B**, **C**, scaphoid in lateral and distal views; **D**-**F**, lunar, in dorsal, lateral, and medial views; **G**, pyramidal, proximal view; **H**, pisiform, dorsal view; **I**-**L**, trapezoid, in distal, proximal, medial and lateral views. It is not possible to asses if the trapezoid articulates with the lunar (area enclosed by dotted line); **M**-**P**, magnum, in proximal, distal, medial, and lateral views; **Q**-**S**, unciform, in proximal, distal, and medial views; **T**, **U**, proximal end of right Mc3, in dorsal and proximal views. Abbreviations: **lu**, lunar; **ma**, magnum; **Mc1**, first metacarpal; **Mc2**, second metacarpal; **Mc3**, third metacarpal; **Mc4**, fourth metacarpal; **Mc5**, fifth metacarpal; **pi**, pisiform; **py**, pyramidal; **ra**, radius; **sc**, scaphoid; **td**, trapezoid; **tr**, trapezium; **ul**, ulna; **un**, unciform.

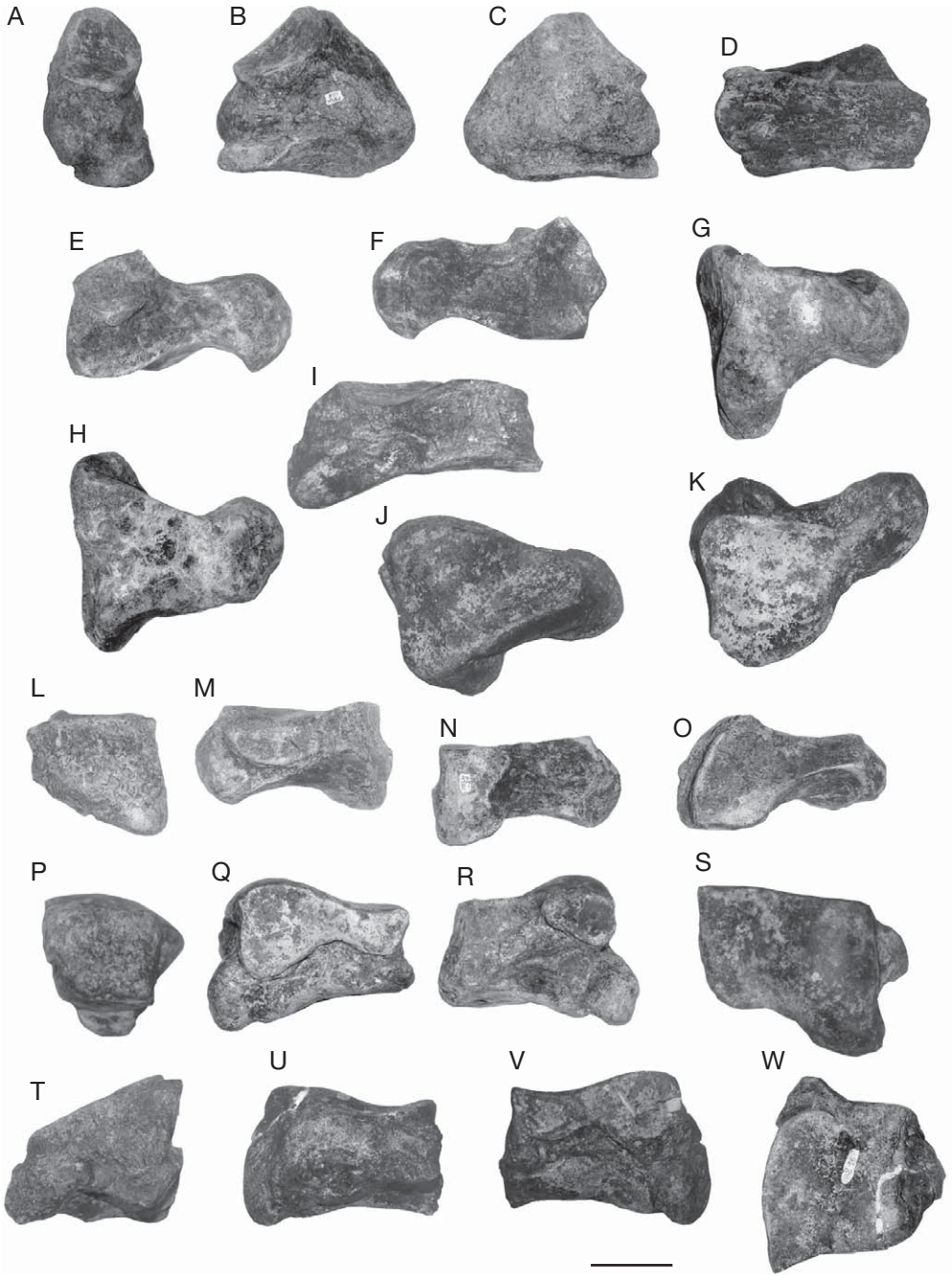


Fig. 15. — *Haplomastodon chimborazi* (Proaño, 1922) from Q. Pistud, Bolivar, Ecuador, carpal bones (MECN 82): **A**-**C**, left scaphoid, in dorsal, medial and lateral views; **D**-**H**, left lunar, in dorsal, medial, lateral, proximal and distal views; **I**-**K**, right pyramidal, in dorsal, proximal and distal views; **L**-**O**, left trapezoid, in dorsal, medial, lateral and proximal views; **P**-**S**, right magnum, in dorsal, lateral, medial and proximal views; **T**-**W**, right unciform, in dorsal, lateral, medial and proximal views. Scale bar: 5 cm.

TABLE 14. — *Haplomastodon chimborazi* (Proaño, 1922) from Bolivar. Measurements (in mm) of metapodials (see Appendix 3). Abbreviations: Mc, metacarpal; Mt, metatarsal.

| | | Measures | | | | | | |
|---|---|---|---|---|---|---|---|---|
| **Metapodial** | **Specimen** | 1. Length | 2. Smallest depth of diaphysis | 3. Smallest breadth of diaphysis | 4. Depth of proximal end | 5. Breadth of proximal end | 6. Depth of distal end | 7. Breadth of distal end |
| Mc2 | MECN 48 | 134 | 55 | 56 | 102 | 57 | 69 | 78 |
| Mc2 | MECN 462 | 125 | 50 | 54 | – | 51 | 63 | 65 |
| Mc2 | MECN 60 | 121 | 48 | 47 | *c.* 79 | *c.* 54 | 62 | 67 |
| Mc3 | MECN 218 | 148 | 55 | 74 | 110 | 86 | 88 | 90 |
| Mc3 | MECN 461 | 134 | 43 | 68 | – | 73 | 65 | 74 |
| Mc3 | MECN 17 | 149 | 45 | 63 | – | 78 | 67 | 80 |
| Mc4 | MECN 220 | 121 | 54 | 71 | 101 | 82 | 77 | 87 |
| Mc5 | MECN 82 | 130 | 64 | 66 | 94 | 82 | 83 | 83 |
| Mt3 | MECN 432 | 105 | 40 | 51 | 70 | 40 | 52 | 62 |
| Mt4 | MECN 431 | 95 | 47 | 56 | 70 | 70 | 64 | 69 |
| Mt4 | MECN 430 | 94 | 45 | 58 | – | 71 | 63 | 69 |

even though the latter might have articulated with the lunar along its dorso-lateral edge. The distal face has the articular face for Mc2. The dorsal face is planar and rough. The palmar margin is made up by a rounded tuberosity. The articulation for the trapezium is found on the medial face of the pyramidal. On the lateral face there are three facets for the magnum. The dorsal one is the larger, running from the proximal to the distal margin. A third, smaller facet for the magnum occurs in a palmar position, near the distal margin of the bone.

The magnum (third carpal bone; Figs 14M-P; 15P-S) is a quadrangular bone. The dorsal face has a squared outline and is very rough. The lateral face is trapezoidal and bears a large facet for the unciform. A second oval facet for the unciform is present dorsally, in proximity of the distal margin of the bone. Palmarly and distally there is a large hooked tubercle, distally directed. The medial side of the magnum has centrally a deep fossa for the interosseous ligaments. A quadratic articular facet for the trapezoid is present along the dorsal margin of the medial side. This facet has a prolongation running palmarly and proximally bordening the central fossa. The prolongation reaches the proximo-palmar facet for the trapezoid. A small fiissure separates the proximal facet from the distal facet for the trapezoid. The latter is linked to the dorsal facet through a dorsally sloping crest. The proximal face is quadrangular. Palmarly, on the medial margin, a process bears the articular surface for the scaphoid. For this reason, the medial margin has a sinuous outline, complementary to that of the lateral margin of the trapezoid. The proximal face is occupied by the articular surface for the lunar and, on the palmar angle, by that for the scaphoid. The articular surface is markedly convex palmarly and concave dorsally. The palmar face has a triangular outline. At the distal vertex of the triangle is a large tubercle, distally bent. The distal face is concave palmo-dorsally, and bears the articular facets for Mc2 and Mc3. The articular facet for the Mc2 does not reach the dorsal margin.

The unciform (fourth carpal bone; Figs 14Q-S; 15T-W) is a massive bone, possessing a trapezoidal outline. The proximal face slopes laterally and articulates with the pyramidal. The unciform articulates distally with the third, fourth and fifth metacarpals. Palmarly, the surface for the Mc5 is contiguous with that of the pyramidal. Two large surfaces for the magnum occur on the medial face.

**Metacarpus (Fig. 16; Table 14).** Three metacarpals are preserved. Mc5 is very short (Fig. 16A, E, H). The proximal articular surface is divided into two facets: a medial one for the unciform and a lateral one articulating with the lateral process of the pyramidal. The lateral face is proximally protruding, forming a tubercle from which a crest departs, dividing the facet for the unciform from that for the pyramidal.

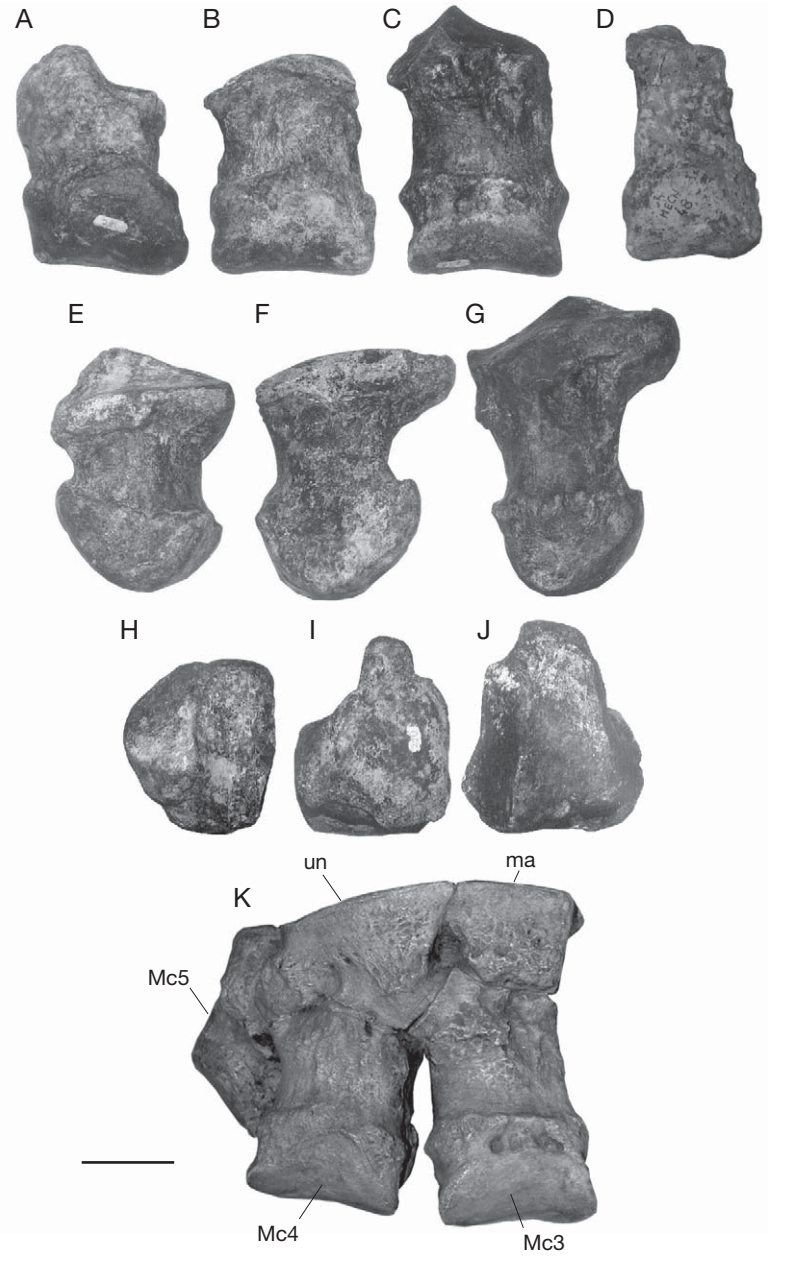


FIG. 16. — *Haplomastodon chimborazi* (Proaño, 1922) from Q. Pistud, Bolivar, Ecuador, metacarpals and partial manus: **A**, **E**, **H**, right Mc5 (MECN 82), in dorsal, medial, and proximal view; **B**, **F**, **I**, right Mc4 (MECN 82), in dorsal, medial and proximal views; **C**, **G**, **J,** right Mc3 (MECN 82), in dorsal, medial and proximal views; **D**, right Mc2 (MECN 462), dorsal view; **K**, partial manus (**cast**) with magnum (**ma**), unciform (**un**), third (**Mc3**), fourth (**Mc4**), and Fifth (**Mc5**) metacarpals in anatomical connection, dorsal view. Scale bar: 5 cm.

TABLE 15. — *Haplomastodon chimborazi* (Proaño, 1922) from Q. Pistud, Bolivar, Ecuador. Measurements (in mm) of the pelvis (see Appendix 4).

| Measures | MECN 82 |
|---|---|
| 1. Maximum length of pelvis | 1110 |
| 2. Maximum length of ilium: from tuber coxae to tuber sacrale | 840 |
| 3. Length of the symphysis | 420 |
| 4. Diagonal height of pelvic aperture: from the pubic symphysis to the lowest point of the tuber sacrale | 490 |
| 5. Diagonal height of pelvic aperture: from the pubic symphysis to the most caudal point of the tuber sacrale | 480 |
| 6. Maximum width of pelvic aperture, between the iliac crests | 460 |
| 7. Maximum breadth across the acetabula | 760 |
| 8. Width between eminentiae iliopubicae | 420 |
| 9. Smallest height of caudal margin of cranial branch of pubis | 80 |
| 10. Smallest height of cranial margin of cranial branch of pubis | 63 |
| 11. Smallest height of medial branch of ileum | 54 |
| 12. Smallest breadth of the shaft of ileum | 207 |

Mc4 is shorter than Mc3 (Fig. 16B, F, I). The proximal articular surface is convex and articulates with the unciform. Medially, the surface for the Mc3 does not reach the dorsal margin. The palmar tubercle is more slender than that of the Mc3.

The body of Mc3 is sub-cylindrical, sturdy, and flattened dorso-palmarly (Fig. 16C, G, J). Its dorsal face is convex, the lateral and medial faces are flat, and the palmar face is slightly concave proximo-distally. The proximal extremity is palmo-dorsally elongated. Proximally, it bears an extended articular surface divided by a sagittal crest. The medial articular facet is for the magnum. This has a trapezoidal outline and narrows palmarly. It is dorso-palmarly convex and medially sloping. The lateral facet articulates with the unciform. It is dorso-palmarly convex, transversely concave except in its palmar edge, where it is strongly inclined laterally. It is less extended palmarly than the facet for the magnum. The two facets are at an angle to one another. The crest dividing the two facets is dorsally elevated, forming a prominence, which slopes and then rises again palmarly. In proximal view the crest appears slightly wavy. Articulations for Mc4 and Mc2 are located, respectively, on the lateral and medial sides. A large tubercle is present palmarly, hanging over the palmar face. The distal extremity is larger than the proximal one. The large articulation for the proximal phalanx is concave transversely and convex dorso-palmarly. A slightly convex facet for the sesamoids bones is found palmarly.

A second right metacarpal (MECN 462; Fig. 16D), not belonging to the MECN 82 skeleton, is present among the Bolivar sample. The facet for the trapezoid is dorso-palmarly extended, while that for the trapezium occupies only the palmar half of the proximal surface.

**Pelvis (Fig. 17; Table 15).** Both halves of the pelvis of the MECN 82 skeleton are preserved. The acetabulum is directed caudally and ventrally. It is bounded by a sub-circular rim, and interrupted ventrally by a deep acetabular notch. The cranial portion of the lunate surface is less developed than the caudal one. Dorsally to the acetabulum, the ischial spine forms a sturdy and short tuberosity. On the cranial surface, at the point of junction with the pubis, the prominent ileo-pubic eminence reaches dorsally and laterally the short and weak arcuate line. Lateralward to the iliac eminence, a wide surface for the attachment of the *m. rectus femuris* is present.

The iliac wing arises from the median part of the hipbone through a short, cranially flattened and transversely broad, neck. The iliac wing is greatly extended transversally, and is cranially inclined. The gluteal (external) surface is plane, and it bends caudally at the level of the sacral tuberosity. The gluteal lines are well marked. The pelvic (internal) surface has a sub-triangular outline, is cranially oriented and it is bounded by the arcuate line medially and by the ventral margin of the ilium laterally. The

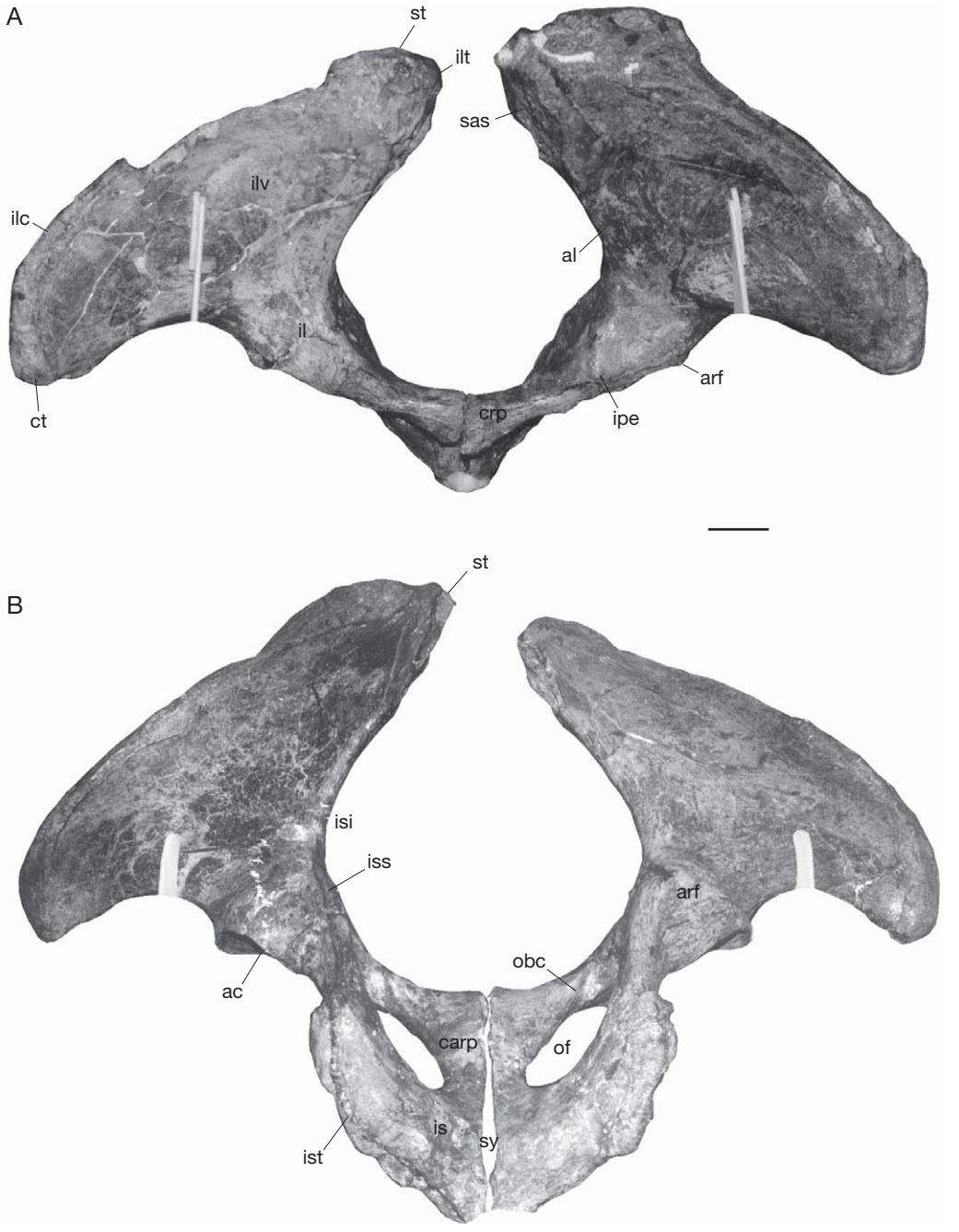


FIG. 17. — *Haplomastodon chimborazi* (Proaño, 1922) from Q. Pistud, Bolivar, Ecuador, pelvis (MECN 82): **A**, cranial view; **B**, caudal view. Abbreviations: **ac**, acetabulum; **al**, arcuate line; **arf**, area for *m. rectus femoris*; **carp**, caudal ramus of pubis; **crp**, cranial ramus of pubis; **ct**, coxal tuberosity; **il**, corpus of ileum; **ilc**, iliac crest; **ilt**, iliac tuberosity; **ilv**, iliac wing; **ipe**, ileo-pubic eminence; **is**, ischium; **isi**, incisura ischiatica; **iss**, ischiatic spine; **ist**, ischiatic tuberosity; **obc**, oblique obturator crest; **of**, obturator foramen; **sas**, sacral surface; **st**, sacral tuberosity; **sy**, ischio-pubic symphysis. Scale bar: 10 cm.

TABLE 16. — *Haplomastodon chimborazi* (Proaño, 1922) from Bolivar and La Carolina, Ecuador. Measurements (in mm) of the femur (see Appendix 5). *, measured at the same location as measure 5.

| | Specimen/site | | | | | | |
|---|---|---|---|---|---|---|---|
| | Q. Pistud | | La Carolina | | | | |
| **Measures** | MECN 98 | MECN 420 | EPN V-168 | EPN V-170 | EPN V-2009 | EPN V-2010 | EPN V-3846 |
| 1. Greatest length from caput | 965 | 960 | 990 | – | – | 1005 | 995 |
| 2. Lateral length | 900 | 890 | 941 | – | 942 | 945 | 915 |
| 3. Greatest breadth of proximal end | *c.* 370 | 360 | – | – | – | – | – |
| 4. Greatest depth of caput | 155 | 150 | 157 | – | – | – | 158 |
| 5. Smallest breadth of diaphysis | 132 | 131 | 158 | 146 | 157 | 145 | 154 |
| 6. Depth of diaphysis* | 88 | 82 | 98 | 92 | 93 | 88 | 94 |
| 7. Greatest breadth of distal end | 221 | 230 | 210 | 202 | 210 | – | 223 |
| 8. Depth of distal end | 226 | 223 | 212 | 210 | 236 | – | 232 |

internal surface is slightly concave. Along the arcuate line no tuberculum for the *m. psoas minoris* has been observed.

The arcuate line reaches dorsally the sacral tuberosity, and separates the pelvic surface from the sacral one. The latter is medially oriented, at an angle with the pelvic surface. The sacral surface is rough. Ventrally, an amphiarthrosial surface articulates with the sacrum, just below the iliac tuberosity. A cranially oriented amphiarthrosis for the fourth lumbar vertebra is situated cranially to the sacral surface. The crest of the ilium is thick and rough, ventrally and laterally directed. The crest ends ventro-laterally into an expanded coxal tuberosity. The ischiopubic part of the hipbone has a squared outline, with one of the vertex represented by the acetabulum. At the center, the great obturate foramen displays an oval outline, with the greater axis sagittally oriented. The body of the pubis enters into the formation of the acetabulum, of which it forms the ventral and cranial parts. The cranial branch of the pubis is robust and has an oval cross-section. Its dorsal surface is transversely concave, while the anterior one (pectineal surface) is planar. The caudal surface is crossed by the oblique obturator crest, which forms part of the medial margin of the obturator sulcus. The medio-cranial angle of the ischiopubic part is thick. Ventrally, it supports a robust ventral pubic spine. The caudal branch of the pubis is thin, depressed and fully fused to the ischium. Its medial border presents the symphysial surface.

The medial branch of the ischium is flattened and very short. It is continuous with the caudal branch of the pubis. The lateral branch of the ischium is characterized by torsion and joins the body of the ischium. The latter forms the caudal portion of the acetabulum. The cranial portion of the medial margin of the lateral branch of the ischium participates in the formation of the pubic symphysis. The caudal margin of the ischiatic table forms a thick and rough vertical margin, ventrally and medially directed. The dorsal extremity forms the tuberosity of the ischium. With its fellow the caudal margin constitutes the ischiatic arch. This has a V shape and its vertex is open ventrally.

**Femur (Fig. 18A-E; Table 16).** The femora of MECN 82 have both epiphyses fused to the shaft. The shaft is long, subcylindrical and flattened cranio-caudally. Narrow in the central portion, it widens approaching the extremities. Proximally, at about one third of the length of the medial margin, there is an elongated prominence slightly caudally placed, probably a homologue of the lesser trochanter. The head of the femur is perfectly hemispheric and delimited by a thick crest from the neck (Fig. 18E, B). Caudally there is, along the crest, a small round depressed surface for the femural ligament. The trochanter is massive, less elevated than the head and expanded cranio-caudally. Distally, the trochanter forms a robust margin, which integrates into the caudal margin of the lateral face of the shaft.

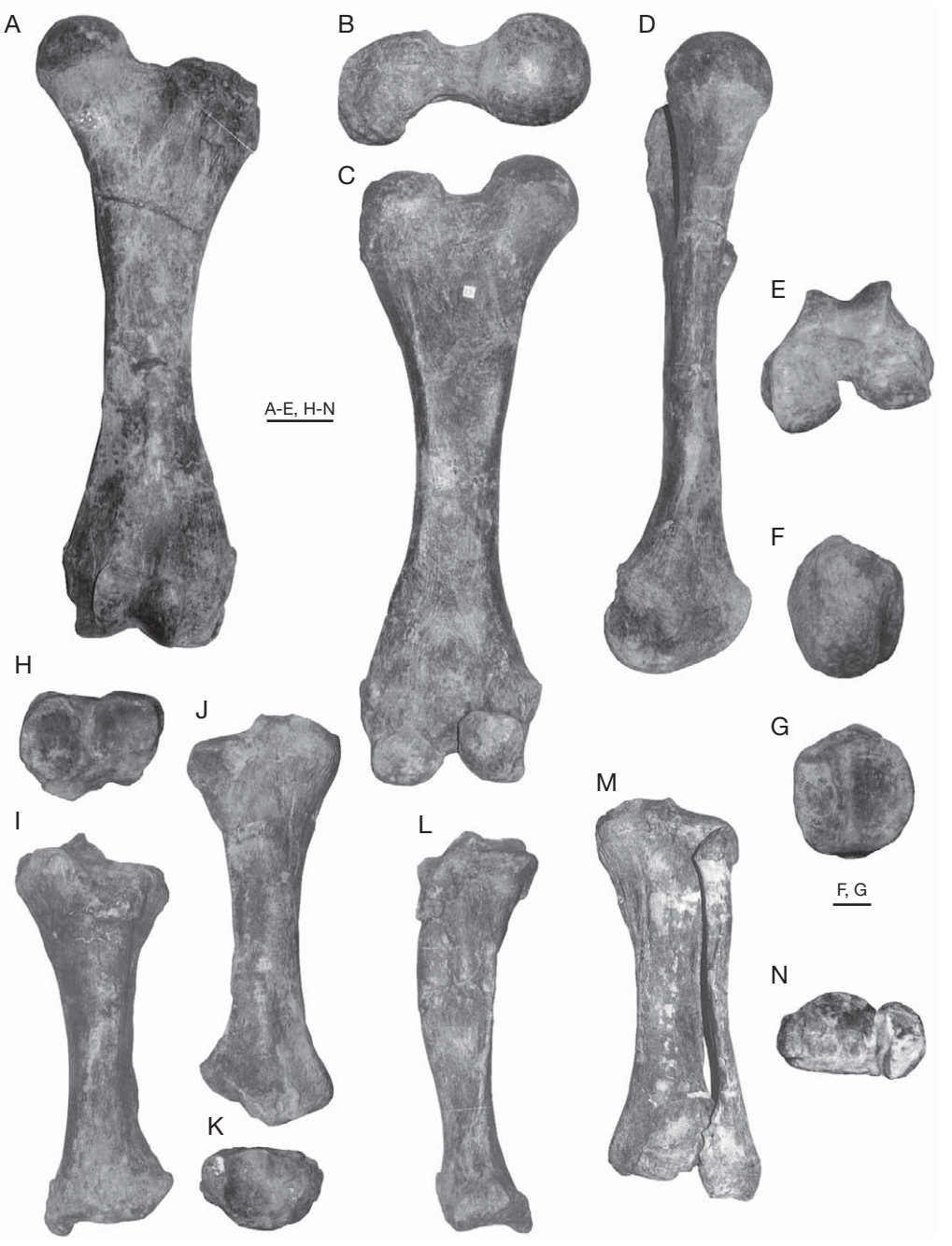


Fig. 18. — *Haplomastodon chimborazi* (Proaño, 1922), from Q. Pistud, Bolivar, Ecuador, hindlimb bones (MECN 82): **A**-**E**, left femur, in anterior, proximal, posterior, medial and distal views; **F**, **G**, right patella, in anterior and posterior views; **H**-**L**, left tibia, in proximal (anterior to the bottom), anterior view, posterior, distal (anterior to the bottom) and lateral views; **M**, **N**, right tibia and fibula in anatomical connection, in posterior and distal views. Scale bars: A-E, H-N, 10 cm; F, G, 5 cm.

TABLE 17. — *Haplomastodon chimborazi* (Proaño, 1922) from Bolivar and La Carolina, Ecuador. Measurements (in mm) of the tibia (see Appendix 5).

| Measures | Specimen/site | | | | | | | |
|---|---|---|---|---|---|---|---|---|
| | Q. Pistud | | La Carolina | | | | | |
| | MECN 83 | MECN 424 | EPN V-167 | EPN V-169 | EPN V-171 | EPN V-173 | EPN V-2010 | EPN V-3847 |
| 1. Greatest length | 605 | 580 | 649 | 606 | 638 | 695 | > 613 | 681 |
| 2. Lateral length | 475 | 480 | – | – | – | – | – | – |
| 3. Medial length | 570 | 575 | 620 | 580 | – | – | – | – |
| 4. Breadth at mid diaphysis | 95 | 96 | 116 | 102 | 111 | 109 | 104 | 114 |
| 5. Depth at mid diaphysis | 89 | 91 | – | – | – | – | – | – |
| 6. Breadth of proximal articular surface | 220 | 215 | 246 | 246 | 252 | 269 | 247 | 272 |
| 7. Depth of proximal articular surface | 160 | 170 | 181 | 176 | 193 | 206 | 165 | 216 |
| 8. Breadth of distal articular surface | 193 | 198 | 180 | 197 | 186 | 196 | 200 | 206 |
| 9. Depth of distal articular surface | 129 | 132 | 148 | 132 | 139 | 161 | 142 | 172 |

TABLE 18. — *Haplomastodon chimborazi* (Proaño, 1922) from Bolivar, Ecuador. Measurements (in mm) of the fibula (see Appendix 5).

| Specimen/site | Measures | | |
|---|---|---|---|
| | 1. Length | 2. Greatest breadth | 3. Greatest depth |
| MECN 422 (Q. Pistud) | 560 | 84 | 118 |

The distal extremity presents the condyles and, anteriorly, the patellar surface (Fig. 18E). The medial condyle is larger and more elongated than the lateral one. It is also slightly bent laterally, while the lateral one is rotated clockwise. From this it follows that the lateral condyle reaches a more distal plane than the medial one. The medial epicondyle is more developed than the lateral one. Two deep fossae, possibly for the insertion of the lateral knee ligament and *m. popliteus*, respectively, are found on the lateral side of the lateral condyle. The patellar surface is relatively large and characterized by wide median concavity.

**Patella (Fig. 18F, G)**. The kneecap has an elliptic outline. The cranial face is convex and rough. The caudal face is flat and bears the articulation for the trochlea. The proximal margin has a small tubercle. The distal margin is flat.

**Tibia (Fig. 18H-M; Table 17)**. The tibia has a prismatic-shaped shaft. The proximal portion is more expanded than the distal one. This is very evident in lateral view. The articular surface for the lateral condyle of the femur is sub-oval and concave. Caudally is the small facet for the fibula. The articulation for the medial condyle is circular and more expanded cranio-caudally. The distal extremity is trapezoidal in outline. On the distal face there is a square surface for the astragalus and latero-caudally a smaller facet of the fibula. A strong medial malleolus borders medially the articulation for the astragalus, on the medial side.

**Fibula (Fig. 18M; Table 18)**. In the MECN 82 skeleton, the left fibula lacks the proximal epiphysis, while the right one is complete. The proximal extremity of the fibula widens to form the head of the bone. On the cranio-medial faces a rounded surface for the tibia occurs. Caudally and laterally there are two tuberosities for ligaments. The lateral face of the distal extremity is convex and very rugose. The medial face bears a complex set of articular surfaces. At the base of a large fossa there is the articulation for the tibia, dorsally oriented. Ventrally and laterally to this there is a triangular articulation surface for the astragalus. On the ventral face there is a concave surface, which articulates with the calcaneum.

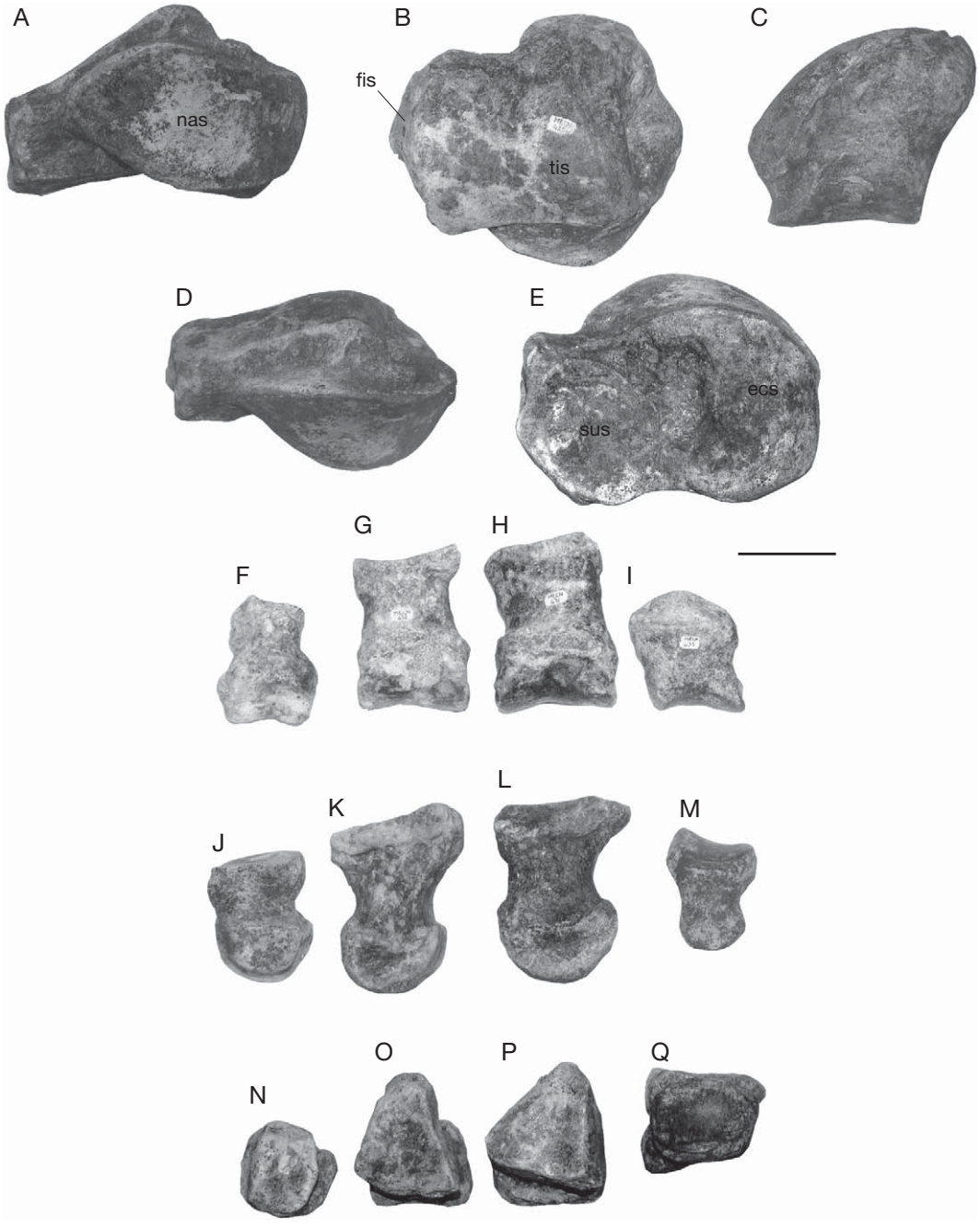


FIG. 19. — *Haplomastodon chimborazi* (Proaño, 1922) from Q. Pistud, Bolivar, Ecuador, astragalus, metatarsals and phalanx (MECN 82): **A**-**E**, right astragalus, in dorso-distal, proximal, medial, dorsal and distal views; **F**, **G**, **N**, right Mt1, in dorsal, medial and proximal views; **G**, **K**, **O**, left Mt3, in dorsal, medial and proximal views; **H**, **L**, **P**, left Mt4,in dorsal, medial and proximal views; **I**, **M**, **Q**, left proximal phalanx, in dorsal, medial and proximal views. Abbreviations: **ecs**, ectal surface; **fis**, articular surface for the fibula; **nas**, articular surface for the navicular; **sus**, sustentacular surface; **tis**, articular surface of the tibia. Scale bar: 5 cm.

TABLE 19. — *Haplomastodon chimborazi* (Proaño, 1922) from Bolivar, Ecuador. Measurements (in mm) of the astragalus (see Appendix 5).

| | Measures | | | | |
|---|---|---|---|---|---|
| **Specimen/site** | 1. Depth | 2. Breadth | 3. Height | 4. Greatest breadth of ectal surface | 5. Greatest breadth of sustentacular surface |
| MECN 425 (Q. Pistud) | 140 | 163 | 99 | 95 | 85 |
| MECN 143 (Q. Cuesaca) | *c.* 152 | *c.* 173 | *c.* 97 | 103 | – |
| MECN 47 (Q. Cuesaca) | 143 | 153 | 96 | 100 | 101 |

**Tarsus (Fig. 19A-E; Table 19).** Of the tarsus of the MECN 82 skeleton, only the astragalus is represented. No other tarsals are present in the Bolivar sample. The right astragalus is complete and not deformed. The surface for the tibia is rectangular, and mediolaterally more elongated in comparison with that of elephants. On the lateral margin is the surface for the fibula. The medial tubercle is poorly developed. The surface for the navicular (central tarsal bone) occupies the two thirds of the antero-distal (dorso-distal) side. The two surfaces for the calcaneum are well separated from each other by a deep sulcus for the attachment of ligaments on the postero-distal (palmo-distal) side (Fig. 19E). The ligamentous surface widens anteriorly. The medial surface (sustentacular) for the calcaneum is bean-shaped and dorso-palmarly directed. The lateral surface (ectal) is oval, with its major axis directed laterally and anteriorly (dorsally).

**Metatarsus (Fig. 19F-Q; Table 14).** Five metatarsals of the Bolivar skeleton are preserved. These are markedly shorter than the metacarpals. The proximal extremity of Mt1 (Fig. 19 F, J, N) has an oval outline. The distal one is much more transversely expanded.

The proximal articular surface of Mt3 (Fig. G, K, O) is triangular and transversely concave. The articulation for the sesamoids forms two distinct condyles.

The proximal extremity of Mt4 is medially rotated (Fig. 19H, L, P). The proximal articular surface is triangular and almost entirely devoted to the articulation with the cuboid.

**Discussion.** The postcranial material of *H. chimborazi* from Bolivar is characterized by a large amount of size variability, without exhibiting any clear (sexual) dimorphic pattern. The mean size of the gomphotheres from Bolivar, as can be deduced from the skeletal elements (Tables 2-19), is greater than that of *C. hyodon*, while it is similar to that of "*S.*" *platensis*. The postcranium of *H. chimborazi* shows a typical elephantoid pattern. *Haplomastodon chimborazi* displays, however, a more robust skeleton than both *Gomphotherium* (e.g., *G. sylvaticum*; Tassy 1977) and more derived elephantoids such as *A. arvernensis* and elephantids.

Brevirostrine and longirostrine elephantoids are characterized by a different proportion between the bones of the anterior limb (Ferretti 1998). In many longirostrine forms (e.g., *Gomphotherium*), the humerus to ulna physiological length ratio is about 1, whilst in brevirostrines it is usually higher than 1.2 (e.g., *A. arvernensis* = 1.3-1.4; in elephantines is >1.25). In *H. chimborazi* (MECN 82) the humerus to ulna ratio is 1.4, displaying thus a typical "brevirostrine" limb proportion.

The structure of the basipodial of *H. chimborazi* is typically elephantoid. *Haplomastodon chimborazi* possesses relatively short basipodials, similarly to other gomphotheres (Fig. 16K). Some elements posses interlocking surfaces. The whole structure appears very robust and firm, a possible adaptation to traversing uneven grounds. The available material prevents us from knowing whether in *H. chimborazi* the lunar articulated distally with the trapezoid, producing the so-called aserial carpus (Weithofer 1889). However, the condition in *C. hyodon* and "*S.*" *platensis*, as reported by Boule & Thevenin (1920: 60), is aserial. In *A. arvernensis*, a brevirostrine ghomphotere from the Old World, the superposition of the lunar on the trapezoid is markedly more developed than in SA gomphotheres. Such differences could have important functional implications related to limb posture and feeding habits (Ferretti & Croitor 2001).

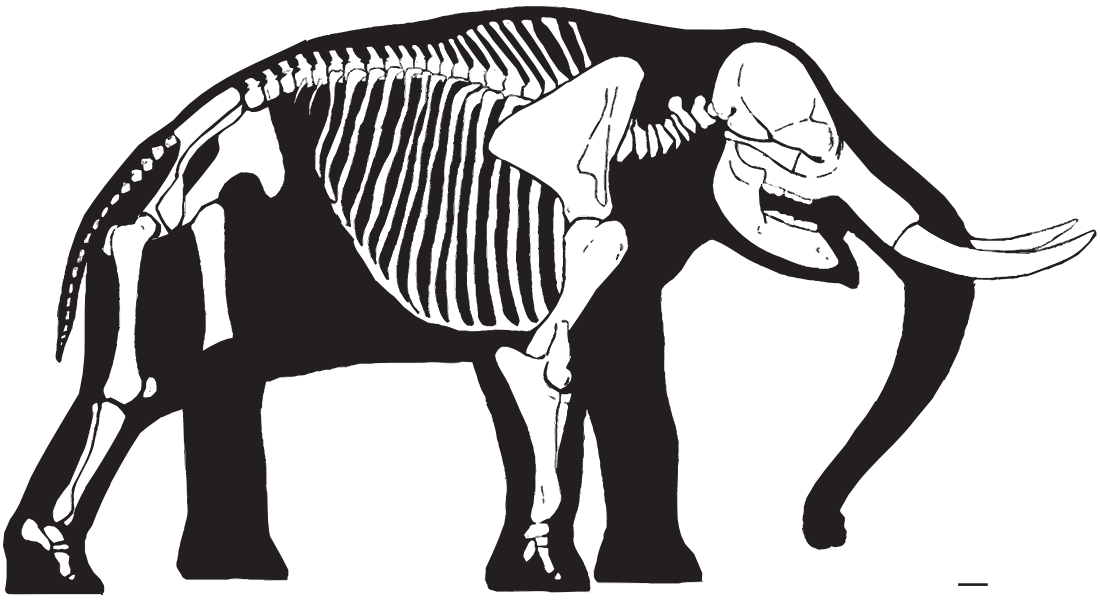

FIG. 20. — Reconstruction of the skeleton of *Haplomastodon chimborazi* (Proaño, 1922), based on MECN 82 and the Punin skull. Scale bar: 10 cm.

SIZE, ONTOGENETIC STAGE AND GENDER DETERMINATION OF INDIVIDUAL MECN 82

Estimates based on humerus length using Harington *et al*. (1974) methods and direct measurements of the associated anterior limb, indicate a shoulder height for individual MECN 82 of about 2.5 m. Body mass estimates for MECN 82, obtained using shoulder height-mass equation based on exant Asian elephant (Roth 1990), is 3125 kg.

The ontogenetic stage of individual MECN 82 was assessed through the stage of skeletal fusion (especially that of the bones of the skull and of the limbs) and, independently, on the base of the molar progression (dental stage), by comparison with the pattern of skeletal fusion and dental progression in living elephants (Sikes 1966; Roth 1994). The cranial sutures of MECN 82 are not discernible, except for the zygomatics, which are yet not fused with the zygomatic processes of the maxillary and of the temporal, and were collected separately from the cranium. In extant elephants the zygomatic remains detached until late in the life of the animal. Among the *Elephas maximus* samples examined (ACM, MNHN, MSNFZ, NHM) there are specimens with the M3 in use that still have not completely fused zygomatic arches. In the MECN 82 postcrania, the dorsal epiphysis of the scapula is completely detached, and the distal radius suture is still open, while in the rest of the bones the epiphyses are well knit. MECN 82 has the M2 in use and the M3 erupting, with wear facets on the first three loph(id)s.

Both the stage of skeletal fusion and the dental progression methods are consistent with MECN 82 representing a prime adult individual (see Roth 1994; Sikes 1966). In terms of African elephants molar age (AEMA; Sikes 1966) MECN 82 died at an age of approximately 25-30 years.

Sexual dimorphism in proboscideans is well marked. In osteological specimens it is revealed by the larger size of the skeletal elements of the males (Deraniyagala 1955; Haynes 1991), the size and robusticity of the tusks (Haynes 1991; Averianov 1996), the morphology of the skull (Beden 1979; Averianov 1996) and by the morphology of the pelvis (Haynes 1991; Kroll 1991; Lister & Agenbroad 1994; Lister 1996; Göhlich 2000). A number of studies have demonstrated that fossil probo-

TABLE 20. — Comparison of measurements ratios of pelvis of *Haplomastodon chimborazi* (MECN 82) and of recent elephants, *Loxodonta africana* (Blumenbach, 1792) and *Elephas maximus* Linnaeus, 1758 (data from Kroll 1991). Labels of measures as in Table 15.

| | Pooled sample of male | | Pooled sample of female | | |
|---|---|---|---|---|---|
| **ratio** | N | min-Max | N | min-Max | **MECN 82** |
| 8/3 | 3 | 0.94-1.01 | 3 | 1.25-1.47 | 01:10 |
| 8/12 | 3 | 1.97-2.28 | 4 | 2.27-3.34 | 02:22 |
| 4/12 | 3 | 2.05-2.56 | 3 | 2.90-3.50 | 02:37 |

scideans display an amount of sexual dimorphism comparable to that of modern elephants (see Tassy 1996b and Haynes 1991 and citations therein). The strength and size of the skeletal elements, and of the tusks, indicate that MECN 82 is a male. The proportions of the pelvis, in particular the relative width of the pelvic aperture and the thickness of the acetabular region, are comparable with those reported for male elephants (Table 20; Haynes 1991; Kroll 1991; Lister & Agenbroad 1994; Lister 1996; Göhlich 2000).

## PHYLOGENETIC ANALYSIS

### RESULTS

The phylogenetic analysis was performed on a matrix of 11 taxa (Appendix 7) and 25 characters (Appendix 6).

Three most parsimonius trees (MPT) of 49 steps each were obtained. They have a consistency index (CI) of 0.65, a retention index (RI) of 0.79, and a homoplasy index (HI) of 0.35. The rescaled consistency index (RC) is of 0.51.

The three trees (Fig. 21) express the conflicting evidence in the phylogenetic resolution of *H. chimborazi*,"*S.*" *platensis*, and *C. hyodon*, i.e. the South American gomphotheres. The three possible hypotheses consist of two paired associations ((*H. chimborazi*,"*S.*" *platensis*) *C. hyodon*) and ((*C. hyodon*,"*S.*" *platensis*) *H. chimborazi*)) respectively, and a trichotomy, (*C. hyodon*,"*S.*" *platensis*, *H. chimborazi*). The strict consensus tree is identical to the MPT with the SA gomphotheres' trichotomous topology (Fig. 21A). Each of the three SA taxa is diagnosed by a set of apomorphies. Two homoplastic apomorphies characterize *H. chimborazi*, both concerning modifications of the upper tusk: presence of markedly upturned upper tusk (13 (2)), and absence of the enamel band of upper tusk at the adult growth stage (14 (2)). One of the MPT (Fig. 21C, node 8') supports a *H. chimborazi*, "*S.*" *platensis* clade, based on three equivocal homoplastic characters (ACCTRAN option): slightly diverging tusk alveoli (4 (1)), enamel band of upper tusk usually absent (14 (1)), and enamel band, when present, without helical torsion (15 (0)), the latter representing a reversal. The alternative hypothesis (Fig. 21B, node 8), that "*S.*" *platensis* is more closely related to *C. hyodon*, is weakly supported by one equivocal character reversal (DELTRAN option): enamel band of upper tusk sometimes present at the adult growth stage (14 (1)). The monophyly of South American gomphotheres (Fig. 21A, node 7) is, on the other hand, well supported by five unambiguous characters, of which four (12 (1): presence of a coronoid fossa; 19 (2): fully trilophodont DP3/dp3; 23 (1): transverse foramen of atlas sometimes absent; 24 (1); atlas with a large dorsal tuberosity) are unique synamoporphies (RI = 1.0).

According to the result of the analysis, *Rhynchotherium* cf. *falconeri* is the sister taxon of South American gomphotheres (Fig. 21A, node 6), a hypothesis supported by four unequivocal characters of which two (5 (1): loss of supraorbital foramen and 6 (1): presence of a subnasal fossa) represent non-homoplastic synapomorphies. Noteworthy, *Stegomastodon texanus* is not closely related neither to "*S.*" *platensis* nor to *H. chimborazi*, but is placed as the sister taxon of the *Rhynchotherium* + South American gomphotheres clade (Fig. 21A, node 5), based on one non-homoplastic synapomorphy (3 (1): robust premaxillaries), and one homoplastic character (21 (1): third loph in DP3 outlined). The Asian *Sinomastodon hanjiangensis* (Fig. 21A, node 4) is united to the New world brevirostrine taxa by five unequivocal characters, three of which are unique synapomorphies (2 (1): wide forehead; 8 (1): symphysis downturned; 18 (1): loss of P2-P4). *Gnathabelodon thorpei* (node 3), *Eubelodon morilli* (node 2), and *Megabelodon lulli* (node 1) are successive outgroups to the bre-

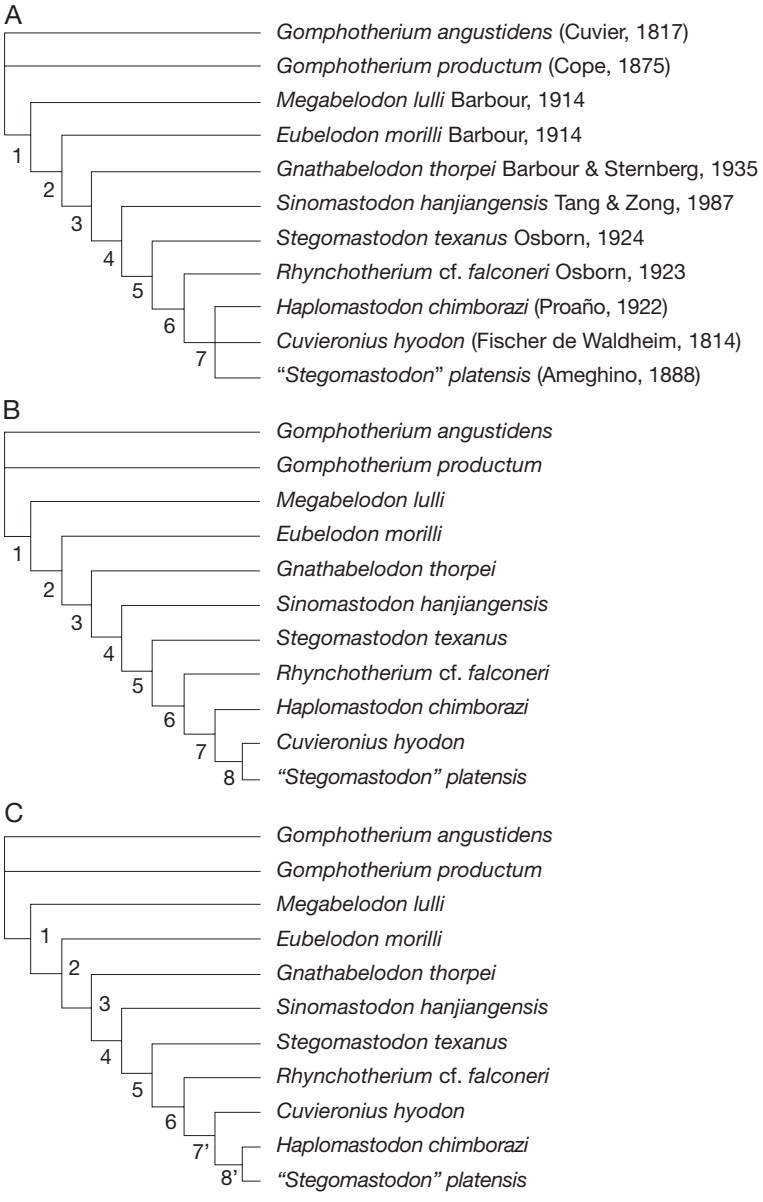


FIG. 21. — The three most parsimonius trees (MPT) of New World gomphotheres from the current study (length = 49 steps; CI = 0.65; RI = 0.79). The topology of the MPT depicted in **A** is identical to that of the strict consensus tree. List of synapomorphies (in bold, non-homoplastic character; *, homoplastic character; in italics, unbiguous character; -, reversal): **A**, node 1: 16 (1)*; node 2: **9 (1)**, 14 (2)*; node 3: 13 (1)*; node 4: 1 (1)*, **2 (1)**, 7 (1)*, **8 (1)**, *10 (1)**, **18 (1)**, ***19 (1)***, 20 (1)*; node 5: **3 (1)**, 21 (1)*, *22 (1)*; node 6: 4 (1)*, **5 (1)**, **6 (1)**, -14 (1)*; node 7: 11 (1)*; **12 (1)**, **19 (2)**, **23 (1)**, **24 (1)**. **B**, node 8: *-14 (1)**; **C**, node 8': *-4 (1)**; *14 (1)**; *-15 (0)**.

virostrine clade. *Gomphotherium productum* and *G. angustidens* are basal to all the rest of the New world gomphothere taxa.

A bootstrap analysis (1000 replicates) showed that all the clades present in the strict consensus topology have relatively high bootstrap proportion

values (BP > 60), except for the clades defined by nodes 3 and 4, which have BP values of 47 and 35, respectively.

### Discussion

Results of the present phylogenetic analysis provide further morphological evidence for a monophyletic South American clade, corresponding to the gomphotheriid subfamily Cuvieroniinae Cabrera, 1929. A major difference from previous studies, however, is that NA *Stegomastodon* is shown not to group within the Cuvieroniinae. The analysis demonstrates that "*S.*" *platensis* is in fact not closely related to NA *Stegomastodon*, as was already suggested by Osborn (1936), Savage (1955), Madden (1984), and Webb (1992), and therefore its removal from *Stegomastodon* is supported. The morphological dataset used in the analysis does not provide unequivocal support for any single, dichotomously branching species tree linking *H. cimborazi*, "*S.*" *platensis* and *C. hyodon*. The hypothesis that *H. chimborazi* and "*S.*" *platensis* are more closely related to each other than either is to *C. hyodon*, as suggested by several authors (Hoffstetter 1952; Savage 1955; Tassy 1985; Prado & Alberdi 2008) is, in fact, just one of the three most parsimonius solutions found. Among these, the hypothesis that the ancestral separation of the three SA gomphothere species is actually the result of a single trichotomous branching event should also be taken into consideration. This last hypothesis would be consistent with the mostly disjunct fossil distribution of the three taxa (Prado *et al*. 2005; Ferretti 2008a). For these reasons, the generic name *Haplomastodon* is conservatively retained as a distinct taxon from South American "*Stegomastodon*".

The analysis supports the hypothesis, advocated by Savage (1955), Miller (1990), and Shoshani (1996), that *Rhynchotherium* is the sister taxon of SA gomphotheres.

This result differs from that provided by Prado & Alberdi (2008), which indicates a sister group relationship between SA gomphotheres and *Sinomastodon*, a hypothesis also presented by Shoshani (1996: 152) as one of the most parsimonious solutions of his own analysis of the Proboscidea. In the Prado & Alberdi's (2008) study, the grouping of *Sinomastodon* with SA gomphotheres is supported by two characters: loss of lower tusk and occurrence of a brevirostrine mandible. However, the first character actually represents a more inclusive feature among NA gomphothere, as also *Eubelodon* Barbour, 1914 and *Gnathabelodon* Barbour & Sternberg, 1935 possess tuskless mandibles (Barbour & Sternberg 1935; Osborn 1936; Lambert & Shoshani 1998). As a matter of fact, the codings of this character for *Eubelodon* (0, i.e. lower tusk present) and *Gnathabelodon* (1, i.e. lower tusk reduced) in the data matrix provided by Prado & Alberdi (2008: table 2) is either a mistake or is based on new observations, which are not discussed or mentioned by the authors. On the other hand, the new characters used in the present analysis and the improved morphological data for *Rhynchotherium* cf. *falconeri* (LVNHM 871) and *Sinomastodon* (based on Zong *et al*. 1989), provide substantial support for a *Rhynchotherium*-SA gomphotheres clade, based on four unequivocal characters. Finally, the analysis does not support the proposed synonymy of *Megabelodon* and *Gomphotherium* advocated by Tobien (1973) and Shoshani (1996), although they are only removed from each other by a single step.

Eleven of the 23 synapomorphies that define the seven nodes depicted by the strict consensus tree topology (Fig. 21A) are homoplastic. Among these homplasies, parallelisms are far more frequent than reversals.

## CONCLUSIONS

The knowledge gained from the abundant and well preserved *Haplomastodon chimborazi* material from Bolivar, Ecuador provided new and improved morphological data to test phylogenetic hypotheses of New World gomphotheres, focusing on the relationships and systematics of South American taxa. New anatomical research and additional specimens are, however, needed to remove much of the missing data and to provide a taxonomically more comprehensive dataset. The systematic revision of *Haplomastodon* indicates that this genus contains only a single South American species, whose valid name is *H. chimborazi*. *Haplomastodon waringi* is

considered a *nomen dubium*. Body size estimates based on an adult male skeleton from Bolivar shows that *H. chimborazi* was comparable is size to the extant Asian elephant, with a shoulder height of about 2.5 m and a body mass of three metric tons. The results of the cladistic analysis provided further morphological support for a monophyletic SA gomphothere clade (the Cuvieroniinae), though the interrelationships within the group could not be definitively resolved. The analysis demonstrates that "*Stegomastodon*" *platensis* represents an endemic SA taxon distinct from NA *Stegomastodon*, the latter being in fact not closely related to the Cuvieroniinae. According to the results of the phylogenetic analysis and based on the known stratigraphic distribution of the taxa considered (see Lambert & Shoshani 1998 and Tobien *et al*. 1986), the Cuvieroniinae originated in North America during the Pliocene from a derived *Rhynchotherium*-like ancestor and then dispersed to South America, where the group differentiated during the Pleistocene, likely triggered by geographic factors. The earliest representatives of NA *Stegomastodon* (referred to *S. primitivus*) are reported from Late Hemphillian sites in the United States (Lambert & Shoshani 1998), indicating that the NA *Stegomastodon* and the *Rhynchotherium*-Cuvieroniinae lineages diverged by the latest Miocene. The split between the Asian *Sinomastodon* and the New World brevirostrine gomphothere lineages can be also traced back to the Late Miocene, corresponding to the age of the oldest finds of *S. intermedius* from China (Tobien *et al*. 1986).

The analysis revealed that, rather than a linear progression from longirostrine to brevirostrine "elephant-like" morphologies, New World trilophodont gomphothere evolution is characterized by extensive homoplasy, especially in the form of parallelisms.

**Acknowledgements**

I dedicate this work to Jeheskel "Hezy" Shoshani (1943-2008), a true teacher and a good friend, whose fundamental contribution to the sudy of proboscidean anatomy and evolution, and dedication to the study and preservation of living elephants, have been, and still are, truly inspiring.

For access to collection, discussions and useful insights, I am grateful to: M. S. Bargo, A. Cione, E. P. Tonni, S. Vizcaino (MLP), M. Moreno Espinosa, G. Roman Jimenez (MECN), F. Rios Paredes (MUT), A. Currant (NHM), J. Meng (AMNH), P. Tassy (MNHN), and L. Werdelin (NMR). I thanks T. Gordón A. and N. E. Báez T., (UCE), for help in locating the type material of *H. chimborazi* in the UCE collections. Particular thanks go to G. Ficcarelli (IGF) for providing the original impetus to my research on SA proboscideans and for his help and encouragements throughout this study. I am also indebted to M.T. Alberdi (Madrid), V. Borselli, F. Cozzini, F. Landucci, L. Rook, M. Rossi, G. Tito (IGF), M. Coltorti, P. L. Pieruccini (University of Siena), U. B. Göhlich (Naturhistorisches Museum Wien), R. Debruyne (MNHN) for help, discussion and constructive criticism. Victoria Herridge (NHM) helped with the English text. I thank Cyrille Delmer (NHM) and Regis Debruyne for the French translation of the abstract. H. Shoshani and L. Rook critically read and commented on an early draft of the paper greatly improving it. I gratefully thank R. W. Graham, A. Ohler, W. J. Sanders, and P. Tassy for helpful review of an early version of the manuscript.

Work supported by grants from the University of Firenze (Fondi di Ateneo), the Italian C.N.R., and M.I.U.R (Cofin 2000, 2002).

## REFERENCES

ALBERDI M. T. & PRADO J. L. 1995. — Los mastodontes de América del Sur, *in* ALBERDI M. T., LEONE G. & TONNI E. P. (eds), Evolucion biologica y climatica de la Region Pampeana durante los ultimos 5 miliones des años. Un ensayo de corrélacion con el Mediterraneo occidental. *Monografias de Museo Nacional de Ciencias Naturales y Consejo Superior de Investigaciones Científicas, Madrid* 12: 277-292.

ALBERDI M. T., PRADO J. L. & SALAS R. 2004. — The Pleistocene gomphotheres (Gomphotheriidae, Proboscidea) from Peru. *Neues Jahrbuch für Geologie und Paläontologie Abhandlungen* 231: 423-452.

ANONYMOUS 1903. — Le Mastodonte du Chimborazo. *Cosmos* Paris, n.s., 48/936: 6-9.

ARÁUZ J. 1950. — Nueva historia de los Mastodontes ecuatorianos. *Boletin de Informaciones Científicas Nacional* 3 (26-27): 419-425.

AVERIANOV A. O. 1996. — Sexual dimorphism in mammoth skull, teeth, and long bones, *in* SHOSHANI J. & TASSY P. (eds), *The Proboscidea. Evolution and Palaeoecology of Elephants and their Relatives*. Oxford University Press, Oxford: 260-267.

BARBOUR E. H. 1914. — Mammalian fossils from Devil's Gulch. *Nebraska Geological Survey* 4: 177-190.

BARBOUR E.H. & STERNBERG G. 1935 — *Gnathabelodon thorpei*, gen. et sp. nov. A new mud-grubbing mastodont. *Bulletin of the Nebraska State Museum* 1: 395-404.

BEDEN M. 1979. — *Les éléphants (*Elephas *et* Loxodonta*) d'Afrique orientale : systématique, phylogénie, intérêt biochronologique*. PhD Thesis, Université de Poitiers, 567 p. (unpublished).

BELL R. H., SWIGART L. L. & ANSON B. J. 1950. — The relation of the vertebral artery to the cervical vertebrae. Based on a study of 200 specimens. *Quarterly Bullettin of the Northwestern University Medical School* 24: 184-185.

BOULE M. & THEVENIN A. 1920. — *Mammifères fossiles de Tarija*. Imprimerie nationale, Mission scientifique G. de Créqui-Monfort et F. Sénechal de la Grange, Paris, 256 p.

CABRERA A. 1929. — Una revision de los mastodontes argentinos. *Revista del Museo de La Plata* 32: 61-144.

CAMPBELL K. E. JR, FRAILY C. D. & ROMERO-PITTMAN L. 2000. — The late Miocene Gomphothere *Amahuacatherium peruvium* (Proboscidea: Gomphotheriidae) from Amazonian Peru: implications for the Great American Faunal Interchange. *Boletin de Estudios Regionales IGEMMET*, Serie D, 23: 1-152.

CAMPBELL K. E. JR, FRAILEY C. D. & ROMERO-PITTMAN L. (2009). — In defense of *Amahuacatherium* (Proboscidea: Gomphotheriidae). *Neues Jahrbuch für Geologie und Paläontologie Abhandlungen* 252 (1): 113-128.

CASAMIGUELA R. M., SHOSHANI J. & DILLEHAY T. D. 1996. — South American proboscideans: general introduction and reflections on Pleistocene extinctions, *in* SHOSHANI J. & TASSY P. (eds), *The Proboscidea. Evolution and Palaeoecology of Elephants and their Relatives*. Oxford University Press, Oxford: 316-320.

COLTORTI M., FICCARELLI G., JAHREN H., ROOK L. & TORRE D. 1998. — The last occurrence of Pleistocene megafauna in the Ecuadorian Andes. *Journal of South American Earth Sciences* 11 (6): 581-586.

COSTALES SAMANIEGO A. 1950. — *Masthodon Chimborazi* Proaño. *Boletin de Informaciones Científicas Nacional* 3 (35): 372-375.

DERANIYAGALA P. E. P. 1955. — *Some Extinct Elephants, their Relatives and the Two Living Species*. Ceylon National Museum Publication, Colombo, 161 p.

EALES N.B. 1928. — The anatomy of a foetal African elephant (*Loxodonta africana*). *Transactions of the Royal Society of Edinburgh* 56: 206-246.

FERRETTI M. P. 1998. — *Gli Elefanti del Plio-Pleistocene dell'Italia*. Doctoral thesis, Modena, Bologna, Firenze, and Roma associated Universities, 272 p. (unpublished).

FERRETTI M. P. 2008a. — A review of South American gomphotheres. *New Mexico Natural History and Science Museum Bulletin* 44: 381-391.

FERRETTI M. P. 2008b. — Enamel structure of *Cuvieronius hyodon* (Proboscidea, Gomphotheriidae) with a discussion on enamel evolution in elephantoids. *Journal of Mammalian Evolution* 15 (1): 37-58.

FERRETTI M. P. 2009. — Comment on the proposed conservation of usage of *Mastodon waringi* Holland, 1920 (currently *Haplomastodon waringi*; Mammalia, Proboscidea) by designation of a neotype. *Bulletin of Zoological Nomenclature* 66 (2): 358-359.

FERRETTI M. P. & CROITOR R. 2001. — Functional morphology and ecology of Villafranchian Proboscideans from Central Italy, *in* CAVARETTA G., GIOIA P., MUSSI M. & PALOMBO M. R. (eds), *The World of Elephants - Proceedings of the 1st International Congress, Rome, 16-20 October*, Consiglio Nazionale delle Ricerche, Roma: 103-108.

FICCARELLI G., AZZAROLI A., BORSELLI V., COLTORTI M., DRAMIS F., FEJFAR O., HIRTZ A. & TORRE D. 1992. — Stratigraphy and Paleontology of Upper Pleistocene deposits in the Interandean Depression, northern Ecuador. *Journal of South American Earth Sciences* 6 (3): 145-150.

FICCARELLI G., BORSELLI V., MORENO ESPINOSA M. & TORRE D. 1993. — New *Haplomastodon* finds from the Late Pleistocene of Northern Ecuador. *Geobios* 26 (2): 231-240.

FICCARELLI G., BORSELLI V., MORENO ESPINOSA M. & TORRE D. 1995. — Taxonomic remarks on the South American mastodonts referred to *Haplomastodon* and *Cuvieronius. Geobios* 28 (6): 745-756.

FICCARELLI G., AZZAROLI A., BERTINI A., COLTORTI M., MAZZA P., MEZZABOTTA C., MORENO ESPINOSA M., ROOK L. & TORRE D. 1997. — Hypothesis on the cause of extinction of the south American Mastodonts. *Journal of South American Earth Sciences* 10 (1): 29-38.

FICCARELLI G., COLTORTI M., MORENO ESPINOSA M., PIERUCCINI P., ROOK L. & TORRE D. 2003. — A model for the Holocene extinction of the mammal megafauna in Ecuador, South America. *Journal of South American Earth Sciences* 15: 835-845.

FRICK C. 1926. — Tooth sequence in certain trilophodont tetrabelodont mastodonts. *Bulletin of the American Museum of Natural History* 56: 122-176.

GÖHLICH U. B. 2000. — On a pelvis of the straight-tusked elephant *Elephas antiquus* (Proboscidea, Mammalia) from Binsfeld near Speyer (Rhineland-Palatinate, Germany). *Paläontologisches Zeitschriftes* 74: 205-214.

HARINGTON C. R., TIPPER H. W. & MOTT R. J. 1974. —

Mammoth from Babine Lake, British Columbia. *Canadian Journal of Earth Science* 11: 285-303.

HAYNES G. 1991. — *Mammoth Mastodonts & Elephants, Biology Behavior and the Fossil Record*. Cambridge University Press, Cambridge, 413 p.

HOFFSTETTER R. 1950. — Observaciones sobre los mastodontes de Sud America y especialmente del Ecuador. *Haplomastodon*, subgen. nov. de *Stegomastodon*. *Publicaciones de la Escuela Politecnica Nacional de Quito*, 1950, 1: 1-49.

HOFFSTETTER R. 1952. — Les Mammifères pléistocènes de la République de l'Équateur. *Mémoires de la Societé géologique de France* 66: 1-391.

HOFFSTETTER R. 1955. — Remarques sur la classification et la phylogénie des mastodontes sud-américains. *Bulletin du Muséum national d'Histoire naturelle, Paris*, 2e sér., 27 (6): 484-491.

HOFFSTETTER R. 1986. — High Andean mammalian faunas during the Plio-Pleistocene, *in* VUILLEUMIER F. & MONASTEIRO M. (eds), *High Altitude Tropical Biogeography*. Oxford University Press, New York: 218-245.

HOLLAND W. J. 1920. — Fossil mammal collected at Pedra Vernelha, Bahia, Brazil, by G. A. Waring. *Annals of the Carnegie Museum* 13: 224-232.

ICZN 1999. — *International Code of Zoological Nomenclature*. International Trust for Zoological Nomenclature, London, 436 p.

KROLL W. 1991. — *Der Waldelefant von Crumstadt. Ein Beitrag zur Osteologie des Waldelefanten*, E. *(*Palaeoloxodon*)* antiquus *Falconer & Cautley (1847)*. Inaugural-Dissertation zur Erlangung der tiermedizinischen Doktorwürde der Tierärztlichen Fakultät der Ludwig-Maximilians-Universität München, 31 p.

LAMBERT W. D. & SHOSHANI H. 1998. — Chapter 43. Proboscidea *in* JANIS C. M., SCOTT K. M. & JACOBS L. L. (eds), *Evolution of Tertiary Mammals of North America*. Volume 1. Cambridge University Press, Cambridge: 606-621.

LAUB R. S. 1996. — The masticatory apparatus of the American mastodon (*Mammut americanum*), *in* STEWART K. M. & SEYMOUR K. L. (eds), *Palaeoecology and Palaeoenvironments of Late Cenozoic Mammals* – Tributes to the Career of C.S. (Rufus) Churcher. University of Toronto Press, Toronto: 375-405.

LISTER A. 1996. — Sexual dimorphism in the mammoth pelvis: an aid to gender determination, *in* SHOSHANI J. & TASSY P. (eds), *The Proboscidea. Evolution and Palaeoecology of Elephants and their Relatives*. Oxford University Press, Oxford: 203-213.

LISTER A. & AGENBROAD L. D. 1994. — Gender determination of the Hot Spring mammoths, *in* AGENBROAD L. D. & MEAD J. I. (eds), *The Hot Spring Mammoth Site*. Mammoth Site Inc., Hot Spring, South Dakota: 208-214.

LUCAS S. G. 2009. — Taxonomic nomenclature of *Cuvieronius* and *Haplomastodon*, proboscideans from the Plio-Pleistocene of the NewWorld. *New Mexico Museum of Natural History and Science Bulletin* 44: 409-415.

LUCAS S. G. 2009. — *Mastodon waringi* Holland, 1920 (currently *Haplomastodon waringi*; Mammalia, Proboscidea): proposed conservation of usage by designation of a neotype. *Bulletin of Zoological Nomenclature* 66 (2): 164-167.

MADDEN C. T. 1984. — The Proboscidea of South America. *Geological Society of America*, abstracts with programs 12: 474.

MILLER W. 1990. — A *Rhynchotherium* skull and mandible from southeastern Arizona. *Brigham Young University Geology Studies* 36: 57-67.

OLSEN S. J. 1979. — Osteology for the Archaeologist. N.3: The american mastodon and the woolly mammoth. *Papers of the Peabody Museum of Archaeology and Ethnology, Harvard University* 56 (3): 1-45.

OSBORN H. F. 1936. — *Proboscidea*. Volume 1. Americam Museum of Natural History, New-York, 802 p.

PRADO J. L. & ALBERDI M. T. 2008. — A cladistic analysis among trilophodont gomphotheres (Mammalia, Proboscidea) with special attention to the South American genera. *Paleontology* 51 (4): 903-915.

PRADO J. L., ALBERDI M. T., AZANZA B., SANCHEZ B. & FRASSINETTI D. 2005. — The Pleistocene Gomphotheriidae (Proboscidea) from South America. *Quaternary International* 126-128C: 21-30.

PROAÑO J. F. 1894. — Mastodonte del Chimborazo. *Memorias del Liceo Chimborazo, 1894, Riobamba, Ecuador*: 31.

PROAÑO J. F. 1922. — *La Virgen del Dios Chimborazo, Tradiciones Puruhaes*. Imprenta "El Observador", Riobamba, Ecuador, 23 p.

ROTH V. L. 1990. — Insular dwarf elephants: a case study in body mass estimation and ecological inference, *in* DAMUTH J. & MACFADDEN B. J. (eds), *Body size in Mammalian Palaeobiology: Estimation and Biological Implications*. Cambridge University Press, Cambridge: 151-179.

ROTH V. L. 1994. — How elephants grow: Heterochrony and the calibration of developmental stages in some living and fossil species. *Journal of Vertebrate Paleontology* 4: 126-145.

SAUER W. 1965. — *Geologia del Ecuador*. Editorial del Ministerio de Educacion del Ecuador, Quito, 383 p.

SAVAGE D. 1955. — A survey of various late Cenozoic faunas of the Panhandle of Texas. Part 2: Proboscidea. *University of California Publication in Geological Sciences* 31: 51-74.

SHOSHANI J. 1996. — Para- or monophyly of the gomphotheres and their position within Proboscidea, *in* SHOSHANI J. & TASSY P. (eds), *The Proboscidea. Evolution and Palaeoecology of Elephants and their Relatives*. Oxford University Press, Oxford: 149-177.

SHOSHANI J. & TASSY P. 2005. — Advances in proboscideans taxonomy and classification, anatomy and physiology, and ecology and behavior. *Quaternary International* 126-128: 5-20.

SIKES S. K. 1966. — The african elephant, *Loxodonta africana*: a field method for the extimation of age. *Journal of Zoology* 150: 279-295.

SIMPSON G. G. & DE PAULA COUTO C. 1957. — The mastodons of Brazil. *Bulletin of the American Museum of Natural History* 112: 131-189.

SPILLMANN F. 1928. — *Tetrabelodon* nov. spec. *ayora* Spillm. *El Ecuador Comercial* 6 (57): 1-70.

SPILLMANN F. 1931. — *Die Säugetiere Ecuadors im Wandel der Zeit*. Quito Universitad Central, 122 p.

SWOFFORD D. L. 2003. — *PAUP* Phylogenetic Analysis Using Parsimony (* and Other Methods). Version 4*. Sinauer Associates: Sunderland, Massachusetts.

TASSY P. 1977. — Le plus ancien squelette de gomphothère (Proboscidea Mammalia) dans la formation burdigalienne des sables de l'Orléanais, France. *Mémoires du Muséum national d'Histoire naturelle,* Série C, *Sciences de la Terre* 37: 3-51.

TASSY P. 1985. — La *place des mastodontes miocènes de l'ancien Monde dans la phylogénie des Proboscidea (Mammalia): hypothèses et conjectures*. Thèse de Doctorat, Université Pierre et Marie Curie, Paris, 862 p. (unpublished).

TASSY P. 1990. — Phylogénie et classification des Proboscidea (Mammalia) : historique et actualité. *Annales de Paléontologie (Vertebrates-Invertebrates)* 76 (3): 159-224.

TASSY P. 1996a. — Dental homologies and nomenclature in the Proboscidea, *in* SHOSHANI J. & TASSY P. (eds), *The Proboscidea. Evolution and Palaeoecology of Elephants and their Relatives*. Oxford University Press, Oxford: 21-25.

TASSY P. 1996b. — Growth and sexual dimorphism among Miocene elephantoids: the example of *Gomphotherium angustidens*, *in* SHOSHANI J. & TASSY P. (eds), *The Proboscidea. Evolution and Palaeoecology of Elephants and their Relatives*. Oxford University Press, Oxford: 92-100.

TEILHARD DE CHARDIN P. & TRASSAERT M. 1937. — The Proboscideans of south-eastern Shansi. *Palaeontologia Sinica*, Series C, 13: 1-58.

TOBIEN H. 1973. — On the evolution of mastodonts (Proboscidea, Mammalia). Prt 1: The bunodont trilophodont Groups. *Notizblatt des Hessischen Landesamtes für Bodenforschung zu Wiesbaden* 101: 202-208.

TOBIEN H., CHEN G. & LI Y. 1986. — Mastodonts (Proboscidea, Mammalia) from the late Neogene and early Pleistocene of the People's Republic of China. *Mainzer Geowissenschaftliches Mitteilungen* 15: 119-181.

WEBB S. D. 1992. — A brief history of New World Proboscidea with emphasis on their adaptations and interactions with man, *in* FOX J. W., SMITH C. B. & WILKINS K. T. (eds), *Proboscidean and Paleoindian Interactions*. Baylor University Press, Waco, Texas: 16-34.

WEITHOFER K. A. 1889. — Einige Bemerkungen über den Carpus der Proboscidier. *Gegenbaurs Morphologisches Jahrbuch* 14: 507-517.

ZONG G., TANG Y., LEI Y. & LI S. 1989. — *The Hanjiang mastodont (*Sinomastodon hanjiangensis *nov. sp.)*. Academic Press, Beijing (in Chinese with English abstract), 84 p.

*Submitted on 14 September 2007;*
*accepted on 27 May 2010.*

# APPENDIX 1

Measurements of *Haplomastodon chimborazi* (Proaño, 1922): **A**, cranium (see Table 2) ; **B**, mandible (see Table 3). Material catalog numbers: see Table 1.

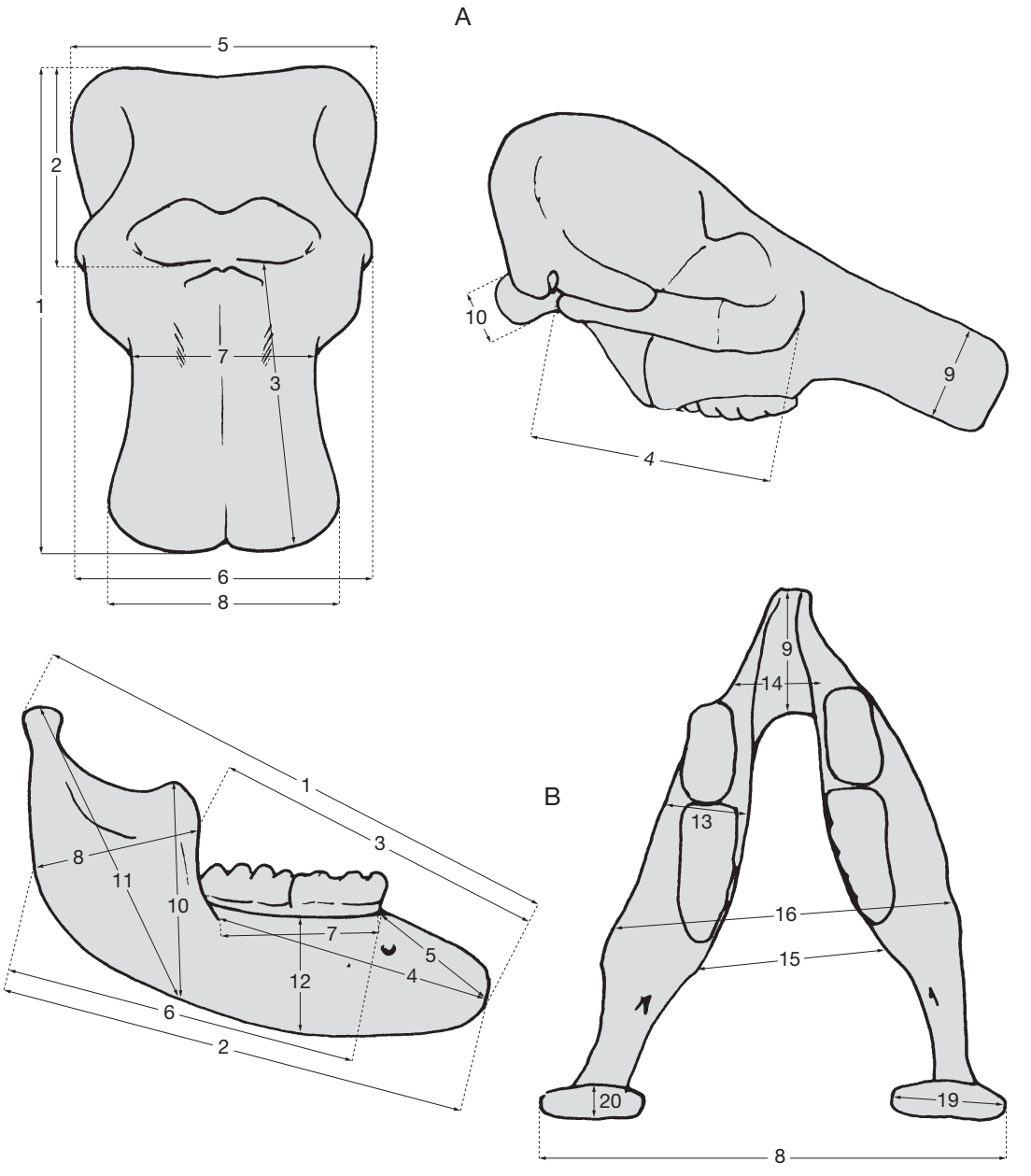

# APPENDIX 2

Measurements of vertebrae of *Haplomastodon chimborazi* (Proaño, 1922): **A**, atlas (see Table 5); **B**, axis (see Table 6); **C**, vertebra C3-L4 (see Table 7); **D**, sacrum (see Table 8). Material catalog numbers: see Table 1.

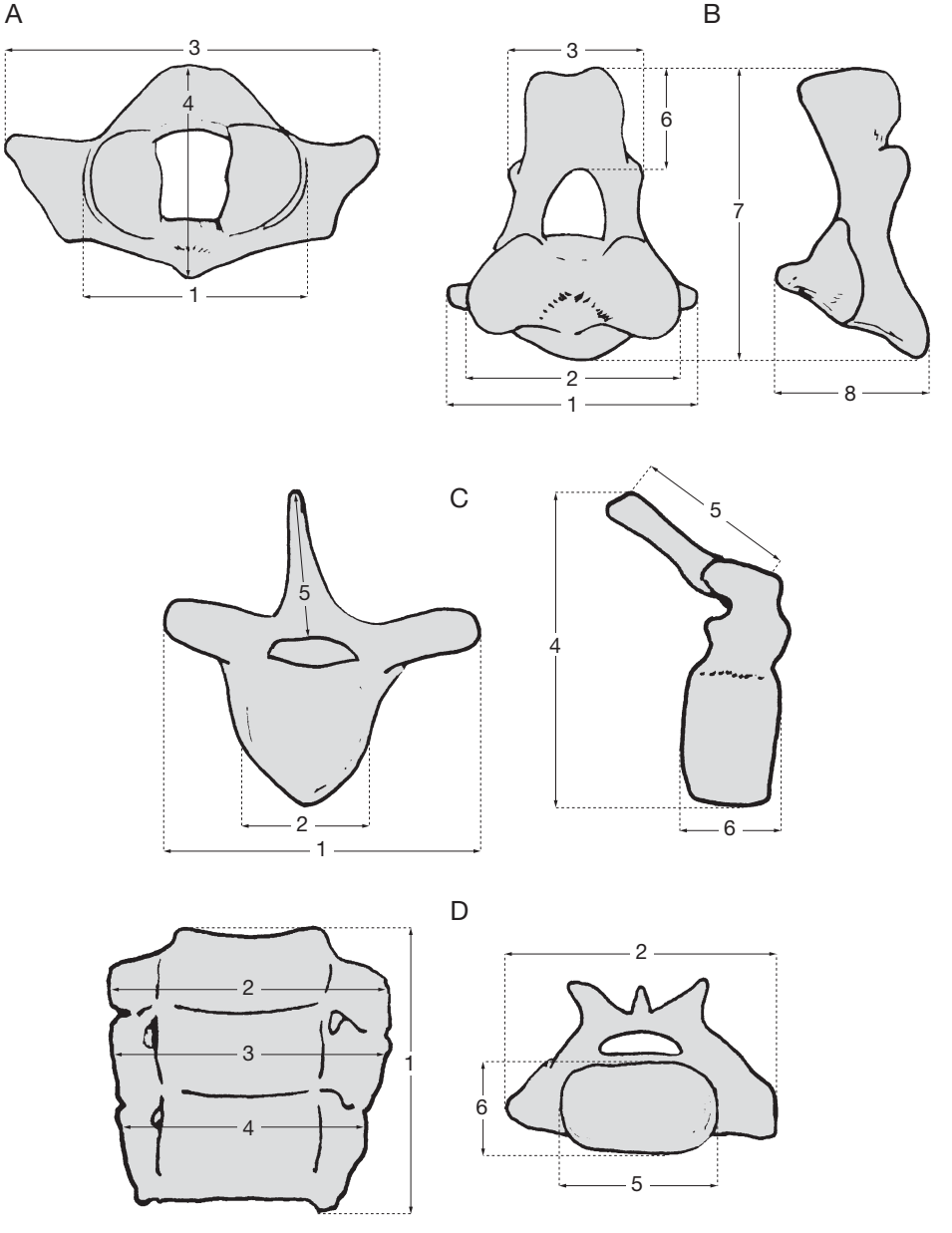

# APPENDIX 3

Measurements of forelimb bones of *Haplomastodon chimborazi* (Proaño, 1922): **A**, scapula (see Table 9); **B**, humerus (see Table 10); **C**, ulna (see Table 11); **D**, radius (see Table 12); **E**, carpal (see Table 13); **F**, metapodial (see Table 14). Material catalog numbers: see Table 1.

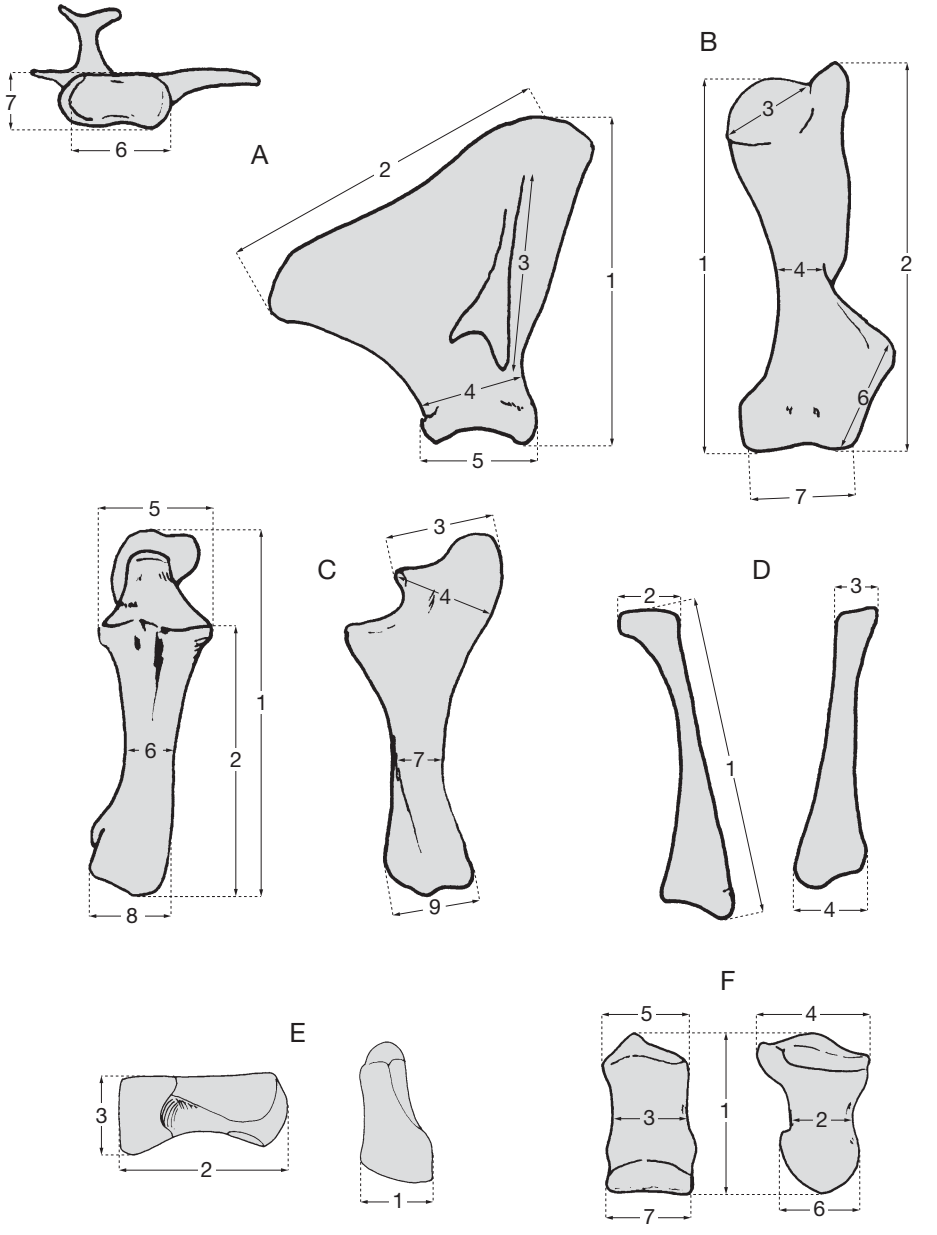

# APPENDIX 4

Measurements of pelvis of *Haplomastodon chimborazi* (Proaño, 1922) (see Table 15). Material catalog numbers: see Table 1.

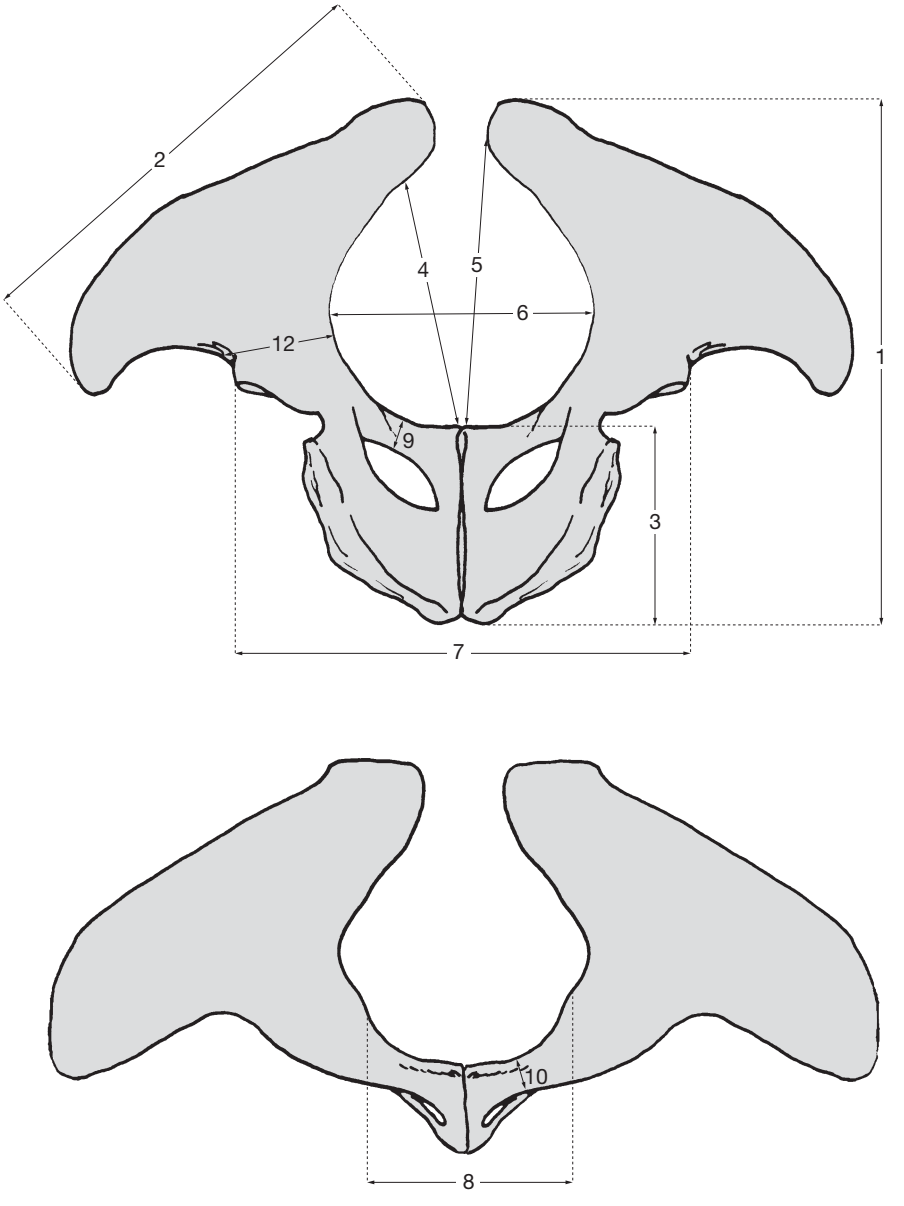

# APPENDIX 5

Measurements of hindlimb bones of *Haplomastodon chimborazi* (Proaño, 1922): **A**, femur (see Table 16); **B**, tibia (see Table 17); **C**, fibula (see Table 18); **D**, astragalus (see Table 19). Material catalog numbers: see Table 1.

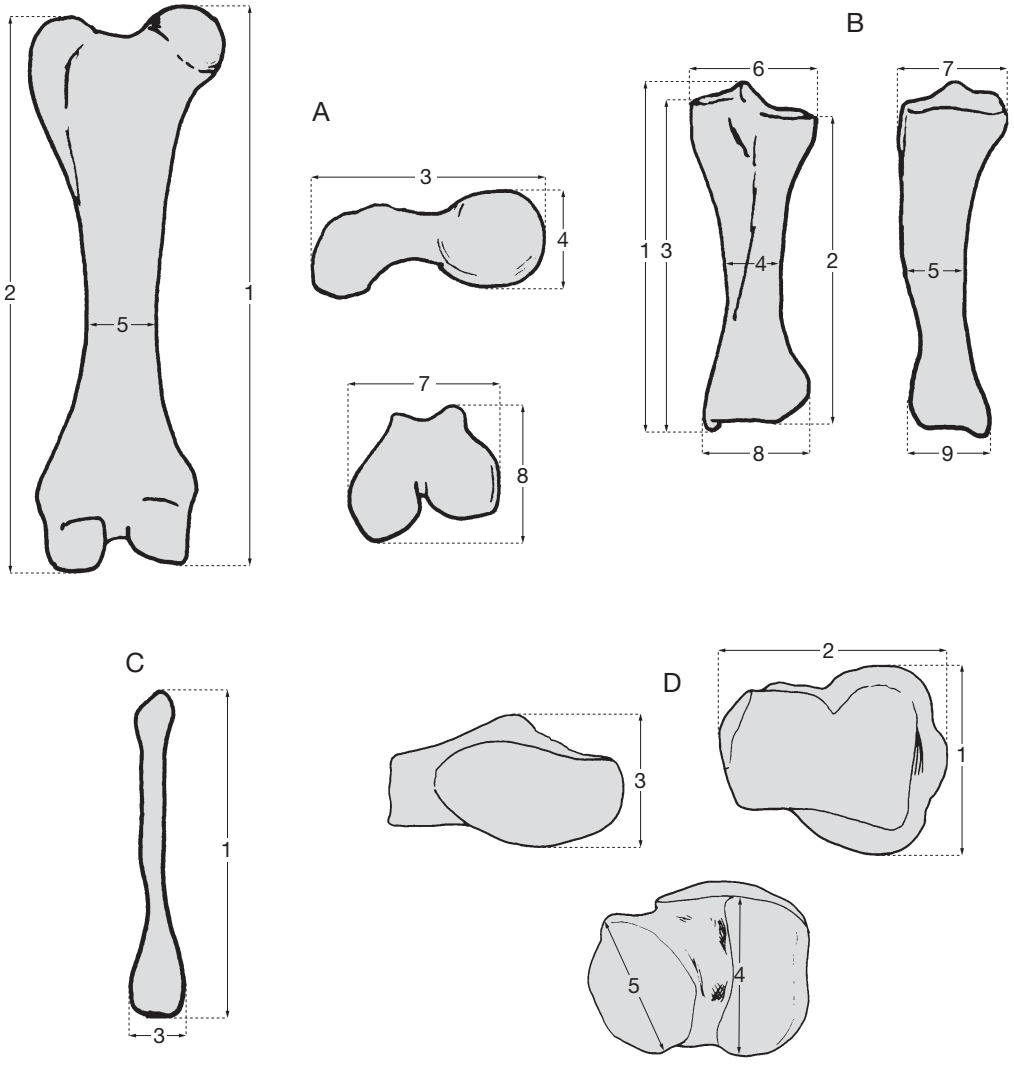

# APPENDIX 6

Skeletal and dental characters used in the cladistic analysis and their primitive (0) and derived (1, 2) states.

*Cranium*

**1. Position of the anterior border of the bony orbit (in lateral view).** 0) laying above or posterior to the mesial-most cheek tooth, 1) forward of the mesial-most tooth.
Modified from character 83 of Shoshani (1996).

**2. Forehead (frontoparietal plane between temporal lines).** 0) narrow, 1) wide.
Modified from character 37 of Tassy (1990).

**3. Premaxillaries (in frontal view).** 0) slender, distal margin much narrower than interorbital width, 1) robust, distal margin equal or wider than interorbital width.
Modified from character 35 of Tassy (1990).

**4. Tusk alveoli (in frontal view).** 0) nearly parallel, 1) distally slightly diverging, 2) distally greatly diverging.
Modified from character 9 of Shoshani (1996).

**5. Supraorbital foramen.** 0) present, 1) absent.
Adapted from character 33 of Tassy (1990).

**6. Subnasal fossa.** 0) absent, 1) present.

*Mandible*

**7. Symphysis.** 0) long, 1) short.
Taken from character 52 of Tassy (1990).

**8. Symphysis (in lateral view).** 0) parallel to ventral margin of mandibular body, 1) downturned.
Modified from character 51 of Tassy (1990).

**9. Symphysis (dorsal view).** 0) slightly widens distally, 1) tapers distally, 2) greatly widens distally.

**10. Ascending ramus.** 0) dorso-posteriorly directed, 1) dorsally directed.

**11. Position of the mandibular foramen.** 0) at or slightly higher than the level of the occlusal plane, 1) much higher than the occlusal plane.

**12. Coronoid fossa.** 0) absent, 1) present.

*Teeth*

**13. Upper tusk, curvature in adult growth stage.** 0) downturned, 1) straight or slightly upturned, 2) upturned, much.
Modified from character 76 of Tassy (1990) and character 7 of Shoshani (1996).

**14. Upper tusk, enamel band in adult growth stage.** 0) present, 1) sometimes present, 2) absent.
Modified from character 72 of Tassy (1990) and character 10 of Shoshani (1996).

**15. Upper tusk, helicoidal torsion of the enamel band.** 0) absent or moderate, 1) strong.
Modified from character 8 of Shoshani (1996).

**16. Lower permanent tusk (i2).** 0) present, 1) absent.
Taken from character 70 of Tassy (1990).

**17. Lower tusk: cross section.** 0) piriform, 1) subcircular.
Taken from character 74 of Tassy (1990).

**18. Definitive premolars (P2-P4).** 0) P2 absent 1) P2-P4 absent.
Adapted from character 86 of Tassy (1990).

**19. Third deciduous premolars (DP3/dp3).** 0) bilophodont, 1) third loph/id outlined, 2) trilophodonty achieved.

**20. Number of complete lophids in lower third molar.** 0) four, 1) five, 2) six or more.
Modified from character 105 of Tassy (1990).

**21. Posttrite central conules in molars (M1-M3/m1/m3).** 0) absent, 1) outlined, 2) present, large.
Modified from character 113 of Tassy (1990).

**22. Crown cement in cheek teeth.** 0) absent, 1) little present, 2) abundant.
Modified from character 116 of Tassy (1990).

*Post-cranial*

**23. Atlas, transversal foramen.** 0) present, 1) sometimes absent.
Based on Hoffstetter (1952) and Tassy (1986).

**24. Atlas, large dorsal tuberosity of dorsal arch.**
0) absent, 1) present.

# APPENDIX 7

Character-taxon matrix used in the cladistic analysis. Missing data (either due to non-preservation or because non-applicable) are coded as "?".

| **Taxon/character** | **1** | **2** | **3** | **4** | **5** | **6** | **7** | **8** | **9** | **10** | **11** | **12** | **13** | **14** | **15** | **16** | **17** | **18** | **19** | **20** | **21** | **22** | **23** | **24** |
|---|---|---|---|---|---|---|---|---|---|---|---|---|---|---|---|---|---|---|---|---|---|---|---|---|
| *Gomphotherium angustidens* | 0 | 0 | 0 | 0 | 0 | 0 | 0 | 0 | 0 | 0 | 0 | 0 | 0 | 0 | 0 | 0 | 0 | 0 | 0 | 0 | 0 | 0 | 0 | 0 |
| *Gomphotherium productum* | 0 | 0 | 0 | 0 | 0 | 0 | 0 | 0 | 0 | 0 | 0 | 0 | 0 | 0 | 0 | 0 | 1 | 0 | 0 | 0 | 0 | 0 | 0 | 0 |
| *Megabelodon lulli* | 0 | 0 | 0 | 0 | 0 | 0 | 0 | 0 | 0 | 0 | 0 | 0 | 0 | 0 | ? | 1 | ? | 0 | 0 | 0 | 0 | 0 | 0 | 0 |
| *Eubelodon morilli* | 0 | 0 | 0 | 0 | 0 | 0 | 0 | 0 | 2 | 0 | 0 | 0 | 0 | 2 | ? | 1 | ? | ? | ? | 0 | 1 | 1 | 0 | 0 |
| *Gnathabelodon thorpei* | 0 | 0 | 0 | 0 | 0 | 0 | 0 | 0 | 1 | 0 | 0 | 0 | 1 | 2 | ? | 1 | ? | 0 | 0 | 0 | 0 | 0 | 0 | 0 |
| *Sinomastodon hanjiangensis* | 1 | 1 | 0 | 0 | 0 | 0 | 1 | 1 | 2 | 1 | 1 | 0 | 1 | 2 | ? | 1 | ? | 1 | ? | 1 | 0 | 0 | 0 | 0 |
| *Stegomastodon texanus* | 1 | 1 | 1 | 1 | 0 | 0 | 1 | 1 | 2 | 0 | 0 | 0 | 2 | 2 | ? | 1 | ? | 1 | 1 | 2 | 2 | 2 | 0 | 0 |
| *Rynchotherium* cf. *falconeri* | 0 | 1 | 1 | 2 | 1 | 1 | 0 | 1 | 2 | 1 | 0 | 0 | 1 | 0 | 1 | 0 | 1 | 1 | 1 | 0 | 1 | 0 | 0 | 0 |
| "*Stegomastodon*" *platensis* | 1 | 1 | 1 | 1 | 1 | 1 | 1 | 1 | 2 | 1 | 1 | 1 | 1 | 1 | 0 | 1 | ? | 1 | 2 | 1 | 2 | 1 | 1 | 1 |
| *Cuvieronius hyodon* | 1 | 1 | 1 | 2 | 1 | 1 | 1 | 1 | 2 | 1 | 1 | 1 | 1 | 0 | 1 | 1 | 1 | 1 | 2 | 1 | 1 | 1 | 1 | 1 |
| *Haplomastodon chimborazi* | 1 | 1 | 1 | 1 | 1 | 1 | 1 | 1 | 2 | 1 | 1 | 1 | 2 | 2 | 0 | 1 | ? | 1 | 2 | 1 | 1 | 1 | 1 | 1 |